Cost Effective Repetitive Control
and Its Application to Magnetic Disk Drives

by

Steven Craig Smith Jr.

B.S. (California Institute of Technology) 1994
M.S. (University of California at Berkeley) 1997

A dissertation submitted in partial satisfaction of the
requirements for the degree of
Doctor of Philosophy

in

Engineering – Mechanical Engineering

in the

GRADUATE DIVISION
of the
UNIVERSITY of CALIFORNIA at BERKELEY

Committee in charge:

Professor Masayoshi Tomizuka, Chair
Professor Andrew Packard
Professor Laurent El Ghaoui

Spring 2000

The dissertation of Steven Craig Smith Jr. is approved:

Chair Date

Date

Date

University of California at Berkeley

Spring 2000

Cost Effective Repetitive Control
and Its Application to Magnetic Disk Drives

Steven Craig Smith Jr.

Abstract

Cost Effective Repetitive Control
and Its Application to Magnetic Disk Drives

by

Steven Craig Smith Jr.
Doctor of Philosophy in Engineering – Mechanical Engineering

University of California at Berkeley

Professor Masayoshi Tomizuka, Chair

Repetitive control is a control scheme which reduces the effects of periodic disturbances on a system when the period is known. Two new discrete time repetitive controller designs are presented. These new designs specifically address the tradeoff between performance and controller complexity. The first new design uses a dual-rate controller to reduce memory requirements. The second new design is restricted to cases where repetitive control is added to an existing feedback control system. Reductions in computational complexity are attained through the direct use of the internal states of the feedback controller. As these developments were motivated by concerns voiced in the computer disk drive industry, problems drawn from this application are used to illustrate these designs. Emphasis is placed on defining a framework for repetitive controller design. Within this framework, the designer of a repetitive control system can examine the achievable performance with varying complexities. Making the connection that complexity implies cost, this information is critical for determining the most cost effective solution – the heart of the problem.

Professor Masayoshi Tomizuka
Dissertation Committee Chair

To my parents,
for their love and support.

Contents

List of Figures **vi**

List of Tables **viii**

1 Introduction **1**
1.1 Motivation . . . 1
1.2 Previous Work . . . 2
1.3 Magnetic Disk Drives . . . 3
1.4 Contributions of this Dissertation . . . 4
1.4.1 Tunable Frequency Domain Performance Objective . . . 5
1.4.2 Dual-Rate Repetitive Control . . . 5
1.4.3 Cascaded Repetitive Controller Design . . . 6
1.5 Outline of the Dissertation . . . 7

2 Preliminaries **8**
2.1 Discrete Time Repetitive Control . . . 8
2.1.1 A Generic Context for Disrete Time Repetitive Control . . . 8
2.1.2 Internal Model Principle . . . 9
2.1.3 Interpretations of Discrete Time Linear Repetitive Control . . . 10
2.1.4 1989 Discrete Time Repetitive Controller Design . . . 12
2.2 Magnetic Disk Drives . . . 20
2.2.1 Physical Plant . . . 20
2.2.2 Cost Concerns Relating to Servo Control Objectives . . . 22
2.2.3 Obstacles to Meeting Positioning Requirements . . . 24
2.2.4 Periodic Disturbance Sources which Motivate Repetitive Control . . . 27
2.3 Cost Effective Repetitive Control . . . 28
2.3.1 Starting Point for Cost Effective Designs . . . 28
2.3.2 Describing the Cost of a Design . . . 29
2.3.3 Describing Performance . . . 30
2.3.4 Frequency Domain Performance Specification . . . 31
2.3.5 Time and Frequency Domain Effects of $q_w(z, z^{-1})$ and ξ . . . 31
2.3.6 Rationale for Performance Criterion . . . 33
2.3.7 Relation of Performance Measure to 1989 Repetitive Controller Design 34

3 Dual-rate Repetitive Controller Design **35**
3.1 Development . . . 36
3.1.1 Structure . . . 36
3.1.2 Design of the Components . . . 38
3.1.3 Stability . . . 40
3.1.4 The Lifted Closed Loop System . . . 45
3.1.5 Best and Worst Case Periodic Disturbances . . . 46
3.1.6 Effects of G_{ptv} on the Closed Loop . . . 48
3.1.7 Frequency Domain Interpretation Tools . . . 51
3.1.8 Relation to Performance Objective of Section 2.3 . . . 53
3.1.9 Closing Comments on the Design . . . 53
3.2 Application to Magnetic Disk Drive . . . 54
3.2.1 The Disk Drive System in Context . . . 55
3.2.2 Stability Issues . . . 57
3.2.3 Performance . . . 65
3.3 Concluding Remarks . . . 80

4 Cascaded Repetitive Controllers **81**
4.1 Development . . . 81
4.1.1 Structure . . . 82
4.1.2 Design Method / Performance . . . 85
4.2 Application to Magnetic Disk Drive . . . 87
4.2.1 Designing for different complexities (σ) . . . 88
4.2.2 Effect of ξ on the resulting designs . . . 89
4.2.3 Comparison to 1989 Design . . . 91
4.3 Concluding Remarks . . . 92

5 Conclusions **93**
5.1 Summary of Results . . . 93
5.2 Future Work . . . 95

Bibliography **97**

A Technical **100**
A.1 Zero-Phase-Error Inverses . . . 100
A.2 Multirate Systems . . . 102
A.2.1 Lifting . . . 102
A.2.2 Frequency Domain Interpretations . . . 104
A.2.3 Decimation . . . 106
A.2.4 Interpolation . . . 107

B Design Example Data **108**
B.1 Experimental Equipment . . . 108
B.2 Disk Drive Servosystem Model used in Chapter 3 . . . 109
B.3 Disk Drive Servosystem Model used in Chapter 4 . . . 110

List of Figures

2.1 Generic Repetitive Control 9
2.2 Augmenting Plant with Model of Periodic Disturbance 11
2.3 Tomizuka *et al* Repetitive Control Structure (1989) 13
2.4 Small gain theorem structure 16
2.5 Realization of PSG in implementation 19
2.6 Various modified periodic signal generators ($N = 30$) 21
2.7 Schematic of a computer disk drive 22
2.8 Disk Drive Track Following Servo 24
2.9 Proposed ideal closed loop frequency response. 32
2.10 Example Proposed ideal closed loop time responses. 33

3.1 Dual-Rate Repetitive Control 37
3.2 Small-gain structure for Dual-Rate Repetitive Control 40
3.3 Uncertainty bound for robust stability 44
3.4 Aliasing effects of the filter $q(z^r, z^{-r}) = \frac{1}{4}z^4 + \frac{1}{2} + \frac{1}{4}z^{-4}$ 48
3.5 Frequency response of nominal and perturbed plants (G_n). 56
3.6 Frequency responses of controller G_c(left), and feedback loop G_nG_c(right). 57
3.7 Frequency response from $u_{rep}(k)$ to $y(k)$ (Γ_y) with inner loop closed. . . . 58
3.8 Frequency response from $d_{out}(k)$ to $y(k)$ (Γ_{out}) with inner loop closed. . . 58
3.9 Frequency response of the approximate ZPE inverse of Γ_y 59
3.10 Frequency response of $z^2 G_{zpe}\Gamma_y$ 60
3.11 Frequency response of $z^3 G_{gain}\Gamma_y$ 61
3.12 Magnitude plots of $(z^{-\delta_r} - \mathcal{DL}^r(G_{zpe}\Gamma_y)\mathcal{I})$ 61
3.13 Magnitude plots of $(z^{-\delta_r} - \mathcal{DL}^r(G_{zpe}\Gamma_y)\mathcal{I})$ with perturbed plant. 62
3.14 Magnitude plots of $(z^{-\delta_r} - \mathcal{DL}^r(G_{gain}\Gamma_y)\mathcal{I})$ with perturbed plant. 63
3.15 Magnitude responses of several $q(z, z^{-1})$ filters defined according to Eq 3.60. 65
3.16 Reduction of Periodic Disturbances with G_{inv} as zero-phase inverse 66
3.17 Reduction of Sinusoidal Disturbances with G_{inv} as a fixed gain 67
3.18 Reduction of Sinusoidal Disturbances with $G_{inv} = G_{zpe}f(z^{-1})$ 67
3.19 Simulated Example of Best Case Periodic Input Disturbance 68
3.20 Simulated Example of Worst Case Periodic Input Disturbance 69
3.21 Simulated Example of Worst Case Periodic Output Disturbance 70
3.22 Simulated Example of Best Case Periodic Output Disturbance 70

3.23 Simulated Example of Best Case Periodic Output Disturbance 71
3.24 Simulated Example of Worst Case Periodic Output Disturbance 72
3.25 Worst case output disturbance for $G_{zpef}(z^{-1})$ 74
3.26 Noises and the nominal system 75
3.27 Simulated comparisons of $r = 1, 2, 4$ designs 75
3.28 Experimental Comparison of Linear Interpolation and Holding of the Repetitive Control Signal for $r = 4$ 77
3.29 Experimental Comparison of $r = 4$ vs. $r = 1$ 78
3.30 Experimental Results for $r = 4$ with $q(z, z^{-1})$ either $q16 = \frac{1}{16}z + \frac{14}{16} + \frac{1}{16}z^{-1}$ or $q64 = \frac{1}{64}z + \frac{62}{64} + \frac{1}{64}z^{-1}$ 79

4.1 Cascaded Repetitive Control Structure 82
4.2 Effect of σ on the system shown in the time domain. 90
4.3 Simulation results for Cascaded designs with varying ξ and constant σ . . 90

A.1 Several interpolation schemes 107

B.1 Bode plots for observer state feedback system. 111

List of Tables

2.1 Elements of Fig 2.3 14

3.1 HDD for dual-rate repetitive control 56
3.2 Magnitude of frequency components of worst case output disturbances when G_{zpe} is used 72
3.3 Magnitude of frequency components of worst case output disturbances when G_{gain} is used 73
3.4 Worst case singular values of G_{ptv} at harmonics 73

4.1 Optimal $\hat{\mathrm{J}}_{\mathrm{rep}}(K_{opt})$ for varying δ and σ 89
4.2 Optimal values of K_{opt} as complexity varies 89
4.3 Performance Index Comparison 91

Acknowledgements

I have to begin by acknowleding the support of my dissertation advisor, Professor Tomizuka. He has played a very large role in the formation of my view of automatic control, and not through intimidation. My perspective on problems was both valued and challenged in constructive ways. I will miss being his student.

Professor Packard has been a particularly good sounding board over the years I have been at Berkeley, especially when I was a new graduate student. Professor El Ghaoui was very helpful with his encouragement and comments during the writing of this dissertation. I have been fortunate that Professors O'Reilly, Hedrick, and Horowitz have given great advice and related their experiences as a graduate students to me. I will be doing my best to cross paths with all of them in the future.

In addition to the faculty members at Berkeley who have been supportive, my fellow graduate students have played a large role in my intellectual development. I recall great philosophical discussions about automatic control with my fellow graduate students in 2103 Etcheverry Hall. It has been a great place to be. Professor Bin Yao and Dr. Matt White in particular need to be noted for great advice they have given me. I'm looking forward to more.

Kenji Takeuchi was first a fellow graduate student, and then my research contact at Iomega Corporation. He made the collection of the experimental data in this dissertation a pleasure. In addition, he gave me valuable insight into the concerns of a practicing controls engineer.

My brother Geoff was very kind to come up to Berkeley one Saturday and spend 15+ hours editing a draft of the dissertation. He deserves profuse thanks. It was a tremendous help to have his comments on grammar and style.

The rest of my family along with a great group of friends here at Berkeley has given me tremendous moral support. I doubt I would have finished without all of them.

Finally, I would like to acknowledge the support of Iomega Corporation in the form of reseach grants.

Chapter 1

Introduction

This dissertation is about designing cost effective repetitive controllers. The motivation for this work is described along with a discussion of previous work in the area of repetitive control. A brief discussion of why magnetic disk drive servosystems are a target application for this work follows. The contributions of this thesis are then introduced. The chapter ends with an outline of the remainder of the dissertation.

1.1 Motivation

Periodic disturbances or process variations are common to mechanical systems undergoing periodic motions. The controlled quantities in these systems must be regulated to their desired values in spite of these disturbances. Systems affected by periodic disturbances include read/write head positioning in magnetic and optical disk drives, robotic manipulators repeating a task, scanning mirrors on satellites, and cartridge motion in inkjet printers. One approach to addressing periodic disturbances to these mechanical systems is to redesign the system to tighter specifications, directly minimizing the causes of variation. Another approach is feedback control, which is often the more practical choice because of its price advantage over precision manufacturing.

Consider a motion control system operating in a linear regime. When viewed in the frequency domain, the output of a periodically disturbed system will show peaks at a fundamental frequency and its harmonics. Simple feedback schemes may be sufficient to reduce the magnitude of these peaks to acceptable levels. However, when these peaks are large and the performance objectives stringent, more sophisticated solutions are necessary.

Repetitive control systems are designed to eliminate the effect of a periodic disturbance on a system. This technique requires that the period of the cyclic disturbance be known; its shape can be arbitrary.

To asymptotically eliminate the effect of periodic disturbances, a repetitive control system must generate a periodic control even as the output error approaches zero. A repetitive control scheme must therefore be sophisticated enough to generate a wide spectrum of periodic control signals. For a linear controller, this corresponds to a controller with high order. For other techniques, a large number of parameters are required. Limiting complexity, and therefore implementation costs, is a challenge in either case.

1.2 Previous Work

Repetitive controllers have been a subject of research for some time due to the significance of periodic disturbances in many applications. The first appearance of repetitive control was in the work of Inoue, Nakano and Iwai (1981) with applications to repeated motions of a servomechanism. Hara, Yamamoto, Omata and Nakano (1988) proposed synthesis methods for continuous time repetitive control systems which guarantee both stability and asymototic elimination of periodic disturbances. Repetitive control in the continuous time is based upon the introduction of a time delay of one period of the repetitive disturbance. Implementation on digital computers in a sampled-data context has led naturally to sampled data (Langari and Francis, 1996; She and Nakano, 1996) and discrete time developments (Tomizuka, Tsao and Chew, 1989).

Developments in sampled-data systems analysis and optimal synthesis methods have spurred developments in repetitive control. Langari and Francis (1996) formulate a robust tracking problem for sampled data repetitive control using tests based on the structured singular value. She and Nakano (1996) describe a discrete time repetitive controller designed with sampled data $\mathcal{H}_\infty$ synthesis techniques.

Discrete time repetitive control has been applied to various mechanical systems. Tenney and Tomizuka (1996) address the effect of non-periodic disturbances when applied to robotic manipulation. Repetitive control has been used to reduce manufacturing errors when turning or boring non-circular profiles (Hanson and Tsao, 1996; Tsao and Tomizuka, 1994). For situations where measurements are not evenly spaced over the period of the disturbance, Hanson and Tsao (1996) describe a repetitive controller for periodically time varying discrete

time systems. Kempf, Messner, Tomizuka and Horowitz (1993) compare four different discrete time repetitive controller designs applied to a computer disk drive servosystem. The comparisons made are in terms of achievable performance, coding complexity, and realtime computational burden.

For more, refer to Hillerstrom and Walgama's (1996) survey of the development and application of repetitive control. The above listed research has been directed toward designs achieving higher levels of robust stability and performance with little regard to controller complexity. The work in this dissertation seeks to include concerns about controller complexity when designing repetitive control systems.

1.3 Magnetic Disk Drives

As stated at the outset of the previous section, magnetic disk drives represent a case where periodic disturbances affect performance. In fact, the study of repetitive control in this dissertation has been motivated by magnetic disk drive applications. The data-storage field is characterized by low margins, continual improvement in data capacity and throughput, and extreme attention to cost, most often measured in dollars per megabyte. While other systems (satellite, military, aerospace) can demand premium performance at high cost, disk drive manufacturers are constantly pressured to find the cheapest way to produce a device with a suboptimal but acceptable level of performance.

The read/write head positioning accuracy in computer disk drives is a critical determinant of storage density. Data is arranged on a disk along concentric circular tracks. A servosystem must position the read/write head radially over the correct track as the disk spins underneath it. This must be done within very tight tolerances to prevent read errors, and, more critically, write errors which result in data loss. Though the servosystem is a critical component of the disk drive, it is not isolated. The specifications for the entire system affect the specifications for the servosystem both directly and indirectly.

The constant rate of rotation of the disk gives rise to periodic disturbances to the servosystem. Their shape is a function of manufacturing variability and material properties. The order of a discrete time repetitive controller depends upon the period of the repetitive disturbance. In the context of magnetic disk drives, this order will be the number of measurement samples per disk revolution. A detailed discussion of these periodic disturbance sources is made in Section 2.2.

The dynamic behavior of the magnetic disk drive servosystem is not complex. A magnetic induction motor applies torque to a pivot, or force to a slider. There are three predominant challenges to this problem. First, only one *sampled* measurement is available to the controller: the relative position of the head over the track. The measurement sample rate is typically long relative to the performance requirements (faster sampling uses up disk space which would otherwise be used for data). Second, a variety of disturbances have an influence on the position of the head. Describing these disturbances and their relative importance for servo controller design is an active area of research in the disk drive community. Third, mechanical resonance of the actuator arm puts a limit on the bandwidth of the closed loop control system. In fact, decreasing the physical size of disk drives allows for higher bandwidths because the length of the actuator arm is decreased, moving the mechanical resonance to a higher frequency.

If commercially available storage density is to appreciably increase, servosystem positioning accuracy must improve at reasonable cost. To this end, more sophisticated control algorithms are being considered. Dual-stage actuation and accelerometer feedback have been introduced to disk drive servosystems. These methods augment the system described above with either an actuator (dual-stage actuation) or a sensor (accelerometer feedback). The dual-stage actuation aims to address the bandwidth constraint on the system imposed by the resonant mode of the actuator arm by adding a small, higher bandwidth actuator in series with the original actuator at the tip of the arm. The accelerometer feedback scheme aims to minimize the performance limitations caused by limited measurement information.

Repetitive control for magnetic disk drives aims to address the periodic disturbances typical of these systems without adding sensors or actuators to the system. This does not mean that when sensors or actuators are added to the system, there will be no need for repetitive control. For disk drives (especially removable media drives), disturbances coperiodic with disk rotation are significant. Repetitive control is considered for disk drive systems primarily to address these disturbances, though its design must incorporate the fact that other disturbances are present.

1.4 Contributions of this Dissertation

The specific contributions of this dissertation are as follows:

- A tunable frequency domain performance objective for repetitive control is proposed.

- A dual-rate repetitive controller design is proposed to reduce storage requirements relative to single rate repetitive control.
- A cascaded repetitive control structure is presented to more efficiently integrate repetitive control into an existing control system.

Some details of each of these contributions are described below.

1.4.1 Tunable Frequency Domain Performance Objective

This performance objective is introduced in Section 2.3 to describe a repetitive control problem independent of the repetitive controller design. Comparisons between repetitive controller designs can then be made. Performance of discrete time repetitive controllers for single-input single-output (SISO) regulator systems is considered. A tunable ideal frequency response for a repetitive control system was specified. The peak magnitude of the frequency response of the difference between the actual and ideal repetitive control systems is used as performance measure. This is a loop-shaping criterion.

The ideal frequency response is defined using the system to which repetitive control is applied. There are two additional design parameters. They describe: 1) the rate of convergence to steady-state vs the effect of non-periodic disturbances, and 2) robustness to uncertainty (and sensitivity to non-periodic disturbances) vs nominal steady-state attenuation of periodic disturbances. The combined selection of these parameters describes a wide variety of repetitive control problems. Though this specification could be used to design a repetitive controller via classical H-infinity synthesis, such a design is not considered because of the unconstrained complexity of the resulting controller. This performance measure is used as an objective function for the design of the cascaded repetitive controller.

1.4.2 Dual-Rate Repetitive Control

A single rate digital repetitive controller will use N states to describe an N-periodic control signal. A dual-rate discrete time repetitive controller structure is proposed in Chapter 3 to reduce memory usage and keep implementation complexity low compared to a single rate design. This dual-rate controller instead uses M states to describe an N-periodic control signal, where $Mr = N$ for some integer r. The memory usage devoted to generating periodic control signals is reduced by a factor of r. Dual-rate linear control introduces

aliasing effects which must be considered when evaluating the performance of the control system.

Lifting techniques are used to analyze the dual rate closed loop system as a multi-input-multi-output linear time invariant system. A specific design methodology is provided, emphasizing simplicity of implementation. Stability is described using the small gain theorem. Frequency domain interpretations of the closed loop system are given, illustrating drawbacks of the dual-rate design. Evaluation of this design using the introduced performance objective is described. Finally, the proposed design and analysis techniques are applied to a computer disk drive servosystem in experiment and simulation.

1.4.3 Cascaded Repetitive Controller Design

In many cases, repetitive control will not be the only feedback control action. Other feedback controllers are initially used to stabilize the system and provide nominal desired performance. Repetitive control is then applied as an additional control measure to eliminate the persistent effect of periodic disturbances. In the literature, repetitive controller design typically proceeds by lumping the plant with these other stabilizing feedback controllers, considering only the input/output behavior of the stabilized plant during the design.

In a departure from this approach, the cascaded structure presented in Chapter 4 uses the internal states of the stabilizing controller. The presented development assumes that this stabilizing controller is an observer state feedback controller. The real-time computation done by the observer in computing state estimates is used by the repetitive controller at no additional cost. A linear combination of the observer states and a filtered plant output is used to update the periodic control signal. The order of the filter applied to the output is a design parameter allowing the complexity of the design to be specified. The proposed frequency domain design specification is directly used to design repetitive controllers with this structure. For a given complexity, the linear combination of observer states and delayed outputs is sought to best approximate this desired performance.

This design method amounts to an $\mathcal{H}_\infty$ optimal design for a fixed structure controller. The optimization problem is not convex, but is approximated with a convex optimization problem. The reasons for making this approximation, as well as its quality, are discussed. Conditions for stability of the resulting control system are given. This design

method is applied to an example disk drive servosystem.

1.5 Outline of the Dissertation

The remainder of this dissertation is organized as follows:

- In Chapter 2, some background material on discrete time repetitive control and servo control for magnetic disk drives is given, followed by a description of what is meant by cost effective repetitive control.
- In Chapter 3, dual-rate repetitive control is described along with its application to a magnetic disk drive servosystem.
- In Chapter 4, a cascaded repetitive controller design is described with application to a magnetic disk drive servosystem.
- In Chapter 5, a review of what was done along with a vision for future work is presented.
- Mathematical reference material, numerical expressions of the system models used for the example applications, and a description of the experimental system are provided in Appendices.

Chapter 2

Preliminaries

The aim of this chapter is to establish a foundation for the later chapters of this dissertation. The following three sections describe: (1) discrete time repetitive control, (2) the computer disk drive servo control problem, (3) cost effectiveness of the new designs. In the last section, a frequency domain objective for repetitive controllers is introduced.

2.1 Discrete Time Repetitive Control

Repetitive control systems are designed to use past input/output data and knowledge of system dynamics to eliminate the effect of periodic disturbances. In this section, discrete time repetitive control applied to linear servosystems is described. The general setting in which repetitive control is discussed in the remainder of this dissertation is first described, followed by a description of the Internal Model Principle in this context. Then various interpretations of linear repetitive control are given, with an eye to the design methods they suggest. Finally, the discrete time repetitive controller design proposed by Tomizuka et al. (1989) is described in some detail.

2.1.1 A Generic Context for Disrete Time Repetitive Control

The block diagram in Figure 2.1 depicts a generic setting for repetitive control. Assume the following: (1) all systems are linear and signals are discrete time; (2) the period of the repetitive disturbances is an integer number of samples, N; (3) the plant (possibly augmented by feedback control) is asymptotically stable and subject to periodic

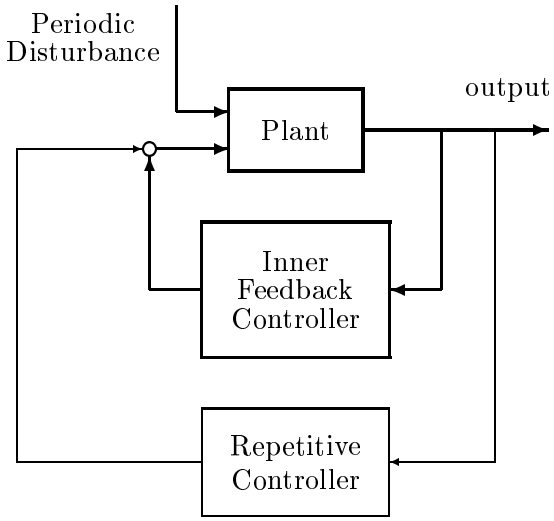

Figure 2.1: Generic Repetitive Control

disturbances ; (4) the control objective is regulation of the output to zero. The repetitive controller will be a single-input single output system in this setting.

Because of the assumption that repetitive control is applied to an asymptotically stable system, repetitive control is typically used in an "outer" loop, as depicted in Figure 2.1. It cleans up the uncompensated effect of a repetitive disturbance on a system – it may be designed after an "inner" loop controller which provides a nominal performance (stability) with respect to the other control objectives. In this dissertation, the asymptotically stable system to which repetitive control is to be applied is assumed to be given.

2.1.2 Internal Model Principle

As mentioned, a popular class of repetitive controllers is based on the Internal Model Principle (IMP) of linear controller design (Francis and Wonham, 1975). When a system is forced with an unknown periodic disturbance with known period, the IMP states that a periodic signal generator(PSG) must be a part of the feedback controller if the output is to be asymptotically driven to zero. The discrete time repetitive controller design proposed by Tomizuka et al. (1989) falls into this category. As a technical note, the

$\mathcal{Z}$-transform of an N-periodic discrete time signal, $d(k)$, can be written as follows:

$$\mathcal{Z}\{d(k)\} = D(z^{-1}) = \frac{\sum_{i=0}^{N-1} d(i)z^{-i}}{1-z^{-N}} \tag{2.1}$$

Accordingly, if $y(k)$ is defined as the output of the filter $1-z^{-N}$ forced with the periodic signal $d(k)$ as

$$\mathcal{Z}\{y(k)\} = Y(z^{-1}) = (1-z^{-N})\mathcal{Z}\{d(k)\} \tag{2.2}$$

then $y(k)$ will be zero for $k > (N-1)$. The impulse response of a system with transfer function $D(z^{-1})$ will be the discrete time signal $d(k)$. For repetitive control, the IMP states that $1-z^{-N}$ should be part of the characteristic equation of a repetitive controller. The output of an appropriately designed closed loop when forced with a periodic disturbance, $d(k)$ will have the generic form (specific example given in Eq 2.5):

$$\begin{aligned} \mathcal{Z}\{e(k)\} &= E(z^{-1}) \\ &= \frac{B_{cl}(z^{-1})}{A_{cl}(z^{-1})}(1-z^{-N})\mathcal{Z}\{d(k)\} \\ &= \frac{B_{cl}(z^{-1})}{A_{cl}(z^{-1})}\sum_{i=0}^{N-1} d(i)z^{-i} \end{aligned} \tag{2.3}$$

Assuming no roots of $1-z^{-N}$ are shared by $A_{cl}(z^{-1})$, the resulting error is the inverse $\mathcal{Z}$-transform of a quantity whose poles are those of the closed loop system (the roots of $A_{cl}(z^{-1})$). When the closed loop was designed to be asymptotically stable, the error will converge to zero.

2.1.3 Interpretations of Discrete Time Linear Repetitive Control

The internal model principle is a tool for linear controller design. The design of discrete time linear controllers is a broad topic, thus other interpretations are offered here along with any design methods they may immediately suggest. Alone, the IMP does not provide a design method, merely a necessary condition for the controller if it is to be capable of asymptotically eliminating the effect of a periodic disturbance.

By far the most intuitive way to think about discrete time repetitive control is on a cycle to cycle basis (N samples make up one disturbance cycle). Consider the periodic disturbance in this context as N independent constant disturbances. Then consider

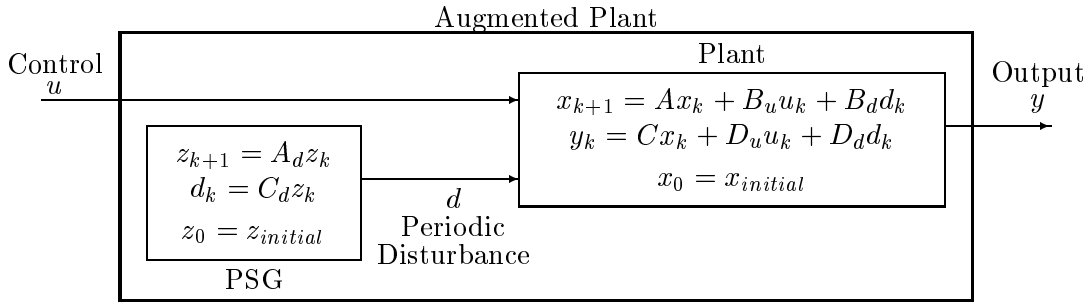

Figure 2.2: Augmenting Plant with Model of Periodic Disturbance

repetitive control as N independent estimators of these N constant disturbances. Recalling that an integrator in a feedback controller can act as an estimator of a constant input disturbance (again the IMP), internal model based repetitive control can be interpreted as N independent integrators. With some effort, this cycle by cycle notion of repetitive control can be naturally connected to a time invariant linear control scheme. Using a cycle by cycle interpretation of repetitive control for design typically suffers from an implementation complexity point of view. The controller is designed as an N-input-N-output system. Unless some sort of sparseness of the controller is specified, such a scheme will be overly complex. The presented dual-rate controller design can be thought of in this way satisfying a sparseness condition.

The repetitive disturbance may also be considered as an observable but uncontrollable part of an augmented plant (see Fig 2.2). This state space approach perspective leads to a full-state observer design for control. The observer will contain a periodic signal generator, so a state feedback control scheme based on the observer states will have a periodic signal generator as a component. In this sense, repetitive controller design is an observer state feedback controller design. This was a useful perspective during the development of the structure described in Chapter 4 where repetitive control is integrated with state feedback control. A potential problem with directly using a full-state observer with full-state feedback to eliminate the effect of the periodic disturbance can be found in designing and implementing the high order observer (there are N states representing the periodic disturbance).

For a naive pole placement design, the realization of the feedback control scheme presents problems in practice. There is the question of where to place the poles in a pole placement scheme. As noted by Tomizuka et al. (1989), if a Diophantine equation based

pole placement technique is used to design the internal model based repetitive controller, the high order of the polynomials involved can lead to numerical sensitivity of the solution, and instability of the control system in implementation. An Nth order canonical form of such a control will often suffer from numerical problems; more numerically favorable realizations will require more calculation during each sample interval. Computationally efficient designs implicitly rather than explicitly assign the closed loop poles.

In the frequency domain, periodic disturbances have components at isolated frequencies. The discrete fourier transform can be used to determine the components at the fundamental and its harmonics (referred to as the repetitive frequencies). External model based repetitive controllers seek to identify the periodic disturbance in terms of these components (Tomizuka, Chew and Yang, 1990). Such a scheme is typically nonlinear, learning phases and magnitudes of different sinusoidal components of the disturbance. A disadvantage of this type of repetitive control action relative to linear IMP-based schemes is typically the computational load of the adaptation algorithms.

In a linear controls context, a frequency domain characterization of repetitive control is as a feedback controller to decrease sensitivity at the frequencies which make up periodic signals. This outlook influenced the choice of performance criterion described later. Design based on frequency response specifications can typically be interpreted in an $\mathcal{H}_\infty$ control context. Using $\mathcal{H}_\infty$ optimal methods for repetitive control does not generally result in controllers which are cheaply implemented.

2.1.4 1989 Discrete Time Repetitive Controller Design

The primary weaknesses of the repetitive controller design methods above is the complexity of the resulting control. By imposing structure on the controller, the complexity of the design can be made tractable. The discrete time repetitive controller design proposed by Tomizuka et al. (1989) has been a popular choice for several reasons and will be referred to as the 1989 repetitive controller. Its design is highly structured and its implementation complexity is low.

Structure

A block diagram representation of the 1989 design is shown in Fig 2.3 with a description of various elements given in Table 2.1. Other than the blocks describing the

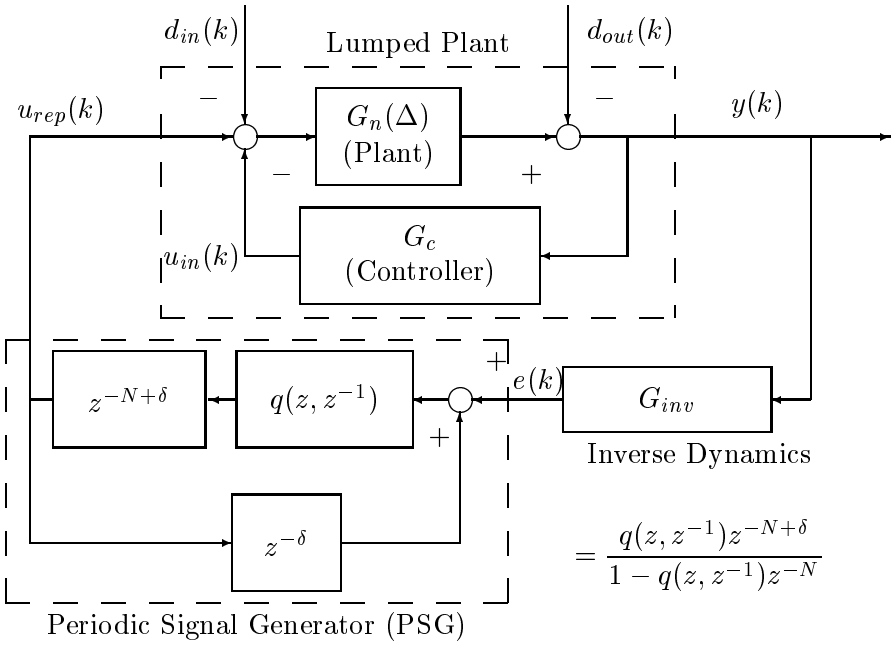

Figure 2.3: Tomizuka *et al* Repetitive Control Structure (1989)

repetitive controller, this structure fits into the generic form shown in Figure 2.1. The structure of the controller is naturally divided into two components: the inverse dynamics and the PSG (or Internal Model). This design allows performance and stability to be interpreted in terms of this natural division. It is convenient to consider the repetitive disturbances as lumped ($d_{in}(k)$), matched with the repetitive control signal ($u_{rep}(k)$).

The suggested choice for the inverse dynamics, G_{inv}, is a gain adjusted zero-phase-error(ZPE) inverse (see Appendix A.1) of the lumped plant dynamics, Γ_y. This leads to clean guarantees of stability and some guarantees about performance. Also note that for $q(z, z^{-1}) = 1$, the PSG has the characteristic equation described in Eq 2.2. As a result, for $q(z, z^{-1}) \neq 1$, this repetitive controller will not be able to asymptotically reject all N-periodic disturbances. Reasons for introducing choices for $q(z, z^{-1})$ other than 1 will be described.

Closed Loop Transfer Functions

The closed loop performance of the repetitive control system can be evaluated in the frequency domain, focusing on the steady state attenuation at the frequencies which

Table 2.1: Elements of Fig 2.3

$d_{in}(k)$	input disturbance
$d_{out}(k)$	output disturbance
$y(k)$	output (regulated)
$u_{rep}(k)$	repetitive control signal
$u_{in}(k)$	internal control signal
N	period of repetitive disturbance (samples)
$q(z, z^{-1})$	zero-phase lowpass filter
$\frac{q(z,z^{-1})z^{-N+\delta}}{1-q(z,z^{-1})z^{-N}}$	PSG transfer function
$e(k)$	estimate of uncancelled periodic disturbance

make up the periodic disturbance. After some algebraic manipulation, the closed loop transfer function (referring to Fig. 2.3) from the repetitive disturbance, $d_{in}(k)$, to output, $y(k)$, is:

$$\Phi_y = \left(\frac{G_n}{1 + G_n G_c}\right) \frac{1 - q(z, z^{-1})z^{-N}}{1 - q(z, z^{-1})z^{-N+\delta}(z^{-\delta} - \Gamma_y G_{inv})} \tag{2.4}$$

The first factor in this expression is nothing more than the transfer function of the nominal feedback control system, Γ_y. The second factor describes the contribution of repetitive control.

The asymptotic elimination of repetitive disturbances follows when Φ_y is asymptotically stable and $q(z, z^{-1})$ is 1. Consider the $\mathcal{Z}$-transform of the output given a periodic disturbance $d_{in}(k)$:

$$\mathcal{Z}\{y(k)\} = \left(\frac{G_n}{1 + G_n G_c}\right) \frac{1 - q(z, z^{-1})z^{-N}}{1 - q(z, z^{-1})z^{-N+\delta}(z^{-\delta} - \Gamma_y G_{inv})} \frac{\sum_{i=0}^{N-1} d_{in}(i)z^{-1}}{1 - z^{-N}} \tag{2.5}$$

With the pole-zero cancellations of $1 - z^{-N}$, only the asymptotically stable poles of Φ_y remain. The output will asymptotically approach zero, and the disturbance will be eliminated.

Stability

The asymptotic stability of Φ_y will be shown after describing the selection of G_{inv} and δ. First consider the purpose of the parameter δ. Repetitive control aims to use deviations from the expected input/output behavior to estimate and cancel the periodic disturbance (assumed to be lumped at $d_{in}(k)$). This means that ideally, $u_{rep}(k)$ will equal

$-d_{in}(k) = -d_{in}(k-N)$. Assuming that the effect of $u_{rep}(k)$ is first seen in the output at time $k+\delta$, measurements at time k describe the uncancelled disturbance at time $k-\delta$. They will not influence the repetitive control signal until almost one cycle later, at time $k+N-\delta$. The parameter δ is thus used to synchronize the previously applied repetitive control signals with estimates of the uncancelled periodic disturbance.

In this light, consider the design proposed by Tomizuka et al. (1989), for the case where Γ_y is a stable non-minimum phase system. Via pole/zero cancellations, G_{inv} and δ can be selected to satisfy $\Gamma_y G_{inv} = z^{-\delta}$. When Γ_y is asymptotically stable, but not minimum phase (i.e. has zeros outside the stability boundary), G_{inv} is selected as the zero-phase-error (ZPE) inverse of Γ_y described in Appendix A.1. This effects pole/zero cancellations where possible. Using the form of the plant transfer function given in Eq (A.2) and the corresponding zero-phase-inverse G_{zpe} defined in Eq (A.5), define

$$\alpha(z, z^{-1}) = \frac{B^+(z^{-1})B^+(z)}{B^+(1)^2} = z^{d+d_p}\Gamma_y G_{zpe} \tag{2.6}$$

This is not a causal filter; it requires advance knowledge of its input to compute its output. The number of advance steps is finite, $d+d_p$, as indicated. The system components Γ_y and G_{zpe} are both causal. A consequence of the zero-phase-error inverse design is that the frequency response of $\alpha(z, z^{-1})$ will take on positive real values. When the unstable zeros of Γ_y all lie in the left half plane (a typical situation in digital control) the coefficients of $\alpha(z, z^{-1})$ will all be positive. A consequence of this fact is that $\alpha(z, z^{-1})$will have lowpass characteristics and a peak gain of 1. This has been assumed in forming the ZPE inverse as described in Appendix A.1. When there are no uncancellable zeros of the system Γ_y ($d_p = 0$), $\alpha(z, z^{-1}) = 1$.

The stability of this repetitive control system is proven using the small gain theorem. The condition used is therefore only a sufficient condition for stability. It is conservative in terms of stability, but not in terms of robust performance (which requires robust stability as a precondition). The block diagram in Fig. 2.3 can be reorganized into the form shown in Fig. 2.4. The system denoted by Γ_y represents the nominal lumped plant in Fig. 2.3. Deviations of the lumped plant from its nominal behavior are captured by Δ, with $\Delta = 0$ corresponding to the nominal case. The allowable values of Δ depend on the uncertainty model.

Applying the small gain theorem, the system will be asymptotically stable if the portion inside the dashed box has infinity norm less than 1 (since $z^{-N+\delta}$ has infinity norm

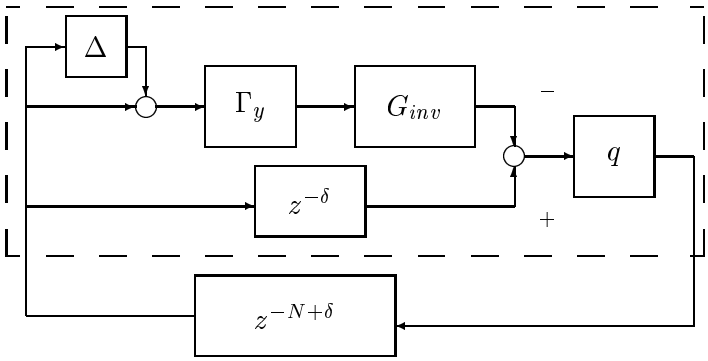

Figure 2.4: Small gain theorem structure

equal to 1):

$$\|(z^{-\delta} - (1+\Delta)\Gamma_y G_{inv}) q(z, z^{-1})\|_\infty < 1 \tag{2.7}$$

If for $\Delta = 0$ the above infinity norm is much smaller than 1, some measure of stability robustness is naturally indicated. The above condition for stability depends upon δ, $q(z, z^{-1})$, and G_{inv}, but not N. The same design will be stable for all disturbance periods longer than δ.

When $d_p = 0$ and $\alpha(z, z^{-1}) = 1$, these relationships simplify Eq 2.7. A sufficient condition for stability of the repetitive control system is then

$$\|\Delta q(z, z^{-1})\|_\infty < 1. \tag{2.8}$$

Robust stability follows if this condition is satisfied for all values of Δ allowed by the uncertainty model.

For the general case, with $\alpha(z, z^{-1})$bounded by 1, the block diagram in Fig. 2.4 is used again. The sufficient condition for asymptotic stability of the closed loop system takes the form:

$$\|(1 - \alpha(z, z^{-1}) - \Delta\alpha(z, z^{-1})) q(z, z^{-1})\|_\infty < 1 \tag{2.9}$$

The zero-phase properties of $\alpha(z, z^{-1})$, along with the assumption that its magnitude is less than one (see Appendix A.1), allow for the following statement:
If

$$\|\Delta q(z, z^{-1})\|_\infty < 1 \tag{2.10}$$

for all possible Δ, the condition given in Eq. (2.9) will be satisfied, and the repetitive control system will be robustly stable.

This condition does not depend upon the plant model. It clearly places the component $q(z, z^{-1})$ (which is ideally equal to 1 for asymptotic rejection of periodic disturbances) in a position to accomodate uncertainty in the closed loop system, Γ_y. Typically, the uncertainty in $\Gamma_y$will be smaller at low frequencies and larger at higher frequencies – feedback control reduces the effect of uncertainty within the bandwidth of the closed loop system. This relaxation of the robust stability condition into the much simpler sufficient condition on $q(z, z^{-1})$ relies on the ZPE design of the inverse dynamics. The realization of $q(z, z^{-1})$ as a zero phase error finite impulse response (FIR) filter with DC gain 1 (in effect a moving average like $\alpha(z, z^{-1})$) was proposed by Chiu et al. (1993). This choice goes far toward keeping $q(z, z^{-1})$ near 1 when its gain is less than 1. This keeps the frequency response of $1 - q(z, z^{-1})z^{-N}$ near zero at the repetitive frequencies.

More on Performance

The ideal situation (perfect cancellation of all repetitive disturbances) may need to be compromised to meet the stability robustness requirement described above. Another typical reason to compromise perfect cancellation of all repetitive disturbances is that the important components of the periodic disturbances are usually at lower harmonics. The effect of higher harmonic components are usually dominated by other process noises (or uncertainty). Since the disturbance sources are indistinguishable at the error, it is then appropriate to react to high frequency errors as being caused by non-periodic disturbances. The term in the closed loop which effects the cancellation of periodic disturbances $(1 - q(z, z^{-1})z^{-N})$ also effects amplification of disturbances $d(k) = Ae^{j\omega k}$ when $e^{-j\omega N}$ lies in the left half plane.

The transient response characteristics of the control system can be described in terms of the closed loop poles. Recall the form of the closed loop transfer function from input disturbance to output given in Eq 2.4. Noting that the lumped plant, Γ_y, was stable by design, assume

$$\|(z^{-\delta} - \Gamma_y G_{inv})q(z, z^{-1})\|_\infty = \gamma < 1. \tag{2.11}$$

The poles associated with the second factor of Φ_y will then have magnitudes less than $\gamma^{(1/N)}$. When γ is near zero, the system will have nearly deadbeat characteristics. Larger values of γ

roughly correspond to longer settling times in response to a new repetitive disturbance. This is not necessarily a bad property for the closed loop system to have – it does not preclude perfect cancellation of the repetitive disturbance in the steady-state, but corresponds to a more conservative reaction to perceived changes in the periodic disturbance. The effect of non-periodic disturbances on the repetitive control signal may be diminished.

To force longer settling times on the system, G_{inv} can be selected as follows (with γ roughly corresponding to the γ above):

$$G_{inv} = z^{-\delta}(1-\gamma)G_{zpe} \tag{2.12}$$

For all values of $\gamma \in [0,1]$, this choice of G_{inv} results in a stable repetitive control system when the above conditions on $q(z,z^{-1})$ in Eq 2.10 are satisfied (Tomizuka et al., 1989).

Other choices of inverse dynamics, perhaps lower order approximations of the zero-phase-error inverse may also be made. For these values of G_{inv}, stability of the closed loop may be proven with the condition in Eq 2.7. The characterization of performance and robustness in terms of $q(z,z^{-1})$ will not be as simple with other choices for the inverse dynamics. To reduce implementation costs, it may be pragmatic to make this compromise.

$q(z,z^{-1})$ and the PSG

"Periodic Signal Generator" is a misnomer when $q(z,z^{-1}) \neq 1$. It is very nearly correct when $q(z,z^{-1})$ is near 1, so the term is still used in this paper. The effect of various $q(z,z^{-1})$ on the PSG and hence the on the repetitive controller are described. Asymptotic rejection of periodic disturbances is sacrificed, but significant rejection is still possible if the PSG generates signals which die out very slowly.

The internal model portion of the repetitive controller is composed partly of a delay chain (represented in Fig. 2.3 by the blocks $z^{-N+\delta}$ and $z^{-\delta}$). The positive feedback around this delay chain allows these memories to generate a periodic control signal. When $q(z,z^{-1}) = 1$ and the estimate of the uncancelled portion of the periodic disturbance is zero ($e(k) = 0$) for all k, the repetitive control signal will repeat with period N: $u_{rep}(k) = u_{rep}(k-N)$. Ideally, this periodic control will cancel the periodic disturbance.

The delay chain can be efficiently implemented as a circular buffer with moving indices as described in Fig 2.5 for the case when $q(z,z^{-1}) = 1$. The period of the disturbance (N samples) determines the size of the buffer.

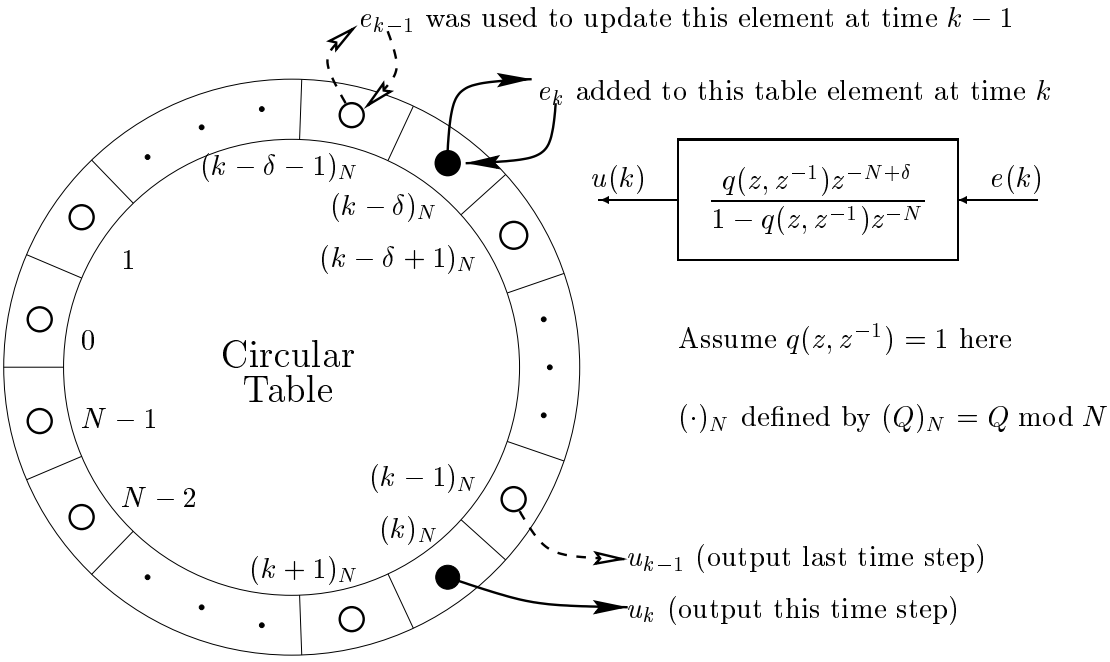

Figure 2.5: Realization of PSG in implementation

The filter within the PSG shown in Fig. 2.3 ($q(z, z^{-1})$), is a zero-phase FIR low-pass filter with unity DC gain. This strips higher frequency components from the generated periodic signal. With $q(z, z^{-1}) = 1$ the poles of the controller associated with the periodic signal generator are all on the stability boundary (the unit circle). The higher frequency poles of the controller associated with the periodic signal generator are moved away from the unit circle. Incorporation of this filtering action (provided it has low order) does not add much complexity to the circular buffer realization depicted in Fig 2.5. The effect of various choices of $q(z, z^{-1})$ on the poles of the PSG and the signals generated by the PSG are shown in Fig 2.6. For the time domain simulations, a desired periodic signal was generated randomly. The initial conditions of each of the PSGs was then assigned to generate that output over the first 30 samples of simulation.

2.2 Magnetic Disk Drives

Computer disk drives are sophisticated electromechanical systems which have evolved tremendously since their introduction. Research in the field is typically directed toward increasing storage capacity and data transfer rates while lowering the cost to the consumer. The relative importance of each of these objectives is constantly in flux; the constraints and demands on each subsystem vary with these changes.

In this section, computer disk drives are discussed from the point of view of the controls engineer, who is predominantly concerned with the design of the positioning system for the read/write head. The characteristics of the physical plant to be controlled, the servo problem and its complexity, recent research activity in this area, and the place of repetitive control in this picture are described in succession.

2.2.1 Physical Plant

A partial schematic of a computer disk drive is shown in Fig 2.7. Only those characteristics related to the positioning of the magnetic read/write head over the appropriate position on the disk are shown. The read/write head is mounted on the end of a pivot arm which can be rotated through the action of a voice coil (magnetic induction) motor. The connection of the read/write head to the on-board electronics is accomplished with a flexible printed circuit (FPC).

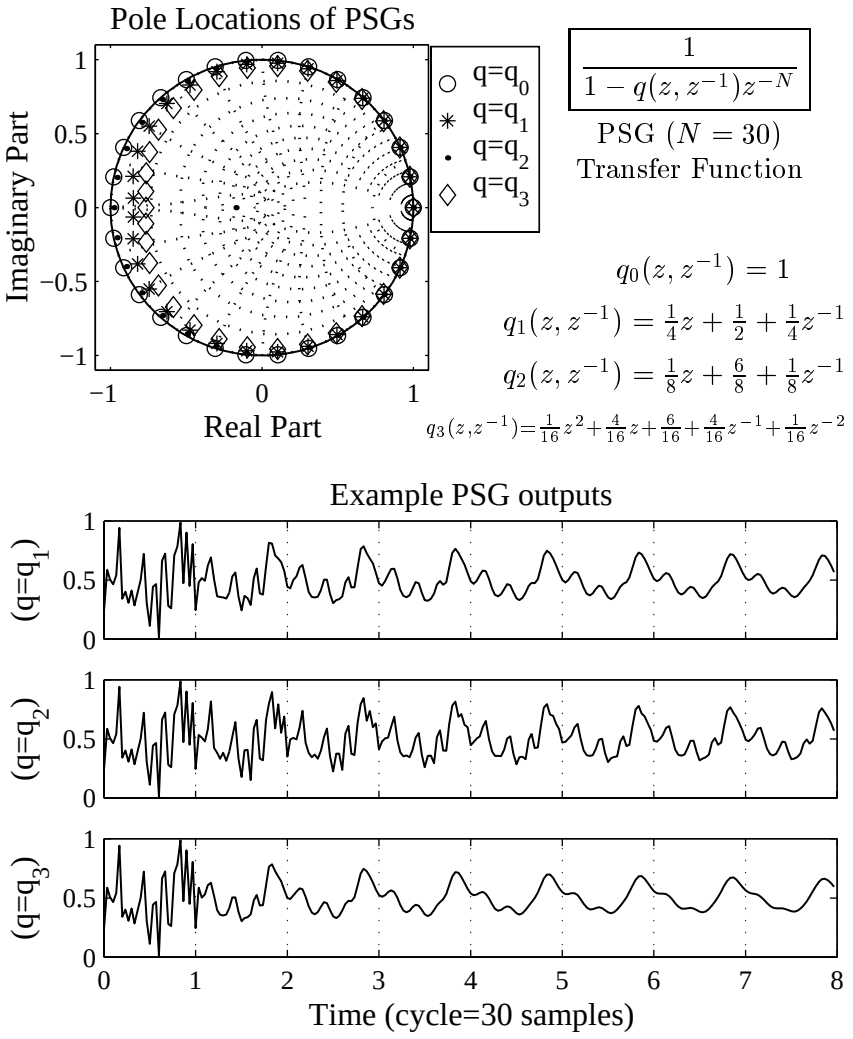

Figure 2.6: Various modified periodic signal generators ($N = 30$)

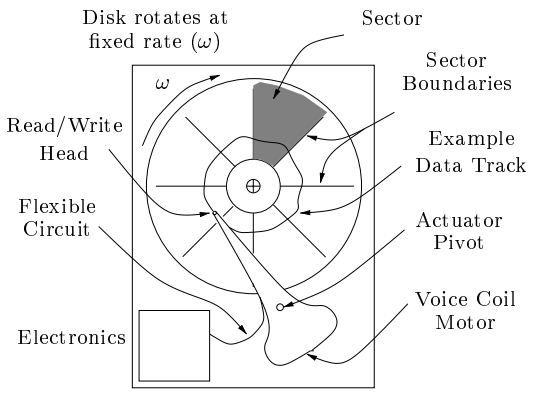

Figure 2.7: Schematic of a computer disk drive

Data is organized on the disk as sequences of bits along concentric circular data tracks. As the disk spins at a fixed rate, the magnetic head can read or write bits of information along a data track, provided the head can be kept directly above the desired track.

The relative radial position of the head over a particular data track is detected by means of a *sector servo* scheme. Radial positioning information is distributed along the circular data tracks at equally spaced intervals; the resulting equally divided areas of the disk are called sectors (see Fig 2.7), with the radial positioning information written at the sector boundaries. In the figure only eight sectors are shown for purposes of illustration (50–100 is typical in practice). The disk rotates at a fixed angular velocity, so the head passes over sector boundaries at fixed time intervals. This sampled measurement is typically the only information available for control, and it measures only the relative position of the head, referred to as the Position Error Signal (PES). The controller is implemented digitally in discrete time. Computation, A/D, and D/A delays are incorporated into the discrete time system model.

2.2.2 Cost Concerns Relating to Servo Control Objectives

This section is an overview of concerns relating to constraints on servo control, setting the servo problem in the context of the entire disk drive system.

Implementation cost concerns are significant for a mass produced item such as computer disk drives. The servosystem controller uses microcontroller hardware resources,

typically taking up six or seven percent of total clock cycles. The microcontroller in many cases operates with fixed point precision, and does not have a built-in multiplier. Multiplication is written in assembly as bit-shifting and adding. A servo controller design will ideally utilize the cheapest possible hardware at the limit of its capability. During development, emphasizing computational savings on the order of clock cycles and memory savings on the order of bytes can lead to overall hardware cost savings.

The density with which information can be stored on the disk surface (bit/cm^2) can be conveniently expressed as the product of the linear storage density along a data track ($bit/(track\,cm)$) and the radial data track density ($track/cm$). The computer disk drive industry seeks to minimize the cost per megabyte of storage, and therfore to increase storage densities. Improvements in linear density are nearly independent of the read/write head positioning system, and have recently outpaced improvements in radial density (Tomizuka, 1997). With linear densities near their practical limit much attention is being directed at radial positioning improvements with the aim of increasing radial density (Ehrlich, 1999).

A compromise between improving the areal storage density and limiting the cost per bit of storage must be made. For this reason, hardware and software concerns play a large role in the design of read/write head positioning servosystems. The interplay of the many subsystems comprising the disk drive will continually affect allocation of resources to the head positioning servosystem.

The Servo Problem

The control of the read/write head during normal operation of a disk drive is typically separated into two modes:

1. **Track Following**: keeping the read/write head on a particular data track
2. **Track Seeking**: moving the head from one track to another

During track following, the input/output behavior from the voltage control of the voice coil motor to the head position is appropriately modeled by a double integrator. This linear model is no longer appropriate during track seeking, during which saturated control signals are used to achieve the fastest possible transition between data tracks. A typical design separately addresses each of these modes, and switches between controllers during operation of the disk drive. The design of track seeking controllers typically involves the generation

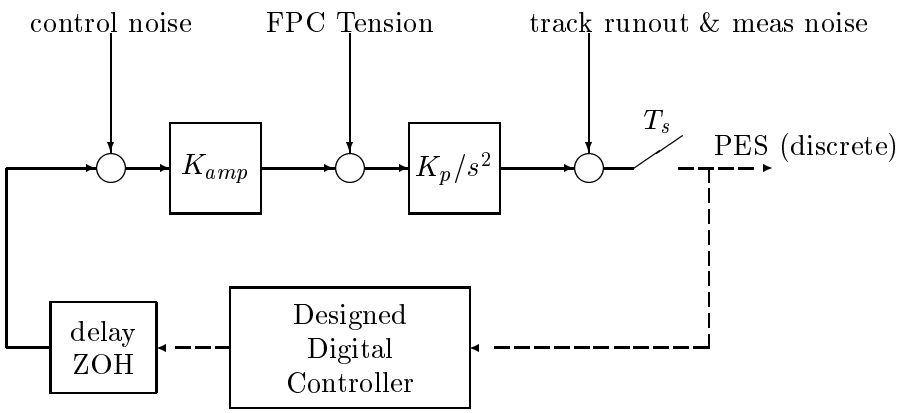

Figure 2.8: Disk Drive Track Following Servo

of appropriate reference signals, and may also involve the design of a different feedback controller. The track following control, however, will be the active one during the reading or writing of data on the disk surface. The accuracy required for these operations relates directly to storage density objectives as described above.

A schematic of the track following control loop with a digital controller is shown in Fig 2.8. The double integrator characteristics from the control signal to head position make stabilization of the position control system for the read/write head possible with a proportional plus derivative (PD) controller (implemented in discrete time).

Additional control beyond PD for stabilization is required because the design concern is not merely stability, but also performance. To prevent corruption of data on adjacent tracks when writing information on the disk, a typical constraint is that the head be within 10% of a track width from its desired position. For currently achieved tracks per inch (TPI), this is roughly between $0.1\mu m$ and $0.4\mu m$, corresponding roughly to 20,000 and 5,000 TPI (Tomizuka, 1997).

2.2.3 Obstacles to Meeting Positioning Requirements

The dynamics of the system are nominally uncomplicated. This does not mean that the servo control problem is easy. There are barriers to the achievement of satisfactory tracking accuracy. Several are itemized below, followed by some discussion of each along with ways they are being addressed in current research activity.

- Limited information from the sampled measurement of position error

- Controller bandwidth limitations due to resonant modes in the actuator arm
- Disturbances to the system (other than periodic ones)

Other variables in the process (such as mechanical wear, environmental conditions, and production tolerances) have been dealt with in the servo controller through specification of stability margins.

Limited Measurement Information

The position error measurements are sampled at a rate equal to the product of the number of sectors and the rotation rate of the disk. Slower sample rates limit the control authority near the associated Nyquist frequency. Two obvious ways to increase the measurement sample rate are increasing the rotation rate of the disk and increasing the number of sectors. There are problems with both. The rotation rate of the disk is typically fixed by the linear data density specification and radius of the disk. Increasing the number of sectors increases the number of sector boundaries. The position information on the sector boundaries takes up disk surface area that would otherwise be used to store user data.

Likewise, decreasing the number of sectors to increase storage capacity will impose limitations on the feedback positioning control (due to a slower measurement sampling rate). Typically, the number of sectors is set such that the radial track density specification is barely attained. This means that if the measurement sample rate is not making servo controller design a challenge, the number of sectors should be reduced until it does!

To address the (inherent) measurement limitations of this sector servo scheme, some researchers have proposed the addition of accelerometers to the system (White and Tomizuka, 1996). With accelerometers mounted on the body of the disk drive, external mechanical disturbances can be detected. The effect on head position can be deduced, allowing improvements of tracking performance. Accelerometers have also been mounted on the actuator arm in efforts to compensate for the effects of friction at the pivot. Resonances in the actuator arm can also be detected. The sampling rates of these schemes are not constrained by concerns about storage capacity, but their use is constrained by the cost of adding sensors to the system.

Actuator Arm Resonance

When the actuator arm has a smaller moment of inertia, a given torque accelerates the head faster. For track seeking, this means the head can be moved more quickly from one track to another. This conflicts with a desire to keep the mechanical resonant modes of the actuator arm above the desired bandwidth of the track following controller. A stiffer arm will be heavier, requiring a larger motor to accelerate it quickly. If the actuator arm resonance is far above the bandwidth of the track following controller, the actuator arm will be redesigned to allow for faster seeking. The resonance will always be a concern for track following.

This problem has been addressed through the use of smaller and smaller disks. This allows the length of the actuator arm to be decreased, increasing the frequencies of mechanical resonances. The increases in storage densities on the disk surface have been so great that though disks have become smaller, capacities have increased.

Another way to address this problem has recently garnered a great deal of attention. It involves the design of dual-stage actuators (Hernandez, Park, Horowitz and Packard, 1999; Shroeck and Messner, 1999; Evans, 1999). A smaller, higher bandwidth actuator with small range of motion is placed on the end of a traditional pivot actuator. This secondary actuator is not constrained by the resonant modes of the actuator arm, and thus the bandwidth of the track following controller can be increased, hopefully allowing for better positioning accuracy.

Disturbances

A variety of disturbances affect the servosystem. One is the result of the combined effects of windage (aerodynamic head/disk interaction) and the flexible printed circuit tension (Fig 2.7). It can be represented by a constant torque disturbance to the actuator during track following. To eliminate steady-state biases in tracking which would otherwise occur, integral action can be added to the feedback controller.

The position error signal is influenced by a variety of factors. The disk has resonant modes which may introduce radial tracking errors. The position error signal measurement is not free of noise. There is process variability in torquing the actuator arm using the digital control signal. These disturbances are indicated in Fig 2.8. Modeling these disturbances has been an active area of theoretical and experimental research (Yi, 2000). These

efforts are motivated by a desire to separate the effects of different sources of errors. These disturbances, along with the previously mentioned constraints guide the design of the servo controller.

2.2.4 Periodic Disturbance Sources which Motivate Repetitive Control

Repetitive control is useful for disk drive servosystem design when periodic disturbances have a significant effect on tracking errors. The predominant source of periodic tracking errors is the shape of the data track. Because of the structure of the control system, with only relative position error available for control, one could consider the radial position of the desired data track as the reference signal to a regulator system. However, since this absolute desired position is unknown and unmeasureable, two-degree-of freedom controllers are not an option. It is better considered as a disturbance. It is indicated as such in Fig 2.8.

Ideally, the data tracks are concentric circles centered at the axis of rotation of the disk, but in reality they are not be perfect circles (as exaggerated in Fig 2.7), nor will they be perfectly centered. Deviations from the ideal occur during the manufacture of the disk, and are referred to as repetitive runout because they repeat as the disk rotates. For removable media (such as floppy) disk drives, centering error upon insertion of the disk will cause most of the repetitive runout. In the frequency domain, the repeatable runout will then be concentrated at the (fixed) frequency of disk rotation. The same centering errors are possible in non-removable media drives due to slippage in the mounting assembly of the disk. The remainder of the repetitive runout can be written in terms of harmonics of this fundamental frequency (discrete fourier transform). These frequencies will be referred to as repetitive frequencies.

If the disk is made of an anisotropic material (e.g. typical flexible media), contraction or expansion (due to temperature or humidity changes) of the disk will make circular tracks elliptic. The effect of this change on the repeatable runout will be a significant component of runout at the first harmonic frequency (double the fundamental).

Repetitive runout components around the sixth harmonic and higher can appear due to mechanical faults in the spindle assembly. The higher harmonics in the repetitive runout are typically not large enough to significantly affect the tracking performance, although interaction with the aforementioned resonant modes in the system may amplify their effects if not carefully considered.

Integral action increases the gain of the feedback loop at lower frequencies, and thus serves to reduce the effect of the lower frequency components of the repetitive runout. If this reduction is not sufficient to guarantee the desired tracking performance, the elimination of the periodic disturbances can be accomplished with repetitive control.

2.3 Cost Effective Repetitive Control

The engineer's perennial task is to get the most perfomance at the smallest cost. Cost effectiveness is concerned with the tradeoffs between these two quantities.

For repetitive control applied to computer disk drives, there is strong pressure to keep implementation costs low, even to the point of accepting a suboptimal level of performance. It is in this type of cost driven scenario that the proposed designs will be of interest. In other applications, cost may not be such a significant concern though typically some compromises must be made. Each application brings a host of other concerns that determine what designs are cost effective. A framework within which a wide variety of repetitive controllers can be designed and compared with relative ease will be a useful tool for the engineer seeking a cost effective solution. Information about what can be achieved at a given cost may justify changes to the system at a higher level. In any practical setting, the design of the repetitive control system must be viewed as both influencing and being influenced by outside factors.

2.3.1 Starting Point for Cost Effective Designs

The developments of stability and performance for the 1989 structure used discrete time $\mathcal{H}_\infty$ norms. One might be tempted to apply optimal loop-shaping methods ($\mathcal{H}_\infty$ synthesis) to design the filters q and G_{inv}. Unless the complexity of the controller is considered during such a design, this technique will not typically produce computationally sleek controllers. Several methods for eliminating the effect of repetitive disturbances other than the 1989 repetitive controller are described by Kempf et al. (1993). Their comparative work identifies the 1989 repetitive controller as a good starting point for computationally efficient designs. The dual-rate and cascaded designs presented in Chapters 3 and 4 aim to reduce costs relative to this design.

To work toward cost effectiveness, one could design succesively higher order controllers, starting with PD control, comparing the incremental cost with the incremental

performance. The approach taken here removes complexity from a repetitive controller design that initially achieves a desirable performance. The emphasis is on what performance is lost, rather than what is gained.

2.3.2 Describing the Cost of a Design

Implementation (as opposed to development) costs, are the primary focus of this discussion of cost effectiveness. They are evaluated in terms of resources used by the repetitive controller. Savings in resource usage may enable the use of cheaper hardware, or the use of that resource for another purpose. Thus an economic measure of cost savings is problem specific and may be discontinuous. In a general setting, however, the resource usage associated with implementation of a digital control algorithm can be quantified in terms of memory and computation.

The actual computational usage depends upon the capabilities of the hardware and the complexity of the algorithm. Since this study aims to be general, the computational complexity will be considered in abstract terms. Algorithms are considered in terms of the number of certain types of basic processor level operations they must perform (addition, multiplication, comparison, data movement). This is further abstracted. The implementation of a second order filter is naturally more complex than the implementation of a first order filter. The realizations of digital filters affect their actual computational usage. The assembly language details of the implementation are problem specific, and are not discussed here, but were kept in mind while developing the proposed designs. For example, multiplication and division by powers of 2 is used where possible. In software, this is accomplished via bit shifting rather than actual multiplication, potentially creating large computational savings.

Another potentially significant source of resource usage, and hence implementation costs, is that of memory. Any repetitive controller must store enough information to generate a control signal to cancel the periodic disturbance. Schemes such as compression may be used to minimize the storage required, but the computational effort required to extract the appropriate control signal must also be considered. The 1989 structure for repetitive controllers (Fig 2.3) is a linear controller which stores this information in a number of states roughly proportional to the period of the disturbance. The implementation of the PSG component of this structure (as shown in Fig 2.5) is such that the appropriate repetitive control

signals are directly stored, making their retrieval extremely efficient. Efforts to retain this efficiency were made in the proposed designs.

2.3.3 Describing Performance

Repetitive control is used to eliminate the effects of periodic disturbances with known periods on an existing control system. The following are additional important points beyond this specification:

1. Nominal system performance w/o periodic disturbances
2. Frequency content and variability of the periodic disturbance
3. Other disturbances to the system
4. Uncertainties in plant dynamics

Performance for linear servosystems is characterized as making the error small, a term which bears some consideration. The peak magnitude may be important, as well as the variability. Stating a desired closed loop sensitivity (i.e. loop shaping) is one way to define what is small. This implicitly uses the expected frequency content of disturbances, including the periodic disturbance. This measure of performance is a specification of the steady-state behavior. The transient behavior of the repetitive control system is related to this steady-state behavior.

To focus on the design of the repetitive controller rather than the total control scheme, the design objective was defined in terms of the nominal system. In other words, the system to which repetitive control is being added is assumed to achieve desirable performance in the absence of periodic disturbances. This assumption suggests a description of the repetitive control objective in terms of a difference from the nominal system. Thus, a loop-shaping specification defined in terms of the nominal system and a parameterized weighting function is proposed.

The following two tradeoffs are proposed to capture the essence of most repetitive control problems.

1. There is a tradeoff between adaptability to changes in the periodic disturbance and steady-state rejection of non-periodic disturbances. The effects of periodic and non-periodic disturbances cannot be distinguished at the output. The repetitive controller

has no hope of quickly learning new periodic disturbances without also falsely assuming that non-periodic disturbances will repeat. Thus, a compromise between fast learning of the periodic disturbance and sensitivity to non-periodic disturbances must be made. This is referred to as the learning rate, and will be specified by the parameter ξ.

2. There is a tradeoff between robustness to uncertainty and steady-state rejection of periodic disturbances. When less is known about the plant dynamics in some frequency range, it makes sense to use less aggressive control action in that frequency range. For repetitive control, this corresponds to accepting some steady-state tracking errors due to periodic disturbances in order to insure stability. This was decribed in Section 2.1 for the 1989 repetitive controller design, in terms of the filter $q(z, z^{-1})$, and appears in the performance measure as $q_w(z, z^{-1})$. Additionally, if the periodic disturbance is concentrated at lower frequencies, reducing efforts to cancel higher frequency periodic disturbances can allow faster learning of the periodic disturbance without amplifying the effects of high frequency non-periodic disturbances.

2.3.4 Frequency Domain Performance Specification

Independent of the repetitive controller design, but dependent on the parameters $q_w(z, z^{-1})$ and ξ, the performance of the closed loop system can quantified with the following performance index (smaller is better):

$$\mathrm{J}_{\mathrm{rep}}(\Phi_y) = \max_{|z|=1} \left| \left(\Gamma_y - \frac{1 - \xi q_w z^{-N}}{1 - q_w z^{-N}} \Phi_y \right) \frac{1}{\Gamma_y} \right|, \tag{2.13}$$

where Γ_y and Φ_y are the disturbance to output transfer functions before and after the application of repetitive control. The independence of this measure of performance from the controller design allows for well defined comparisons between designs.

2.3.5 Time and Frequency Domain Effects of $q_w(z, z^{-1})$ and ξ

The two parameters $q_w(z, z^{-1})$and ξ are used to capture the performance tradeoffs listed earlier in frequency domain terms. The proposed performance criterion specifies an ideal frequency response of the repetitive control system in terms of the original closed loop system, Γ_y. This can be thought of in terms of a weighting function for the original closed

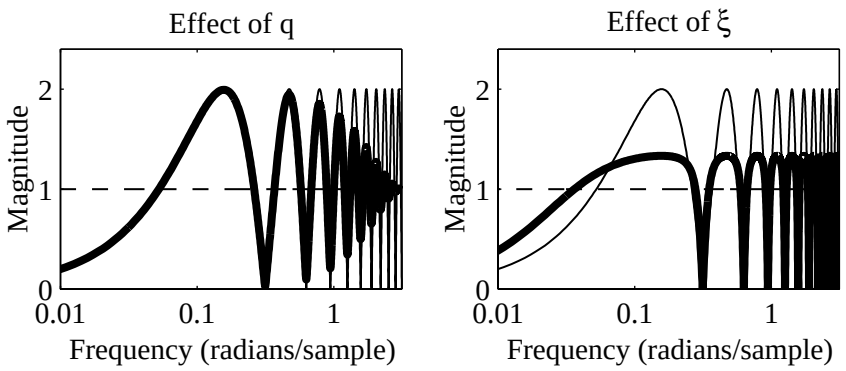

Figure 2.9: Proposed ideal closed loop frequency response.

loop, Γ_y, describing the ideal closed loop frequency response as:

$$\Phi_y^{\text{ideal}} = \frac{1 - q_w(z, z^{-1})z^{-N}}{1 - \xi q_w(z, z^{-1})z^{-N}}\Gamma_y \tag{2.14}$$

The effects of $q_w(z, z^{-1})$ and ξ are illustrated in Fig 2.9, showing an example relation between the original and ideal closed loop frequency responses for $N = 20$. In the figure, the nominal design $\Gamma_y = 1$ is indicated by the dashed line. The thin solid line corresponds to the ideal closed loop when $q_w(z, z^{-1}) = 1$ and $\xi = 0$. The thick line corresponds to the ideal closed loop when $q_w(z, z^{-1}) = 0.25z + 0.5 + 0.25z^{-1}$ (left), or $\xi = 0.5$ (right) instead. Note that the magnitude scale is absolute rather than logarithmic.

The comparison of the ideal closed loops in the time domain is shown in Figure 2.10. Ideal closed loop systems with zero initial conditions were forced with the same randomly generated periodic disturbance (with period 20 samples). The input/output dynamics correspond to the frequency responses shown in Figure 2.9. The measurements of time are given in terms of cycles, where 1 cycle is 20 samples of the system, corresponding to one period of the disturbance. Here, the thick lines show the time response when $q_w(z, z^{-1}) = 1$ and $\xi = 0$. The thin lines correspond to either $q_w(z, z^{-1}) = 0.25z + 0.5 + 0.25z^{-1}$ (left), or $\xi = 0.5$ (right) as before. The response of the nominal system $\Gamma_y = 1$ is not shown, but would show the output over the first cycle in Figure 2.10 repeated for subsequent cycles. Note that high frequency components of the periodic disturbance remain in the output for the non-unity choice of $q_w(z, z^{-1})$, and that the effect of the periodic disturbance decreases exponentially over time with the nonzero choice of ξ.

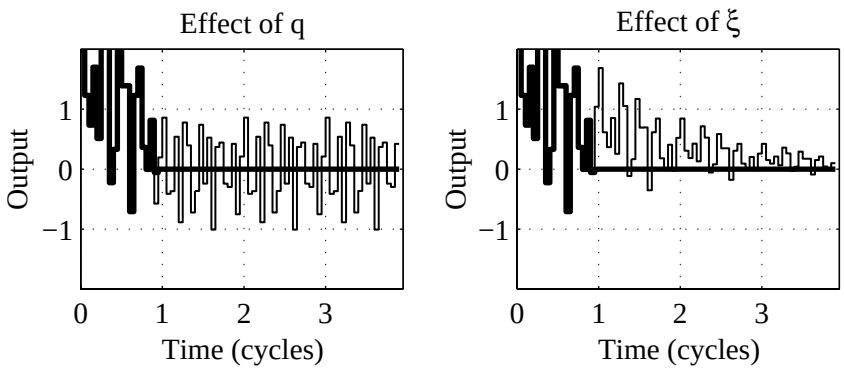

Figure 2.10: Example Proposed ideal closed loop time responses.

2.3.6 Rationale for Performance Criterion

The appearance of $q_w(z, z^{-1})$ in the weighting is symptomatic of the backward approach used in its development; this filter may be the same as the $q(z, z^{-1})$ which is used in the PSG component of the 1989 repetitive controller structure. The filter $q_w(z, z^{-1})$ plays a practical role in the ideal frequency response. For $q_w(z, z^{-1}) = 1$, the quantity $1 - q_w(z, z^{-1})z^{-N}$ is zero at each of the repetitive frequencies, so the ideal closed loop frequency response is *zero* at those frequencies, i.e. perfect cancellation of all repetitive disturbances is achieved. Uncertainty in the plant and noises at higher frequencies are typical, preventing the achievement of this feat in practice, so the requirements at higher frequencies are relaxed with a lowpass filter (DC gain one) choice of $q_w(z, z^{-1})$.

The parameter ξ is intended to be selected from the interval between -1 and 1, and though it appears in a frequency domain expression, it is most easily understood as the desired time constant of repetitive control on a cycle to cycle basis (the learning rate).[1] Choosing $\xi = 0$ corresponds to deadbeat rejection of a repetitive disturbance (the repetitive disturbance is completely rejected after one cycle). Other values between -1 and 1 correspond to exponentially approaching complete rejection (refer again to Fig 2.10). For example, $\xi = 0.3$ corresponds to cancelling seventy percent of the repetitive disturbance after one cycle, ninety-one percent after two cycles, 97.3% after three cycles, and so on. Choosing $\xi = 1$ corresponds to no learning, and no repetitive control! Decreasing the rate

[1]The introduction of ξ to the criterion wqas inspired by the repetitive controller gain K_r found in (Tomizuka et al., 1989). The 1989 structure with G_{inv} equal to the zero-phase error inverse times K_r was shown to be stable for $0 < K_r < 2$. The relation $K_r = 1 - \xi$ transforms that range to $-1 < \xi < 1$

of learning (setting ξ near 1) averages out the effects of non-periodic disturbances at the expense of slowing the reaction to changes in the periodic disturbance. The effect on steady-state amplification of non-periodic disturbances relative to the original system associated with $\xi = 0.5$ relative to $\xi = 0$ can be seen in Figure 2.9.

Specification of the performance in terms of these tradeoffs was used primarily in the development of the design proposed in Chapter 4. The design and specification were jointly structured such that changes in the specification lead to changes in the design. This performance criterion might be made significantly more complex by explicitly considering the frequency content of the repetitive control signal and the other disturbances to the system. Such an approach is a possibility for continued research, but will only be as good as the assumptions about the frequency content of the disturbances. The general nature of the tradeoffs is captured by the proposed criterion.

2.3.7 Relation of Performance Measure to 1989 Repetitive Controller Design

This performance criterion was influenced by the 1989 design. When the closed loop system from the 1989 design (Fig 2.3) is substituted into the performance index with $q(z, z^{-1}) = q_w(z, z^{-1})$, It can be simplified into the following form:

$$\mathrm{J}_{\mathrm{rep}}(\Phi_y) = \max_{|z|=1} \left| \frac{q z^{-N+\delta} \left((1-\xi) z^{-\delta} - \frac{G_n}{1+G_n G_c} G_{inv} \right)}{1 - q z^{-N+\delta} (z^{-\delta} - \frac{G_n}{1+G_n G_c} G_{inv})} \right| . \tag{2.15}$$

The inverse dynamics, G_{inv}, was selected as $(1-\xi)$ times the zero-phase inverse of the closed loop transfer function, $\frac{G_n}{1+G_n G_c}$. With δ equal to the sum of the number of pure plant delays and the number of unstable zeros in the closed loop plant (see Appendix A.1), the quantity in the numerator of $\mathrm{J}_{\mathrm{rep}}(\Phi_y)$ will be small. In fact, when the nominal plant is stable and minimum phase, the performance will be perfect according to this criterion, $\mathrm{J}_{\mathrm{rep}}(\Phi_y) = 0$.

Chapter 3

Dual-rate Repetitive Controller Design

In this chapter, a dual-rate digital repetitive controller design is described. The motivation for this dual-rate design is to reduce the memory used for discrete time repetitive control. For a repetitive controller to have the capability to eliminate all possible N-periodic disturbances, it must have the capability to generate all possible N-periodic control signals (Sec 2.1.2). This generically requires N free parameters, captured in the 1989 design by the states of the PSG.

One way to reduce the memory used by the 1989 design would be to reduce the amount of memory used to store each state. Another method would be to reduce the total number of storage elements. Both of these measures place a limit on the types of periodic signals which might be perfectly cancelled.

In the former case, decreased numerical resolution limits the smoothness of the control signal and/or introduces rounding errors. Rounding errors can be considered as additional disturbances to the closed loop system resulting in steady-state tracking errors. In practice, there is a size of storage elements determined by the hardware used. Software overhead would be required to implementing decreased numerical resolution, even with clever programming. For this reason, the number of storage elements is reduced.

Fewer storage elements are able to describe a subset of all possible periodic control signals. Two parameterizations for discrete time N-periodic signals are in the time and frequency domain. In the time domain, N-periodic signals are described by N values over

one period. In the frequency domain, N-periodic signals are described by the N coefficients of their discrete fourier transform. A reduction in memory in either case corresponds to parameterizing these N values in terms of $Q < N$ parameters. The repetitive disturbances should be predominantly described by Q parameters. A common case is that the fundamental and first several harmonic frequencies are of the most concern. Other repetitive controller designs are able to individually address single components of the disturbance by means of a comb filter (real-time discrete fast fourier transform, or convolution). This is easily done, but not without computation.

The PSG was implemented at a slower sample rate than the measurement rate. Fewer slower samples make up a cycle of the periodic disturbance, so the number of states in the controller is reduced. One state in the new PSG will define several of the repetitive control signals which must be applied. The resulting control system is a dual-rate system, and must be analyzed as such.

A dual-rate repetitive control scheme has been independently developed by James and Sadegh (1999) also using a periodic signal generator implemented at a slower rate. Their design and analysis of the controller does not use lifted system representations and uses a different treatment of stability.

After descriptions of analysis and design, some simulation and experimental results for the application of such a design to a magnetic disk drive system are described.

3.1 Development

In this section, assumptions on the systems and the structure of the dual-rate control system are described first. Selections of the controller components are given and stability is shown. This is followed by a discussion of performance.

Lifting of SISO discrete time systems is extensively used in this development. It is described in Appendix A.2 along with related discussions of polyphase and modulated representations of discrete time signals (and hence systems). Induced norms on these systems figure prominently in the development.

3.1.1 Structure

A discrete time single-input-single-output (SISO) system is subject to periodic disturbances. Refer to the diagram in Fig 3.1. Stabilizing feedback control has been applied

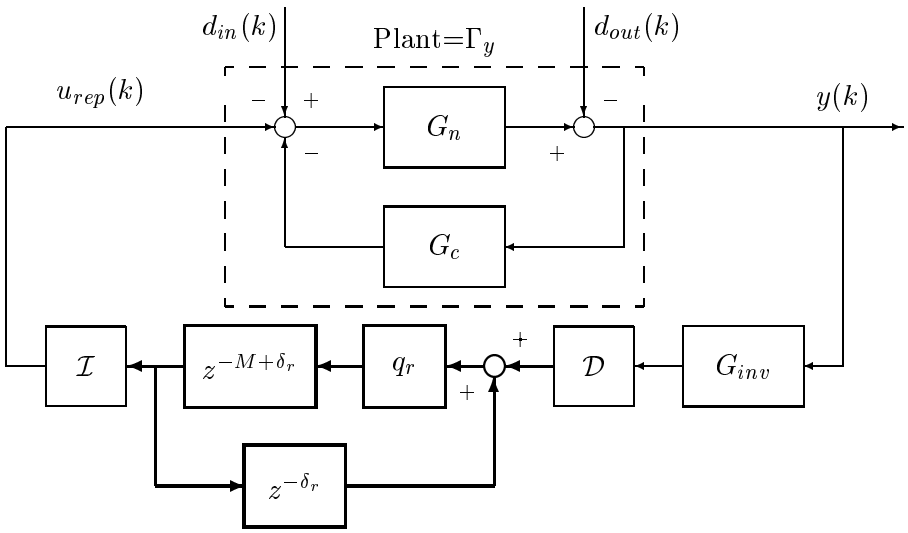

Figure 3.1: Dual-Rate Repetitive Control

to this system. The combination of these two components is considered as a lumped plant, Γ_y. The transfer function representation of the input output dynamics of the plant is used for design, and assumed to to have all poles insude the unit disk. Zeros may be outside the unit disk only if they lie in the left half plane. Left half plane zeros such as these are common in digital control systems, they often result when sampling continuous systems (Astrom, Hagander and Sternby, 1984).

The period of the repetitive disturbance is an integer N measurement samples, divisible by a reduction ratio, r ($M = N/r$). Relaxation of this condition on N and r will be briefly discussed in the closing comments of this section. For now, no further assumptions on this periodic disturbance are made.

Much of the structure of the 1989 design is retained for this dual-rate structure. The design may be separated into two components, the PSG and inverse dynamics. The difference is the design of the PSG. The inverse dynamics is designed based on the nominal closed loop dynamics from $u_{rep}(k)$ to $y(k)$, as in the 1989 design.

The PSG from the 1989 design is replaced with a PSG of the same form, implemented at a sampling rate r times slower (indicated by the bold portion of Fig 3.1), using only $M = N/r$ delays. The new system has signals at two sampling rates (dual-rate system). Of these rates, the measurement rate (that of $y(k)$) will be referred to as the fast

rate, and the sample rate of the PSG will be referred to as the slow rate (r times slower than the fast rate).

For measuring frequencies, time is normalized to the fast sampling interval. This corresponds to the Nyquist frequencies of $\Omega_f = \pi$ and $\Omega_s = \pi/r$ for fast and slow sampled signals respectively. Each polyphase component of a fast signal is a slow rate signal, with frequency content only up to Ω_s.

The interfaces between slow rate signals and fast rate signals are accomplished with interpolation, $\mathcal{I}$, and decimation, $\mathcal{D}$. Several different schemes for interpolation and decimation are described in Appendix A.2. The parameters $q_r(z, z^{-1})$ and δ_r in the slow-rate PSG serve a similar purpose to $q(z, z^{-1})$ and δ described for the 1989 design in Section 2.1.

The linear single rate components, whether at the fast or slow rate, are described in terms of their input sequence to output sequence mappings as transfer functions in z^{-1}. The interpretation of z^{-1} as the unit delay operator corresponds to different physical time delays depending upon the signal.

3.1.2 Design of the Components

To design this control system, begin by choosing G_{inv} as a ZPE inverse of Γ_y, as described in Section A.1. That is:

$$G_{inv}\Gamma_y = z^{-\delta}\frac{B^+(z^{-1})B^+(z)}{(B^+(1))^2} = z^{-\delta}\alpha(z, z^{-1}) \tag{3.1}$$

which has phase contributions only from $z^{-\delta}$. If Γ_y has no unstable zeros, $\alpha(z, z^{-1})$ will equal 1. This case is described first in later sections. Because of the assumptions on the locations of the unstable zeros, $\alpha(z, z^{-1})$ can be expanded into the following form:

$$\alpha(z, z^{-1}) = \alpha_0 + \sum_{i=1}^{\delta}\alpha_i(z^i + z^{-i}), \quad \alpha_i > 0, \quad \alpha_0 + 2\sum_{i=1}^{\delta}\alpha_i = 1 \tag{3.2}$$

This filter is not causal, to compute its current output it requires future inputs δ samples in advance. Furthermore $|z| = 1$, $\alpha(z, z^{-1})$ takes on real values in the interval $[0, 1]$, attaining a maximum value of 1 at $z = 1$ by definition.

Based on the values of δ and r, the remaining parameters of the design, $\mathcal{I}$, $\mathcal{D}$, and

δ_r (hence $z^{-\delta_r}$), will be selected. Choose $\mathcal{I}$ dependent only on r in the following form:

$$\mathcal{I}_{interp} = \begin{bmatrix} 1/r \\ 2/r \\ \vdots \\ (r-1)/r \\ 1 \end{bmatrix} + \begin{bmatrix} (r-1)/r \\ (r-2)/r \\ \vdots \\ 1/r \\ 0 \end{bmatrix} z^{-1} \tag{3.3}$$

This is a linear interpolation scheme between slow samples (Appendix A.2.4). Here z^{-1} is operating on the input to the interpolator, a slow rate scalar signal, therefore corresponds to a delay of one slow rate sample. A choice for $\mathcal{I}$ which effects a hold is used in comparisons, and takes the following form:

$$\mathcal{I}_{hold} = \begin{bmatrix} 1 \\ 1 \\ \vdots \\ 1 \\ 1 \end{bmatrix} \tag{3.4}$$

Use δ and r to define δ_r and ν as follows:

$$\delta_r = \lfloor (\delta - 1)/r \rfloor + 1 \tag{3.5}$$

$$\nu = [(\delta - 1) \bmod r] + 1 \tag{3.6}$$

Finally, using ν and the Kroneker Delta, define $\mathcal{D}$ as:

$$\mathcal{D} = \begin{bmatrix} \delta_\nu^1 & \delta_\nu^2 & \cdots & \delta_\nu^{r-1} & \delta_\nu^r \end{bmatrix} \tag{3.7}$$

This decimation scheme extracts every rth value from a fast rate input signal. Which of the polyphase components of the input signal is selected depends upon ν.

The result of choosing ν and δ_r according to this relationship is that:

$$\mathcal{D}\mathcal{L}^r(z^{-\delta}) = \begin{bmatrix} 0 & 0 & \cdots & 0 & z^{-\delta_r} \end{bmatrix} \tag{3.8}$$

$$\mathcal{D}\mathcal{L}^r(z^{-\delta})\mathcal{I} = z^{-\delta_r} \tag{3.9}$$

These relations are used extensively for algebraic manipulations. The above selections of $\mathcal{D}$ and $\mathcal{I}$ are not the only possible selections for which Eq 3.9 is true. The choices proposed were made with simplicity in mind. These choices are not optimal, as described later.

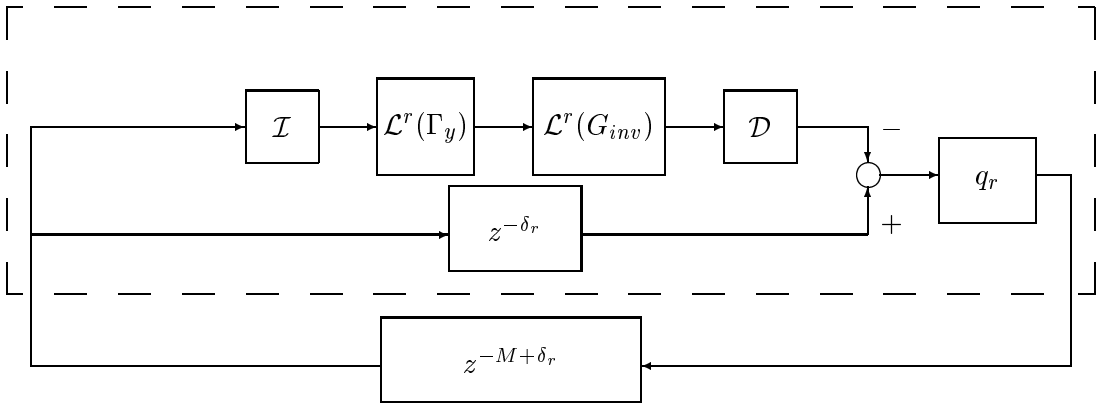

Figure 3.2: Small-gain structure for Dual-Rate Repetitive Control

The parameter $q_r(z, z^{-1})$ is considered to be a lowpass zero-phase filter with DC gain 1. Its usefulness in the context of the dual rate design is limited. It is set to have very mild lowpass characteristics, as the frequencies where uncertainties dominate are most likely above Ω_s.

3.1.3 Stability

In this subsection, the small-gain theorem is used to describe nominal and robust stability for the dual-rate design. The multirate characteristics of the system are easily accomodated for nominal stability. A sufficient condition for stability is posed as an upper bound on the infinity norm of a particular *SISO* slow rate system. The development of this condition follows that in Section 2.1. The block diagram given in Fig 3.1 is rearranged into the form shown in Fig 3.2 to clarify how the small gain theorem is applied. In the figure, $\mathcal{L}^r(\cdot)$ is the lifting operator (Appendix A.2.1).

The discussion of the dual rate system stability relies upon a conversion of system components to equivalent slow rate systems via lifting. The fast rate discrete time signals are put into a polyphase representation. Interpolation, decimation, and lifting are described in Section A.2. The system components in Figures 3.1 and 3.2 considered as time invariant linear systems at the slower sampling rate.

Referring to Fig 3.2, since $z^{-M+\delta_r}$ has infinity norm equal to 1, the following is a

sufficent condition for stability of the closed loop (small gain theorem):

$$\|(z^{-\delta_r} - \mathcal{DL}^r(G_{inv}\Gamma_y(1+\Delta))\mathcal{I})q_r(z,z^{-1})\|_\infty < 1 \tag{3.10}$$

The system inside the dashed box in the figure corresponds to the expression inside the norm. If necessary, delays are moved from $z^{-M+\delta_r}$ to $q_r(z,z^{-1})$ to make the arguement of the norm causal. The stability of the norm's arguement follows from the assumed stability of the plant and the defined stability of the other components.

The possibility of variations from the nominal behavior of the system Γ_y are captured by the stable SISO LTI system Δ, representing the perturbed system as $\Gamma_y(1+\Delta)$. This description of uncertainty places no bounds on Δ, it is used as a placeholder to describe the possible effects of uncertainty on the control system.

The condition given in Eq 3.10 for the nominal case, $\Delta = 0$, in terms of the zero-phase filter $\alpha(z,z^{-1})$ defined in Eq 3.1, takes the following form:

$$\|(z^{-\delta_r} - \mathcal{DL}^r(z^{-\delta}\alpha(z,z^{-1}))\mathcal{I})q_r(z,z^{-1})\|_\infty < 1 \tag{3.11}$$

Note that if $\alpha(z,z^{-1}) = 1$, cancellation using Eq 3.9 guarantees stability. This condition is guaranteed to be satisfied when $q_r(z,z^{-1}) = 1$ and $\mathcal{I} = \mathcal{I}_{interp}$. The properties of $\alpha(z,z^{-1})$ given in Eq 3.2 are used. Additionally note that for $0 < k < r-1$,

$$\mathcal{DL}^r(z^{-\delta-\gamma r-k})\mathcal{I} = \frac{r-k}{r}z^{-\delta_r-\gamma} + \frac{k}{r}z^{-\delta_r-\gamma-1} \tag{3.12}$$

and therefore, for a single term of $\alpha(z,z^{-1})$, $\alpha_i(z^i + z^{-i})$

$$\begin{aligned} i &= \gamma r + k, \quad 0 < k < r-1 \\ \mathcal{DL}^r(z^{-\delta}\alpha_i(z^i+z^{-i}))\mathcal{I} &= z^{-\delta_r}\alpha_i\left(\frac{r-k}{r}(z^{-\gamma}+z^{\gamma}) + \frac{k}{r}(z^{-\gamma-1}+z^{\gamma+1})\right) \end{aligned} \tag{3.13}$$

Each term of $\alpha(z,z^{-1})$ transforms according to this relationship to a zero-phase filter times $z^{-\delta_r}$. The total transformed $z^{-\delta}\alpha(z,z^{-1})$ will be a zero-phase filter $\alpha_r(z,z^{-1})$ times $z^{-\delta_r}$. The peak magnitude of $\alpha_r(z,z^{-1})$ is the sum of its coefficients. This is trivially equal to the sum of the coefficients of $\alpha(z,z^{-1})$, which was 1 by design. Rewrite the stability condition as:

$$\|z^{-\delta_r}(1-\alpha_r(z,z^{-1}))q_r(z,z^{-1})\|_\infty < 1 \tag{3.14}$$

With $q_r(z,z^{-1})$ bounded by 1, and the frequency response of $\alpha_r(z,z^{-1})$ bounded above by 1, it is sufficient for stability to show that the frequency response of $\alpha_r(z,z^{-1})$ is strictly positive.

This can be shown with the following arguement. Start by noting that for a given r, $\mathcal{I}$ can be realized as follows:

$$\mathcal{I} = \mathcal{L}^r \left(1 + \sum_{i=1}^{r-1} \frac{i}{r}(z^i + z^{-i}) \right) \begin{bmatrix} 0 \\ 0 \\ \vdots \\ 0 \\ 1 \end{bmatrix} \tag{3.15}$$

Define the fast rate zero-phase error filter $\beta_r(z, z^{-1})$ as the arguement of the lifting operation.

$$\beta_r(z, z^{-1}) = 1 + \sum_{i=1}^{r-1} \frac{r-i}{r}(z^i + z^{-i}) \tag{3.16}$$

It depends only on r, has zero-phase characteristics. An additional critical property is that its frequency response takes on only positive values as seen by the factored form:

$$\beta_r(z, z^{-1}) = (\sum_{i=0}^{r-1} z)(\sum_{i=0}^{r-1} z^{-i}) \tag{3.17}$$

Using this definition of $\mathcal{I}$ in terms of β_r along with the designed relation between $\mathcal{D}$ and $\mathcal{L}^r(z^{-\delta})$ shows the following:

$$z^{-\delta_r}\alpha_r(z, z^{-1}) = \mathcal{D}\mathcal{L}^r(z^{-\delta}\alpha(z, z^{-1}))\mathcal{I} \tag{3.18}$$

$$= z^{-\delta_r} \begin{bmatrix} 0 & \cdots & 0 & 1 \end{bmatrix} \mathcal{L}^r(\alpha(z, z^{-1})\beta_r(z, z^{-1})) \begin{bmatrix} 0 \\ \vdots \\ 0 \\ 1 \end{bmatrix} \tag{3.19}$$

It can be easily shown, using the modulated representation of the system (Appendix A.2.2), that the frequency response of $\mathcal{L}^r(\alpha(z, z^{-1})\beta_r(z, z^{-1}))$ takes on Hermitian positive semidefinite matrix values. It is diagonalized to a positive semidefinite matrix according to the orthogonal eigenvectors in S_r^{-1}. Positive semidefiniteness of $\mathcal{L}^r(\alpha(z, z^{-1})\beta_r(z, z^{-1})$ at each frequency guarantees that the scalar valued product with the column and its transpose has a nonnegative value at each frequency. Then the frequency response of $\alpha_r(z, z^{-1})$ will be non-negative as well.

The frequency response of $\alpha_r(z, z^{-1})$ takes on real values in the interval $[0, 1]$. Thus $(1 - \alpha_r(z, z^{-1}))$ takes on values in the same range over frequency, and the stability

condition of Eq 3.14 is satisfied. Such a proof does not extend to the case when $\mathcal{I}_{hold}$ is used. However, it does imply that the sum of the coefficients of $\alpha(z, z^{-1})$ may be allowed to be as large as 2 provided its values are still positive. In other words, the gain of the ZPE inverse may be increased by up to a factor of 2 without destabilizing the nominal system. This is an indication of some robustness for this design.

Robust Stability

In this section, a conservative frequency bound on the allowable uncertainty is described. For robust stability, consider the sufficent condition for stability including multiplicative uncertainty in the plant (using Eq 3.9):

$$\|\mathcal{D}\mathcal{L}^r(z^{-\delta}(1-\alpha(z,z^{-1})(1+\Delta)))\mathcal{I}q_r(z,z^{-1})\|_\infty < 1 \tag{3.20}$$

This condition must be satisfied for all Δ. Because the uncertainty is represented in a lifted form, defining the tolerance to uncertainty in a particular frequency range presents a challenge. The combined effect of uncertainties at aliased frequencies needs to be taken into account. The interpolation and decimation schemes, $\mathcal{I}$ and $\mathcal{D}$, will define this effect. Note that lowpass characteristics of $\alpha(z, z^{-1})$ will allow for larger uncertainties.

Consider the case when $\alpha(z, z^{-1}) = 1$ (i.e. $B^+(z^{-1}) = 1$). The above condition simplifies to the following:

$$\|\mathcal{D}\mathcal{L}^r(\Delta)\mathcal{I}q_r(z,z^{-1})\|_\infty < 1 \tag{3.21}$$

To consider the effect of $\mathcal{I}$ and $\mathcal{D}$ on allowable uncertainty the frequency domain, put $\mathcal{L}^r(\Delta)$ in modulated form (refer to Appendix A.2.2), and consider the equivalent condition (inserting identity in the form of $S_r S_r^{-1}$):

$$\max_{0<\omega<\pi/r} \left|(\mathcal{D}S_r)(S_r^{-1}\mathcal{L}^r(\Delta)S_r)(S_r^{-1}\mathcal{I}q_r(z,z^{-1}))\right|_{z=e^{j\omega r}} < 1 \tag{3.22}$$

The uncertainty, Δ, is assumed to be linear time invariant so $(S_r^{-1}\mathcal{L}^r(\Delta)S_r)$ will be diagonal at each frequency. The diagonal elements correspond to the frequency responses of Δ at the aliased frequencies of ω. Since the uncertainties at these aliased frequencies can constructively combine, only a conservative frequency domain bound can be made on Δ. For several values of r, with the associated choices of $\mathcal{D}$ and $\mathcal{I}$, such a bound is shown graphically in Figure 3.3. It was computed using a grid over the frequency range $0 < \omega < \pi/r$. At

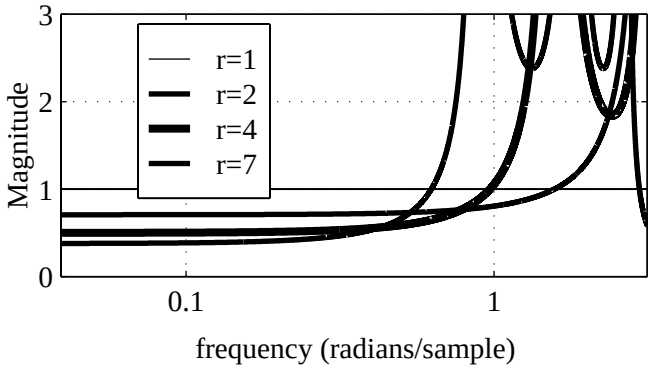

Figure 3.3: Uncertainty bound for robust stability

each frequency, r bounds were computed, corresponding to the bound at each of the aliased frequencies of ω. The following formula was used, with the magnitude of $B(\gamma)$ denoting the inverse of the uncertainty bound at frequency γ:

$$\begin{bmatrix} B(\omega_1) \\ B(\omega_2) \\ \vdots \\ B(\omega_r) \end{bmatrix} = \sqrt{r}\,\mathrm{diag}\left(S_r^{-1}(\omega_1)(\mathcal{ID}|_{z=e^{jr\omega_1}})S_r(\omega_1)\right); \tag{3.23}$$

where the function "diag" is used to extract the diagonal elements of its matrix arguement, and place them in a column.

The same bounds can be used to determine a tolerance to uncertainty when $\alpha(z, z^{-1})$ is not equal to 1. Separate the nominal stability condition out as follows:

$$\|\mathcal{DL}^r(z^{-\delta}(1-\alpha(z,z^{-1})))\mathcal{I}q_r(z,z^{-1}) - \mathcal{DL}^r(z^{-\delta}\alpha(z,z^{-1})\Delta)\mathcal{I}q_r(z,z^{-1})\|_\infty < 1 \tag{3.24}$$

Then consider the diagonal modulated system as

$$S_r^{-1}\mathcal{L}^r(z^{-\delta}\alpha(z,z^{-1})\Delta)))S_r \tag{3.25}$$

At each frequency, bound the magnitude of these diagonal elements, noting that $\alpha(z, z^{-1})$ will allow larger uncertainty as its gain increases. The tolerable uncertainty increases when the nominal stability criterion is satisfied by a wide margin.

Auxillary Stability Result

The following is an important result allowing the scaling of the inverse dynamics without affecting stability. Assume a given design is robustly stable, satisfying Eq 3.10 for all allowable uncertainties, and that the magnitude of $q_r(z, z^{-1})$ is less than 1 at all frequencies. Use of the triangle inequality trivially guarantees that the closed loop system will be stable if G_{inv} is replaced by $(1-\xi)G_{inv}$ for any $\xi \in [0,1]$. This is shown by the following algebraic manipulation:

$$\begin{aligned}
& \|(z^{-\delta_r} - \mathcal{D}\mathcal{L}^r((1-\xi)G_{inv}\Gamma_y(1+\Delta))\mathcal{I})q_r(z,z^{-1})\|_\infty \\
= & \\
& \|(\xi z^{-\delta_r} q_r(z,z^{-1})) + (1-\xi)(z^{-\delta_r} - \mathcal{D}\mathcal{L}^r(G_{inv}\Gamma_y(1+\Delta))\mathcal{I})q_r(z,z^{-1})\|_\infty \\
< & \\
& \|(\xi z^{-\delta_r} q_r(z,z^{-1}))\|_\infty + (1-\xi)\|z^{-\delta_r} - \mathcal{D}\mathcal{L}^r(G_{inv}\Gamma_y(1+\Delta))\mathcal{I})q_r(z,z^{-1})\|_\infty \quad (3.26)
\end{aligned}$$

Where the last expression is clearly less than 1 if the original robust stability condition was satisfied. Thus, the gain of the inverse dynamics can always be reduced to create a robustly stable repetitive control system when the original design was robustly stable.

3.1.4 The Lifted Closed Loop System

Stability was defined in terms of a single input single output system at the slow rate, but the disturbances and measurements are signals at the fast rate. The input-output behavior between these fast-rate signals for the dual-rate system is not described by a transfer function. A lifting approach, however, can be used to write the input/output behavior in terms of an $r \times r$ transfer matrix. Frequency domain interpretations of these transfer matrices are made according to the material in Appendix A.2.2.

Assume that the periodic disturbance is matched with the repetitive control signal. The transfer matrix from polyphase $d_{in}(k)$ to polyphase $y(k)$ is derived from the following system equations (refer to Fig 3.1):

$$y(k) = \mathcal{L}^r(\Gamma_y)(d_{in}(k) - u_{rep}(k)) \quad (3.27)$$

$$u_{rep}(k) = \mathcal{I}(\frac{q_r z^{-M+\delta_r}}{1-q_r z^{-M}})\mathcal{D}\mathcal{L}^r(G_{inv})y(k) \quad (3.28)$$

To find the transfer matrix from $d_{in}(k)$ to $y(k)$, substitute in for $u_{rep}(k)$ in the first system

equation. This gives the transfer matrix as

$$\Phi_y = \left(I_r + \mathcal{L}^r(\Gamma_y)\mathcal{I}(\frac{q_r z^{-M+\delta_r}}{1-q_r z^{-M}})\mathcal{D}\mathcal{L}^r(G_{inv}) \right)^{-1} \mathcal{L}^r(\Gamma_y) \tag{3.29}$$

The matrix inverse operation above has a structured argument. Because of this structure (rank one perturbation of identity), the inverse can be explicitly written by use of a matrix inversion formula. The transfer function is rewritten using an inverted scalar rather than matrix term as:

$$\Phi_y = \left(I_r - \mathcal{L}^r(\Gamma_y)\mathcal{I} \left(\frac{1-q_r z^{-M}}{q_r z^{-M+\delta_r}} + \mathcal{D}\mathcal{L}^r(G_{inv})\mathcal{L}^r(\Gamma_y)\mathcal{I} \right)^{-1} \mathcal{D}\mathcal{L}^r(G_{inv}) \right) \mathcal{L}^r(\Gamma_y) \tag{3.30}$$

With some algebra, Φ_y can be "simplified" to either of the following two forms (of course among many others):

$$\Phi_y = \frac{(1-q_r z^{-M})I_r + q_r z^{-M+\delta_r}\left((\mathcal{D}\mathcal{L}^r(G_{inv})\mathcal{L}^r(\Gamma_y)\mathcal{I})I_r - \mathcal{L}^r(\Gamma_y)\mathcal{I}\mathcal{D}\mathcal{L}^r(G_{inv})\right)}{1-q_r z^{-M+\delta_r}(z^{-\delta_r} - \mathcal{D}\mathcal{L}^r(G_{inv})\mathcal{L}^r(\Gamma_y)\mathcal{I})}\mathcal{L}^r(\Gamma_y)$$

or (3.31)

$$\Phi_y = \left(I_r - \frac{q_r(z,z^{-1})z^{-M+d'}(\mathcal{L}^r(\Gamma_y)\mathcal{I}\mathcal{D}\mathcal{L}^r(G_{inv}))}{1+z^{-M+d'}(z^{-d'} - \mathcal{D}\mathcal{L}^r(G_{inv})\mathcal{L}^r(\Gamma_y)\mathcal{I})q_r(z,z^{-1})} \right) \mathcal{L}^r\left(\frac{G_n}{1+G_n G_c}\right) \tag{3.32}$$

The first form emphasizes the term $(1-q_r z^{-M})I_r$ in the numerator of the transfer matrix, describing the elimination of the periodic disturbance. The second form emphasizes the original system, describing the new closed loop as the old plus something new. The arguement of the stability condition norm in Eq 3.10 appears in their denominators. This relates back to the connection between stability and performance for the 1989 design discussed in Section 2.1.

3.1.5 Best and Worst Case Periodic Disturbances

When using the dual rate design, sacrifices in the ability of the control system to eliminate periodic disturbances are expected. The development here is motivated toward understanding this sacrifice. A description of the periodic disturbances which can be asymptotically eliminated is found. Associated with this concern, the sensitivity to periodic disturbances which do not fit this profile is also described.

The effect of periodic disturbances at $d_{in}(k)$ on the output $y(k)$ is not immediately clear looking at the transfer matrices given in Equations 3.31 and 3.32. Some more can, however be said, about the effects of using the PSG implemented at a slower sampling

rate. For this discussion, the form given in Eq 3.31 is used. To simplify the discussion, the following assumption is made:

$$\|(z^{-\delta_r} - \mathcal{D}\mathcal{L}^r(G_{inv})\mathcal{L}^r(\Gamma_y)\mathcal{I})q_r(z, z^{-1})\|_\infty \ll 1 \tag{3.33}$$

This assumption corresponds to a selection of $\mathcal{D}$, $\mathcal{L}^r(G_{inv})$, δ_r, and $\mathcal{I}$ for nominal stability of the closed loop system with significant stability margin (refer to Eq 3.10 and discussion of stability in previous section). Using this assumption, the first factor of Φ_y given in Eq 3.31 can be interpreted assuming its denominator is 1. The numerator is separated into two terms:

$$G_{lti} = (1 - q_r z^{-M})I_r \tag{3.34}$$

$$G_{ptv} = q_r z^{-M+\delta_r}\left((\mathcal{D}\mathcal{L}^r(G_{inv})\mathcal{L}^r(\Gamma_y)\mathcal{I})I_r - \mathcal{L}^r(\Gamma_y)\mathcal{I}\mathcal{D}\mathcal{L}^r(G_{inv})\right) \tag{3.35}$$

where "lti" refers to *Linear Time Invariant* and "ptv" refers to *Periodically Time Varying*. More to the point, the G_{lti} portion can be interpreted as an LTI filter at the measurement (fast) sampling rate (see below). The G_{ptv} portion describes the time-varying nature of the sensitivity due to the dual-rate controller design.

Interpreting G_{lti} at the fast rate

Use $q_r(z, z^{-1})$ to define a filter $q_r(z^r, z^{-r})$ at the fast rate according to the following lifting relationship.

$$q_r(z, z^{-1})I_r = \mathcal{L}^r(q_r(z^r, z^{-r})) \tag{3.36}$$

The filter $q_r(z^r, z^{-r})$ is written in terms of rth powers of $z^{-1}$and z. This results in a frequency response which exhibits aliasing-like behavior as shown in Figure 3.4 for $r = 4$ and $q_r(z, z^{-1}) = \frac{1}{4}z + \frac{1}{2} + \frac{1}{4}z^{-1}$. The phase plot is not shown, for this filter has zero phase at all frequencies. Note the folding of the magnitude response about the frequencies indicated on the frequency axis. The number of foldings depends upon the value of r. In the figure, there are three folds to form four regions. The frequency response is shown up to Ω_f, measured in revolutions per sample.

With $G_{ptv} = 0$ (impossible unless $r = 1$ as shown later), the previous assumptions yield the following closed loop characteristics:

$$\Phi_y \approx (1 - q_r(z^r, z^{-r})z^{-N})\Gamma_y \tag{3.37}$$

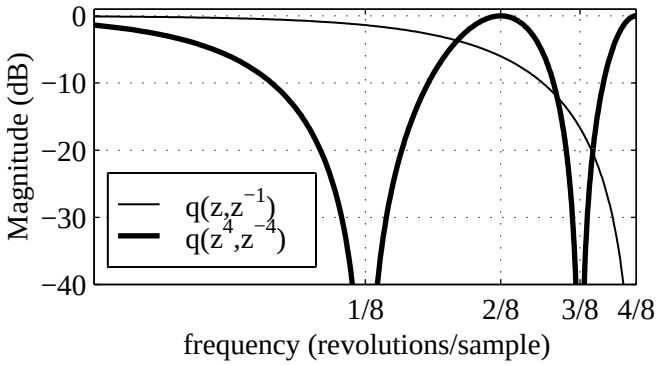

Figure 3.4: Aliasing effects of the filter $q(z^r, z^{-r}) = \frac{1}{4}z^4 + \frac{1}{2} + \frac{1}{4}z^{-4}$

This is now a transfer function between $d_{in}(k)$ and $y(k)$ rather than a transfer matrix between the polyphase components of $d_{in}(k)$ and $y(k)$. Periodic disturbances are then eliminated according to $(1 - q_r(z^r, z^{-r})z^{-N})$.

3.1.6 Effects of G_{ptv} on the Closed Loop

The above remarks describe the performance of the system when the effect of G_{ptv} is ignored ($G_{ptv} = 0$). Taking its effect into account describes the sacrifices made to performance with a dual-rate design.

The $r \times r$ transfer matrix G_{ptv} is a very structured system (at the slow rate). An immediately apparent fact is that:

$$G_{ptv}\mathcal{L}^r(\Gamma_y)\mathcal{I} = \begin{bmatrix} 0 \\ \vdots \\ 0 \end{bmatrix} \in \mathbb{C}^{r\times 1} \tag{3.38}$$

This annihilation of G_{ptv} through series combination with $\mathcal{L}^r(\Gamma_y)\mathcal{I}$ leads to a description of periodic disturbances for which the effect of G_{ptv} on Φ_y *is* effectively zero.

This relation implies that the frequency response of the $r \times r$ system G_{ptv} has at most rank $r - 1$ at each frequency (up to Ω_s). The system G_{ptv} actually describes input output behavior at the fast rate, so its frequency response describes the interrelated gains and phases of r aliased frequency components (Appendix A.2). The $r \times 1$ system $\mathcal{L}^r(\Gamma_y)\mathcal{I}$ maps one frequency below Ω_s to r frequencies below Ω_f according to a modulated

description of the output. At each frequency below π/r, an annihilating combination of sinusoids at the r aliased frequencies can be found. For example, with $0 < \omega < \pi/r$ choose the polyphase components of $d_{in}(k)$ as $e^{jr\omega k}X$ such that

$$X \in \mathbb{C}^{r\times 1} \quad \text{and} \quad (\mathcal{L}^r(\Gamma_y)\mathcal{I})|_{z=e^{jr\omega}} = (\mathcal{L}^r(\Gamma_y))|_{z=e^{jr\omega}}X, \tag{3.39}$$

Choosing $X = \mathcal{I}|_{z=e^{jr\omega}}$ clearly satisfies the above relationship. With the input $d_{in}(k)$defined this way, the steady-state polyphase components of the output, $y(k)$, will be:

$$\left(\frac{(1-q_r z^{-M})I_r}{1-q_r z^{-M+\delta_r}(z^{-\delta_r} - \mathcal{D}\mathcal{L}^r(G_{inv})\mathcal{L}^r(\Gamma_y)\mathcal{I})}\right)\mathcal{L}^r(\Gamma_y)\mathcal{I}\Big|_{z=e^{jr\omega}} e^{jr\omega k}, \tag{3.40}$$

which is independent of G_{ptv}. Doing this at the M repetitive frequencies lying in the range $[0, \pi/r)$ determines M combinations of r repetitive frequencies which may be asympotically eliminated. Since $N = M \cdot r$, this in turn describes the M-parameterized family of N-periodic disturbances for which G_{lti} is the predominant indicator of performance.

It is important to note that if periodic disturbances are injected into the closed loop at different points, the second term of the transfer matrix given in Eq 3.31, Γ_y, will be different. As an example, for computer disk drives, known sources of periodic disturbances are at the output of the plant, G_n. The transfer matrix from $d_{out}(k)$ to $y(k)$ will be:

$$\Phi_y = \frac{(1-q_r z^{-M})I_r + G_{ptv}}{1-q_r z^{-M+\delta_r}(z^{-\delta_r} - \mathcal{D}\mathcal{L}^r(G_{inv})\mathcal{L}^r(\Gamma_y)\mathcal{I})}\left(\frac{1}{1-G_nG_c}\right) \tag{3.41}$$

Following analagous logic to that above, for the polyphase components of $y(k)$ to be given by the expression in Eq 3.40, the output disturbance, $d_{out}(k)$ defined as $Xe^{jr\omega k}$ must be such that:

$$\mathcal{L}^r(\Gamma_y)(e^{-j\omega})\mathcal{I}(e^{-j\omega}) = \left(\frac{1}{1-G_nG_c}\right)|_{z=e^{jr\omega}}X, \tag{3.42}$$

which is a slightly different condition than that in Eq 3.39. Thus, the shapes of periodic disturbances which are completely annihiliated by G_{ptv} depends upon their injection point.

The periodic disturbances which can be asymptotically eliminated have been described dependent upon their injection point into the system. The design of the interpolation scheme plays the most significant role in determining these disturbances. Next, the structure of G_{ptv} is examined to determine what happens to periodic disturbances which do not fall into this category.

A Factorization of G_{ptv}

The singular value decomposition leads to a factorization of G_{ptv}. This factorization in turn leads to a further understanding of the effect of disturbances on the output. Disturbances for which G_{ptv} plays no role were described above. They correspond to null spaces of G_{ptv}'s frequency response matrices.

Evaluate the frequency response of G_{ptv} at some frequency, $0 < \omega < \pi/r$. The analysis which follows is based on this $r \times r$ complex matrix. To simplify the discussion, define the following:

$$\nu = ((\mathcal{D}\mathcal{L}^r(G_{inv}))\,|_{z=e^{jr\omega}})^* \in \mathbb{C}^{r\times 1} \tag{3.43}$$

$$\eta = (\mathcal{L}^r(\Gamma_y)\mathcal{I})\,|_{z=e^{jr\omega}} \in \mathbb{C}^{r\times 1} \tag{3.44}$$

$$\tag{3.45}$$

Then note that

$$G_{ptv}|_{z=e^{jr\omega}} = (q_r z^{-M+d'})|_{z=e^{jr\omega}}(\nu^*\eta I_r - \eta\nu^*) \tag{3.46}$$

and define

$$P = \nu^*\eta I_r - \eta\nu^* \tag{3.47}$$

Now some easily verifiable properties of P can be stated.

$$P\eta = 0 \tag{3.48}$$

$$P^*\nu = 0 \tag{3.49}$$

$$\nu^* w = 0 \;\Rightarrow\; Pw = (\nu^*\eta)w \tag{3.50}$$

$$w^*\eta = 0 \;\Rightarrow\; w^*P = (\nu^*\eta)w^* \tag{3.51}$$

Using these properties, a factorization of P based on the Singular Value Decomposition (SVD) can be made. Choose an $r-2$ dimensional othonormal basis w_i for the subspace orthogonal to both ν and η. This factored P has the following form:

$$P = \left(\sum_1^{r-2}(\nu^*\eta)w_i w_i^*\right) + |\eta||\nu| w_{out} w_{in}^* \tag{3.52}$$

where w_{out} and w_{in} are the unit vectors:

$$w_{out} = \frac{(\nu^*\nu)\eta - (\nu^*\eta)\nu}{|(\nu^*\nu)\eta - (\nu^*\eta)\nu|} \tag{3.53}$$

$$w_{in} = \frac{(\eta^*\eta)\nu - (\eta^*\nu)\eta}{|(\eta^*\eta)\nu - (\eta^*\nu)\eta|} \tag{3.54}$$

Notice that of the singular values of P , one zero and one repeats $r-2$ times (it is $|\nu^*\eta|$). The final singular value is the largest, with size $|\eta||\nu|$. When η is a constant multiple of ν, there will be no difference in magnitude between these two nonzero singular values. The proposed selections of $\mathcal{D}$, $\mathcal{I}$, and G_{inv}were such that $|\nu^*\eta| \approx 1$ at all frequencies. When the gain of G_{inv} is reduced, all of these singular values will drop together. The majority of signals passing through G_{ptv} are amplified by this factor. The design of $\mathcal{D}$ and $\mathcal{I}$ to be computationally efficient, achieve stability, and also achieve $|\nu^*\eta| = |\eta||\nu|$ is touched upon in the application example. It remains a topic for future research.

The worst case amplification of input combinations of r aliased frequencies was described in terms of the frequency response of G_{ptv}. The shape of the worst case input can be found according to the appropriate w_{in}, and should correspond to unlikely disturbances. In the context of dual-rate repetitive control, they should be concentraetd at higher frequencies.

Remarks on Worst Case Disturbance Analysis

A subset of periodic disturbances for which steady-state rejection is described predominantly by $1-q_r z^{-M}$ has been defined. The output sensitivity to deviations from this M-dimensional subset of N-periodic disturbances was given in terms of a factorization of the frequency response of G_{ptv}. Consider the singular values of the frequency response of $G_{ptv}\Gamma_y$ (assuming input disturbance) at the repetitive frequencies. The particular combination of disturbance polyphase components which causes the largest deviation from the performance specified by G_{lti} can be found. Such a combination of polyphase components should be likely to have small magnitude.

The critical parameter for determining which periodic disturbances can be asymptotically eliminated is the interpolation scheme, $\mathcal{I}$. The choice of decimation, $\mathcal{D}$, affects performance through its interaction with $\mathcal{I}$, in combination with G_{inv} and δ_r.

3.1.7 Frequency Domain Interpretation Tools

In addition to looking at the combined effects of r aliased frequencies at a time, consider the effect of forcing the system with a purely sinusoidal disturbance. When a dual-rate repetitive control scheme such as this makes sense, periodic disturbances concentrated at lower frequencies are typically the primary source of concern.

Force the system with a signal consisting of a single sinusoid at a frequency below this threshold, $0 < \omega < \pi/r$. The output will have r frequency components in general. The amplitude of the output component at the forcing frequency and the size of the components of the output at the other frequencies are measures of the system behavior. The calculation of these amplifications is described below, assuming a sinusoidal input signal with unit amplitude. These relations use the modulated representations of signals, and the modulation matrices S_r and S_r^{-1} (Appendix A.2.2).

First, the amplitude of the output component at the forcing frequency is described as:

$$T_{\sin}(\Phi_y, \omega) = \left| \frac{1}{r} \begin{bmatrix} 1 & e^{-j\omega\frac{1}{r}} & \cdots & e^{-j\omega\frac{r-2}{r}} & e^{-j\omega\frac{r-1}{r}} \end{bmatrix} \Phi_y|_{z=e^{jr\omega}} \begin{bmatrix} 1 \\ e^{j\omega\frac{1}{r}} \\ \vdots \\ e^{j\omega\frac{r-2}{r}} \\ e^{j\omega\frac{r-1}{r}} \end{bmatrix} \right|, \tag{3.55}$$

Then the RMS of the amplitudes of all the output frequency components is given as:

$$T_{\text{tot}}(\Phi_y, \omega) = \frac{1}{\sqrt{r}} \left\| \Phi_y|_{z=e^{jr\omega}} \begin{bmatrix} 1 \\ e^{j\omega\frac{1}{r}} \\ \vdots \\ e^{j\omega\frac{r-2}{r}} \\ e^{j\omega\frac{r-1}{r}} \end{bmatrix} \right\|_2, \tag{3.56}$$

Together, these gains measured at the repetitive frequencies will be used in the design example to simply illustrate the closed loop attenuation of periodic disturbances. These closed loop amplifications are different from the maximum singular value of the frequency response matrix, which is often used as a measure of amplification for MIMO systems. These gains more accurately describe frequency response behavior of the system, because Φ_y is a slow sampled system describing the input/output behavior of lifted fast sampled signals. If Φ_y is a lifted SISO linear time-invariant system, these two amplifications will be equal, and also equal to the magnitude of the frequency response of Φ_y at the forcing frequency.

3.1.8 Relation to Performance Objective of Section 2.3

Finally, consider the performance measure proposed in Section 2.3. Lifting can be used to apply the measure in Eq 2.13 to a dual-rate design. Working from the expression for Φ_y in Eq 3.32, the performance measure takes the form:

$$\mathrm{J}_{\mathrm{rep}}(\Phi_y) = \left\| I_r - \mathcal{L}^r\left(\frac{1-\xi q_w z^{-N}}{1-q_w z^{-N}}\right)\left(\frac{1-q_r z^{-M} I_r + G_{ptv}}{1-q_r z^{-M+\delta_r}(z^{-\delta_r} - \mathcal{D}\mathcal{L}^r(G_{inv})\mathcal{L}^r(\Gamma_y)\mathcal{I})}\right)\right\|_\infty \tag{3.57}$$

The motivation for this performance objective lay in guiding parameter selections for repetitive controller designs. The parameters q_w and ξ might be used to guide the dual rate design. The parameters of the dual-rate design are r, $\mathcal{I}$, $\mathcal{D}$, q_r, and G_{inv}. The proposed design was based upon choices for these parameters leading to simple implementations. Working within the proposed design, guided by the above expression of the performance objective, q_w and ξ might be used in the following way:

- Choose r according to q_w such that the repetitive frequencies of interest lie in the range $0 < \omega < \pi/r$.
- Choose the gain of $q_r(z, z^{-1})|_{z=e^{jr\omega}}$ to roughly match that of $T_{\sin}(q(z, z^{-1}), \omega)$.
- Choose G_{inv} to be $(1-\xi)$ times the proposed ZPE inverse.

It is important to note that when dual-rate repetitive control is being considered, the periodic disturbances are concentrated in the lower frequency range. The appropriate design parameter q_w will then have significant attenuation at higher frequencies.

3.1.9 Closing Comments on the Design

The proposed dual-rate structure is parameterized by $\mathcal{I}$, $\mathcal{D}$, r, $q_r(z, z^{-1})$, and G_{inv}. In the analysis provided, the decimation and inverse dynamics, $\mathcal{D}$ and G_{inv}, appeared together. Their order might be reversed, or more generally they might be combined into a single component. These approaches were not taken because of concerns about complexity. However, in either case G_{ptv} will have the same basic properties, characterizing worst case combinations of sinusoidal disturbances.

If r is not a factor of N, this design method does not apply. Several possibilities being examined for dealing with such a case are:

- Choose the filter $q_r(z, z^{-1})$to approximate the phase of a non-integer number of delays. Example: $q_r(z, z^{-1}) = \frac{r-k}{r} + \frac{k}{r} z^{-1}$ at the slow rate is a linear interpolation approximate of the time delay of z^{-k} at the fast rate. This approximation gets worse at higher frequencies.

- Move the interpolation and decimation schemes inside the PSG feedback loop. In this design, the delayed interpolated control signal would be added to the output of G_{inv} and then decimated. The decimation and interpolation would surround only the longer delay chain in the PSG.

3.2 Application to Magnetic Disk Drive

In this section, the dual-rate design is applied to an experimental disk drive servosystem. Offline analysis, simulations, and experiments are used to illustrate the sacrifices in performance associated with two levels of memory savings. Much attention is also given to saving memory while constraining computational complexity. Comparisons to the 1989 design are made (which is the case when $r = 1$).

The repetitive control problem associated with magnetic disk drives was described in Section 2.2. The lumped model of the magnetic disk drive experimental system is given in Appendix B.2, and illustrated in terms of frequency repsonses later in this section. A description of the experimental setup is given in Appendix B.1. Several features of the system repeated here are:

1. The disk drive has 80 sectors. This means periodic disturbances attributed to disk rotation have a period of $N = 80$ samples.

2. The model of the electromechanical system from control signal to head position is the zero-order hold equivalent of a continuous double integrator system with an input delay (computation, A/D, and D/A). This discrete time system has one zero outside the unit disk, on the negative real axis, satifying the assumptions made in the development above.

3. A stabilizing internal feedback control loop provides nominal tracking performance in the absence of significant track runout. The design of this controller, and hence the nominal lumped feedback control system is taken as a given.

4. In the experiment, dominant track runout is at the fundamental frequency of disk rotation.

5. Non-periodic sources of tracking errors play a very large role in the experiment, dictating a conservative learning rate.

6. The hardware for the experimental setup imposed severe limitations on the complexity of the controllers, guiding (forcing) many design decisions.

The stability of repetitive control sytems has been discussed in terms of the small gain theorem. Bode magnitude plots of the critical quantity,

$$(z^{-\delta_r} - \mathcal{D}\mathcal{L}^r(G_{inv})\mathcal{L}^r(\Gamma_y)\mathcal{I})q_r(z, z^{-1}) \tag{3.58}$$

are used to graphically indicate nominal stability and stability margins. The closed loop will be stable if the peak value is less than 1. The amount by which the gain is less than 1 relates to stability robustness of the design (Section 3.1.3).

The measures T_{tot} and T_{sin} introduced in the preceding section are used to compare nominal steady-state reductions of periodic disturbances. A small tolerance to uncertainty for stability corresponds to potentially large effects on performance with small deviations from the nominal plant.

The final method by which designs will be compared is with simulated and experimental data. Experimental tracking errors are averaged to capture the periodic part of position error. Discrete fourier transforms are used to compute the frequency content of the periodic errors.

The remainder of this section is divided as follows:

- The Disk Drive System in Context
- Stability
- Performance

3.2.1 The Disk Drive System in Context

The relationship between the magnetic disk drive servosystems described in Section 2.2 and the repetitive control structure described in Fig 3.1. is described in Table 3.1. The model of the experimental system given in Appendix B.2 is accurate. The behavior of

Table 3.1: HDD for dual-rate repetitive control

Disk Drives (Figs 2.1 and 2.8)	Dual-Rate (Fig 3.1)
control signal	$-u_{in}(k)$-$u_{rep}(k)$
PES	$y(k)$
meas. noise plus track runout	$d_{out}(k)$
ctrl. noise plus FPC tension	$d_{in}(k)$
system from digital control to PES	G_n
inner feedback controller	G_c

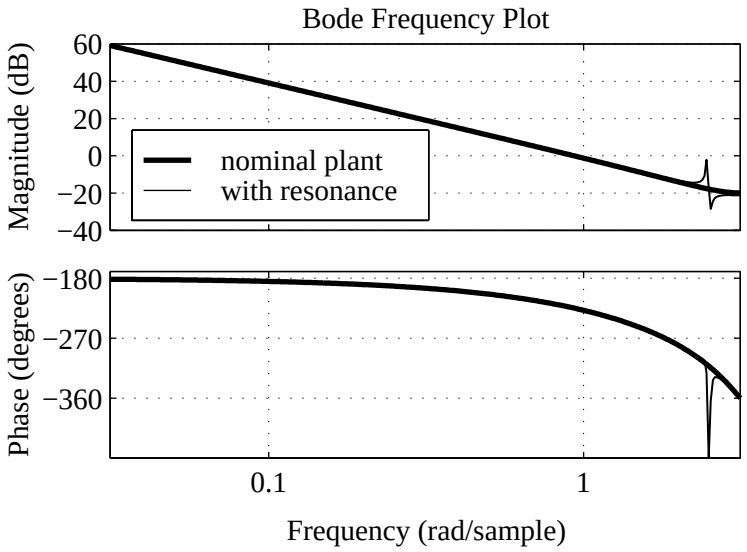

Figure 3.5: Frequency response of nominal and perturbed plants (G_n).

the plant during track following control is as a double integrator. Frequency responses of the nominal discrete time plant model, G_n, and a model which incorporates an exaggerated resonance (representing an actuator arm mode) are shown in Fig 3.5. These are discrete time models which account for assumed computational, D/A, and A/D delays associated with applying the digital discrete time control. Frequencies are given in radians per measurement sample interval.

An observer state feedback design based on pole placement was used for the internal controller, G_c, to achieve a bandwidth below the uncertain resonant mode of the actuator arm, and good gain and phase margins. The numerical form of this controller can be found in Appendix B.2. The frequency response of this controller is shown in Fig 3.6,

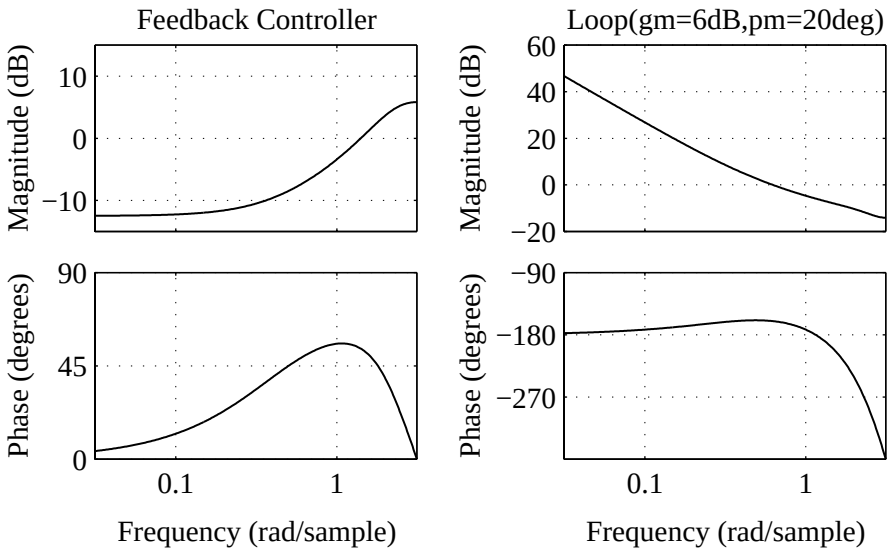

Figure 3.6: Frequency responses of controller G_c(left), and feedback loop G_nG_c(right).

along with the frequency response of the nominal feedback loop (G_nG_c). The gain and phase margins for this design are indicated in the figure. The closed loop frequency response from $d_{in}(k)$ (or $u_{rep}(k)$) to $y(k)$ without repetitive control, Γ_y, is shown for both the nominal and perturbed (with actuator resonance) plant models in Figure 3.7. Finally, the closed loop frequency response from $d_{out}(k)$ (the source of the main periodic disturbance) to the output is shown in Figure 3.8. This system already has significant capability to reduce the effect of low frequency periodic disturbances.

3.2.2 Stability Issues

In this section, the impact of the design parameters on stability margins is described with the aid of the frequency plots of

$$D_{stab}(z^{-1}) = (z^{-\delta_r} - \mathcal{D}\mathcal{L}^r(G_{inv})\mathcal{L}^r(\Gamma_y)\mathcal{I}). \tag{3.59}$$

For stability, $q_r(z, z^{-1})$ is ignored. If the magnitude of $D_{stab}(z^{-1})$ exceeds 1 in some frequency range, $q_r(z, z^{-1})$ must be selected with attenuation at those frequencies. The following variations are discussed:

- approximate selection of G_{inv}.

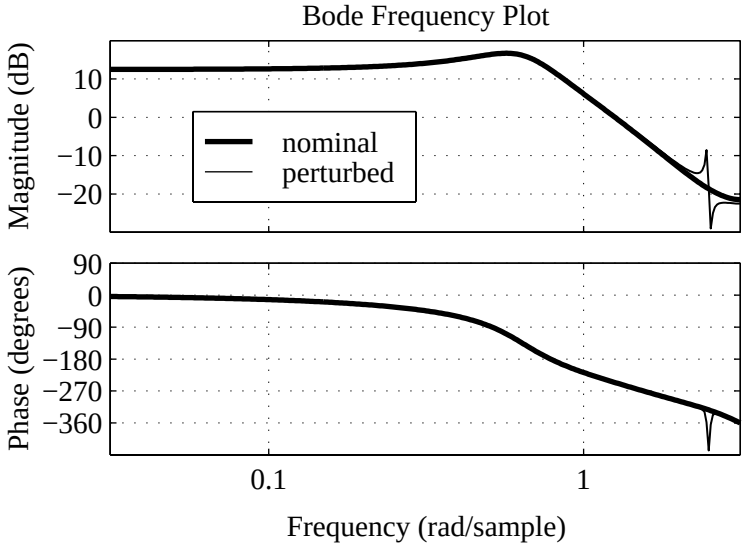

Figure 3.7: Frequency response from $u_{rep}(k)$ to $y(k)$ (Γ_y) with inner loop closed.

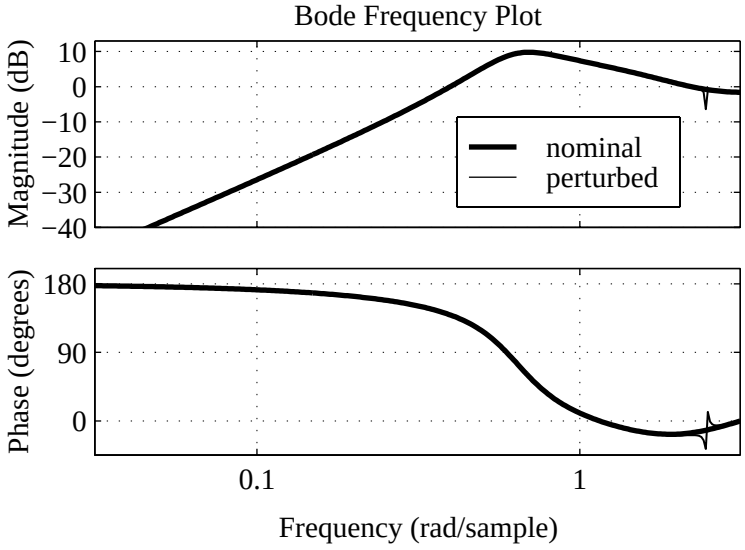

Figure 3.8: Frequency response from $d_{out}(k)$ to $y(k)$ (Γ_{out}) with inner loop closed.

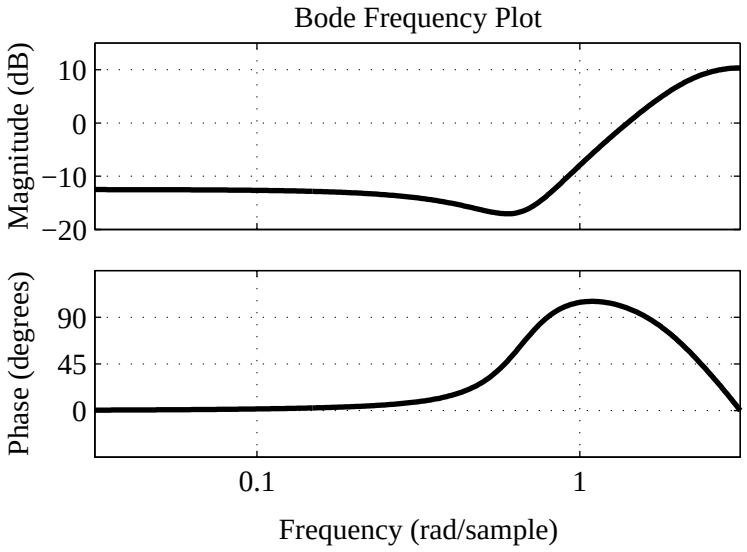

Figure 3.9: Frequency response of the approximate ZPE inverse of Γ_y

- changing interpolation action
- changing r
- plant perturbation

The selections of G_{inv} considered are first described. Proceed by choosing the inverse dynamics, G_{inv}, for Γ_y according to the zero-phase-error inverse rules. This was the proposed choice for both the 1989 design and the dual-rate design. As Γ_y is a sixth order system with one unstable zero, the inverse dynamics thus designed is seventh order. This high order is not necessary. The order is reduced via approximate pole-zero cancellations, maintaining the DC gain. The inverse dynamics referred to as G_{zpe} is then a second order approximation of the full order ZPE inverse of Γ_y(numerical form is in Appendix B.2). The frequency response of the resulting design is shown in Fig 3.9. The plant,Γ_y, had one zero outside the unit disk, and one pure delay, thus $\Gamma_y G_{zpe}$ has approximately the same phase as a two delay system (leading to $\delta = 2$). The frequency response of $z^2\Gamma_y G_{zpe}$ in Fig 3.10 shows that the phase is very nearly zero, and has lowpass filter characteristics.

An alternative inverse, compelling in its simplicity, and so of practical interest consists merely of a fixed gain. Define G_{gain} as the inverse of the DC gain of Γ_y. To

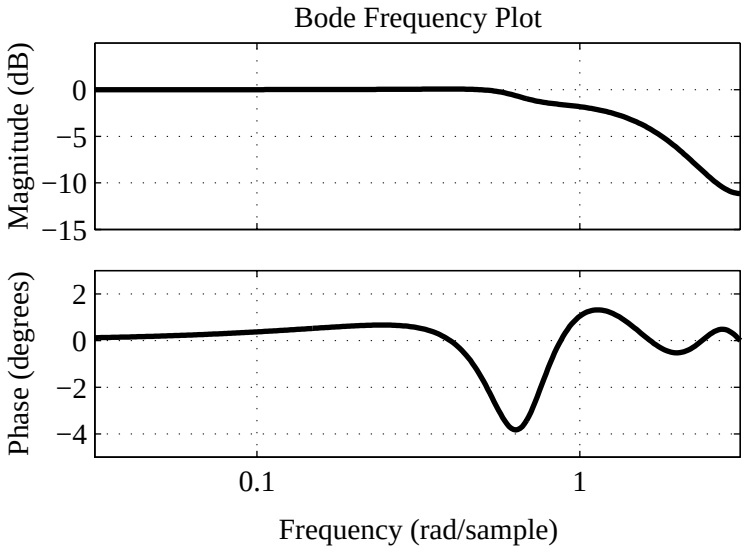

Figure 3.10: Frequency response of $z^2 G_{zpe}\Gamma_y$

satisfy the stability criterion, the most reasonable choice of δ to go along with G_{gain}, was $\delta = 3$. Interpreting this design, the repetitive controller is designed for a three-delay plant. The actual plant characteristics are a deviation from this nominal three-delay system. The frequency response of $z^3 G_{gain}\Gamma_y$ is shown in Fig 3.11. The lowpass characteristics are much larger, as is the phase variation. The phase, however is close to zero at lower frequencies. This inverse dynamics is of practical interest, independent of the resulting performance because of its simplicity. Whichever of these inverses is used, the appropriate δ is used to define the decimation scheme and δ_r as described in Eqns 3.5-3.7.

Frequency responses of $D_{stab}(z^{-1})$ are now shown for several cases. First, take G_{inv} to be G_{zpe} as in Fig 3.9 with $\delta = 2$. The quantities δ_r and ν (hence $\mathcal{D}$) are defined in terms of δ and r as described. The frequency response magnitudes of $D_{stab}(z^{-1})$ for $r = 1, 2, 4$ are shown in Fig 3.12. The interpolation scheme, $\mathcal{I}$, is taken as either a holder or a linear interpolator when r is 2 or 4. The magnitudes for these cases are all less than 1, so the nominal systems are stable. A lowpass $q_r(z, z^{-1})$ will not destabilize the nominal system – the magnitude of the frequency responses will remain less than 1. Notice that linear interpolation of the repetitive control signal can be considered better than holding the repetitive control signal in terms of the increased stability margin.

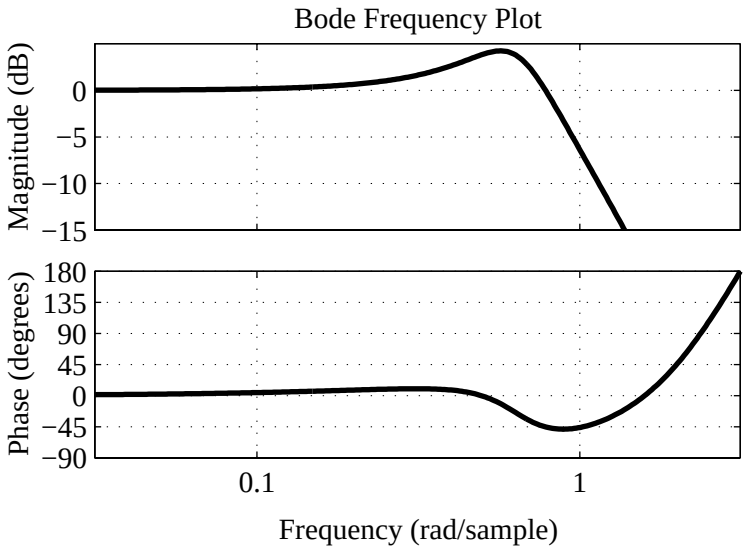

Figure 3.11: Frequency response of $z^3 G_{gain} \Gamma_y$

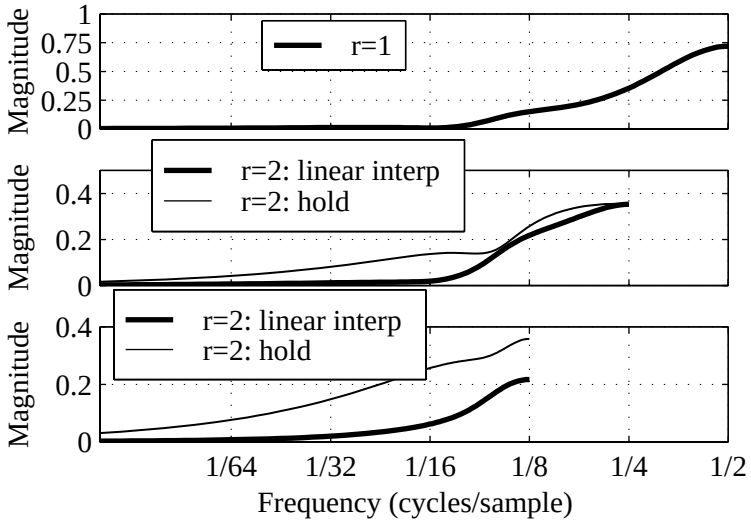

Figure 3.12: Magnitude plots of $(z^{-\delta_r} - \mathcal{DL}^r(G_{zpe}\Gamma_y)\mathcal{I})$

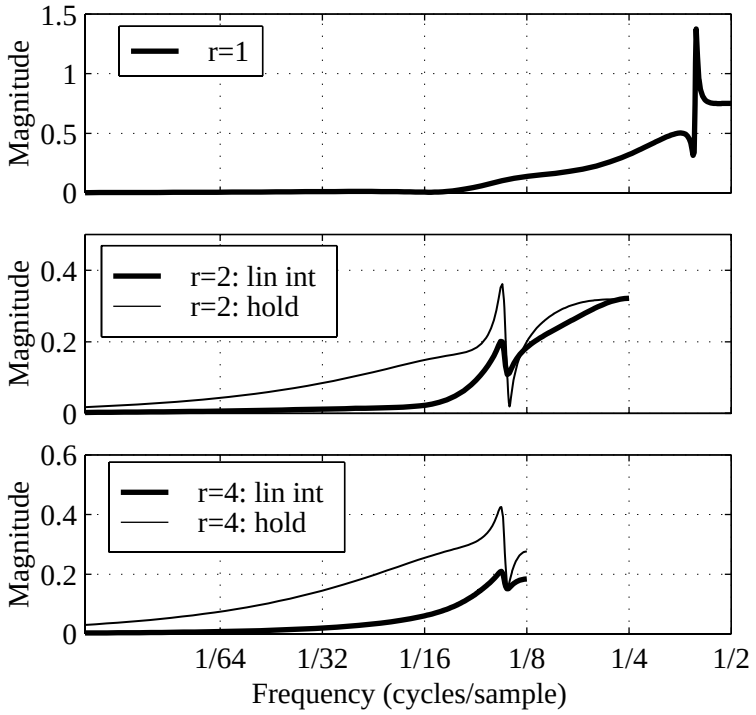

Figure 3.13: Magnitude plots of $(z^{-\delta_r} - \mathcal{D}\mathcal{L}^r(G_{zpe}\Gamma_y)\mathcal{I})$ with perturbed plant.

Next, the effect of a plant resonance on stability is shown through use of a similar set of plots shown in Fig 3.13. Stability is not guaranteed for this design when $r = 1$, which is the 1989 design. Some lowpass action in $q(z, z^{-1})$ would alow the perturbed system to be stable. For the other values of r, the closed loop repetitive control system will be stable for either interpolation scheme– the effect of the perturbation is not significant enough for the stability condition to be violated. The perturbation does, however significantly affect the frequency response magnitudes. This can be attributed to aliasing effects.

The same analysis is performed when G_{inv} is selected as G_{gain}. For this case, $\delta = 3$. The results in Figure 3.14 show the system will be stable for $r = 2$ or 4, but not $r = 1$. For stability of the system when r is one, a lowpass $q(z, z^{-1})$ with sufficient filtering action at higher frequencies may be used. Comparing to the use of the ZPE inverse, the effect of the plant resonance is not as large. This can be attributed to the more significant lowpass characteristics of Γ_y seen in Fig 3.7. The addition of a lowpass filter to G_{zpe} can achieve a

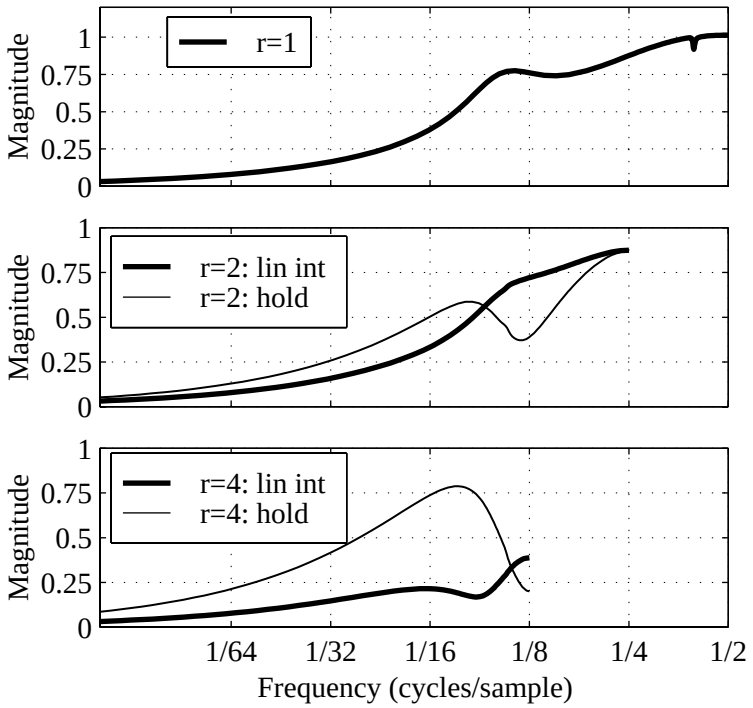

Figure 3.14: Magnitude plots of $(z^{-\delta_r} - \mathcal{D}\mathcal{L}^r(G_{gain}\Gamma_y)\mathcal{I})$ with perturbed plant.

similar effect, though adding complexity. That G_{gain} achieves an otherwise similar stability margin is attributed to the phase of Γ_y. It is very close to that of z^3 below the Nyquist frequency associated with the slow rate, Ω_s. It seems likely that such a choice for G_{inv} will generally be an option, as most closed loop systems are designed for predominantly second order characteristics. The phase of the closed loop at frequencies below the bandwidth will then generally approximate that of some number of pure delays.

As commented earlier, if a design meets the stability criterion in Eq 3.10 for a particular inverse dynamics, G_{inv}, it will also meet this criterion when $(1-\xi)G_{inv},\ 0 < \xi < 1$ is used for the inverse dynamics. Thus there is no need to show plots of $D_{stab}(z^{-1})$ for those cases. Scaling G_{inv} determines the learning rate of repetitive control in terms of closed loop pole locations as described in Section 2.3.

The above discussion did not use values of $q(z, z^{-1})$ other than 1. The reduced order repetitive control does not need any lowpass action for stability. The only reason to add $q(z, z^{-1})$is then for performance reasons, to reduce the effects of non-periodic disturbances. The choices for $q(z, z^{-1})$ or $q_r(z, z^{-1})$ considered are of the following form:

$$q\langle 2^n\rangle(z, z^{-1}) = \frac{1}{2^n}z + \frac{2^n - 2}{2^n}z + \frac{1}{2^n}z^{-1} \tag{3.60}$$

for some integer $n > 1$. Examples for $n = 2, 3, 4$ are:

$$q4(z, z^{-1}) = \frac{1}{4}z + \frac{2}{4} + \frac{1}{4}z^{-1} \tag{3.61}$$

$$q8(z, z^{-1}) = \frac{1}{8}z + \frac{6}{8} + \frac{1}{8}z^{-1} \tag{3.62}$$

$$q16(z, z^{-1}) = \frac{1}{16}z + \frac{14}{16} + \frac{1}{16}z^{-1} \tag{3.63}$$

This set of choices for $q(z, z^{-1})$ have zero-phase properties as well as the property that assembly code instructions to implement them in finite precision arithmetic are very simple. This is illustrated by the following pseudo-code fragment (assuming the next input is known):

```
<assume 'current' input in register 1> shift 'current' input value
down by (n-1) bits -- sub from register 1 shift 'next' input value
down by n bits -- add to register 1 shift 'old' input value down by n
bits -- add to register 1 <register 1 contains output>
```

These filters have zero phase, so only the frequency responses of their magnitude are shown in Figure 3.15. Note that the gain of $q4$ actually approaches zero at frequencies near the

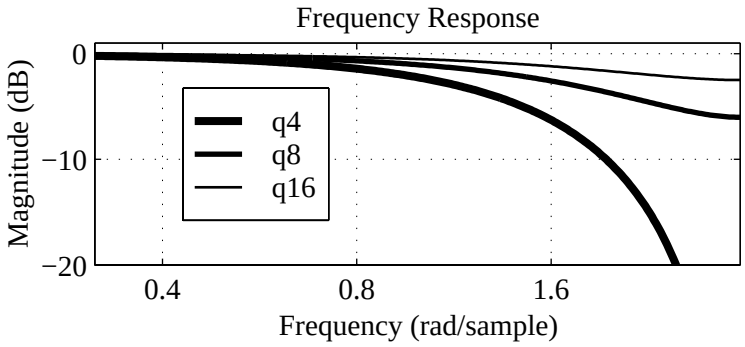

Figure 3.15: Magnitude responses of several $q(z, z^{-1})$ filters defined according to Eq 3.60.

Nyquist frequency, and that the other two filters exhibit comparably mild attenuation.

3.2.3 Performance

Stability was analyzed in terms of SISO transfer functions. To describe performance of the dual-rate systems analytically, a lifting approach was used to allow frequency domain interpretations of performance to be made.

First, the expected steady-state effect of periodic disturbances is described according to several measures. This is followed by a discussion of what the best case and worst case periodic disturbances are for several designs (augmented by simulation results). This is all in an effort to describe the sacrifice in performance inherent to these cost reduction measures. Additionally, time domain experimental and simulated results are shown.

Sensitivity to Sinusoidal Periodic Disturbances

The graph in Fig 3.16 shows the theoretical sensitivity of the PES to sinusoidal disturbances injected matched with the control input. These sinusoids are restricted to be at the frequencies making up the periodic disturbance, that is $2\pi/80$rad/sample and its harmonics. The results may be compared to the nominal sensitivity shown in Fig 3.7. The measures T_{sin} (top) and T_{tot} (bottom) are used to describe this sensitivity. Two reduction ratios, r, are compared, along with the two interpolation schemes. The inverse dynamics used for these designs was the approximate ZPE inverse. When the holding interpolation is used instead of the linear interpolation scheme, the reduction of the periodic disturbances

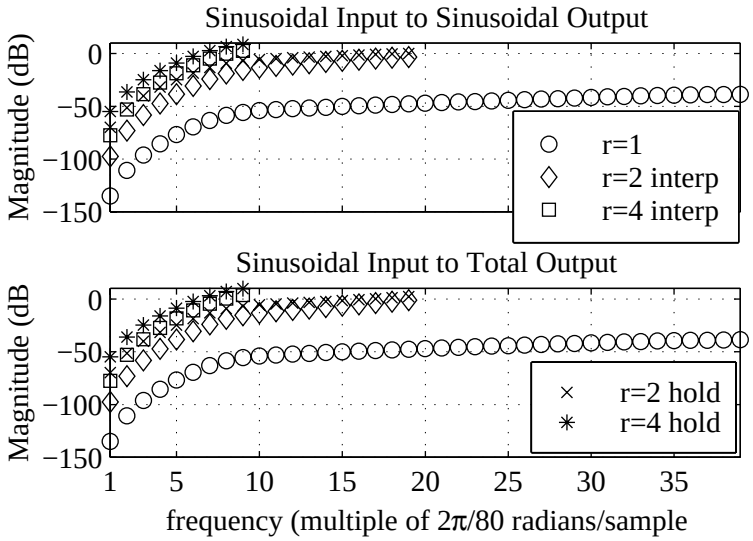

Figure 3.16: Reduction of Periodic Disturbances with G_{inv} as zero-phase inverse

is not as great. For higher reduction ratios, only periodic disturbances up to the Nyquist frequency of the slow rate were considered.

In comparison, Figure 3.17 shows the case when the inverse dynamics is selected as G_{gain}. For the single rate design, the benefit of using the ZPE inverse is apparent, but for the dual-rate designs the ZPE inverse is inferior to merely using a gain. The amplification of high frequencies by the ZPE inverse is the source of this difference. The results of adding the filter

$$f(z^{-1}) = z^{-2}\frac{6 + 4(z + z^{-1}) + (z^2 + z^{-2})}{16} \tag{3.64}$$

to G_{zpe} are shown in Fig 3.18. The design of δ_r and ν is modified accordingly to accomodate the two extra delays. This filter is a binomial filter based upon powers of 2, and will be easily implemented in hardware. Significant improvements in the reduction of the lower harmonic sinusoidal disturbances can be seen. In all three of these figures, the advantage of using linear interpolation over holding is apparent. In addition, the difference between the two measures of attenuation is not very significant. Sinusoidal disturbances at low frequencies do not introduce significant output errors at higher frequencies. A general trend is that higher reduction ratios correspond to less attenuation of periodic disturbances. In the next section, sacrifices of the dual-rate designs are further described.

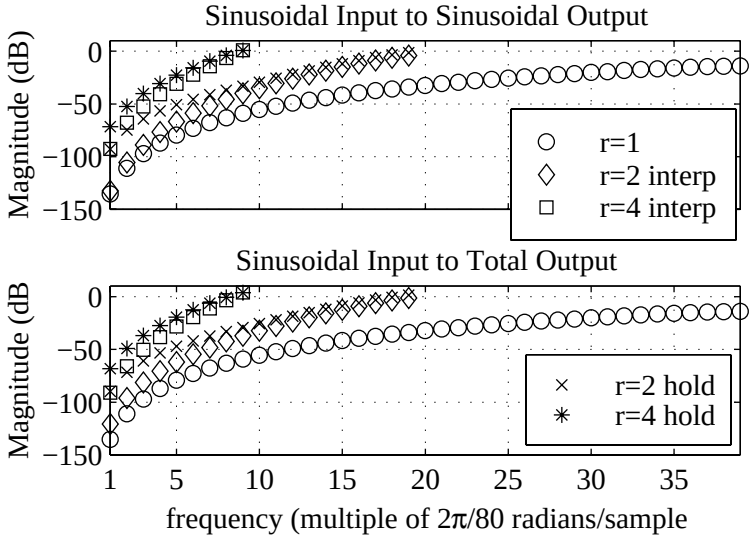

Figure 3.17: Reduction of Sinusoidal Disturbances with G_{inv} as a fixed gain

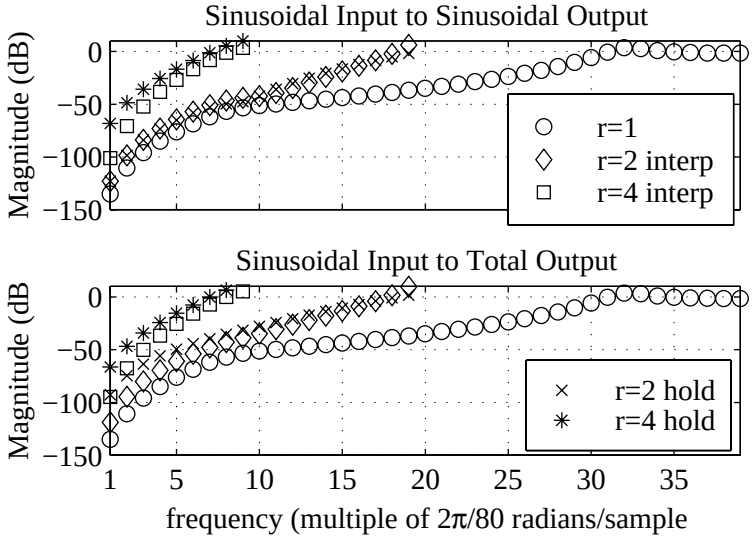

Figure 3.18: Reduction of Sinusoidal Disturbances with $G_{inv} = G_{zpe}f(z^{-1})$

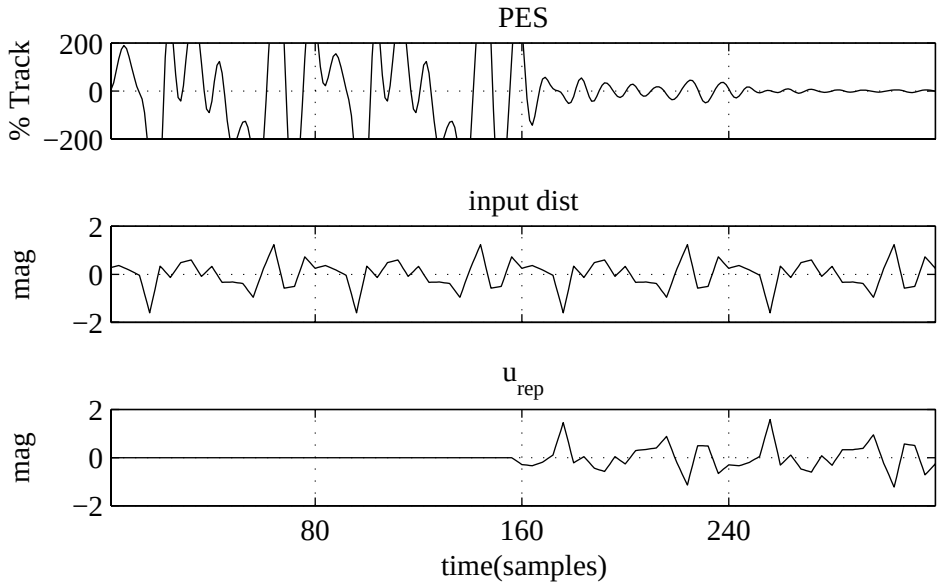

Figure 3.19: Simulated Example of Best Case Periodic Input Disturbance

Best and worst case disturbances

The effect of forcing the system with sinusoidal disturbances at the repetitive frequencies was described. In Section 3.1.5, descriptions of the periodic disturbances which are easiest to reject and most difficult to reject were made in terms of the quantity G_{ptv}. Simulation results show how these effects manifest themselves for the proposed designs. The reduction ratio, r, is set to be 4 for these examples, and the ZPE inverse, G_{zpe} is used. The simulations are conducted free of noise. The repetitive control loop is not closed until the 80th sample. This means that the first control signal does not appear until around the 160th sample. All initial conditions are set to zero. Referring to the development in the previous section, $\mathcal{D}$ and G_{inv} together with $\mathcal{I}$ determine the worst case inputs. For these examples, $\mathcal{I}$ is selected as a linear interpolation.

A best case input disturbance (any signal which could be the output of the interpolation scheme is a best case input disturbance) is randomly generated and the simulated time response of the repetitive control system shown in Figure 3.19. The response of the nominal system is indicated by the time response over the first cycle of the periodic disturbance. Note the approach to perfect rejection, and that the repetitive control signal

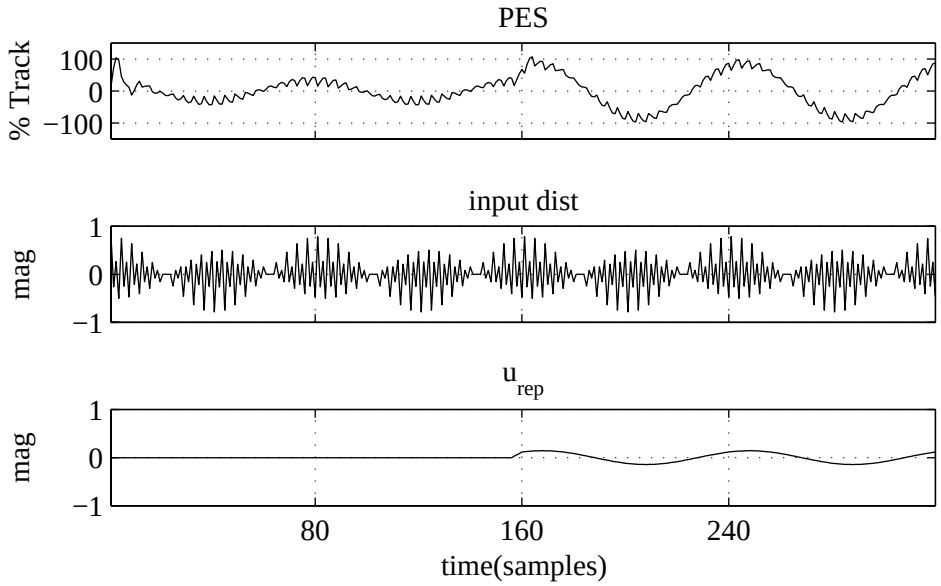

Figure 3.20: Simulated Example of Worst Case Periodic Input Disturbance

matches the input disturbance with flipped sign.

The worst case combination of aliased signals based at the fundamental period of the disturbance was then found by using G_{ptv} as described in Section 3.1.5. This disturbance is composed of the following frequencies:

$$\omega_1 = 2\pi/80,\ \omega_2 = 42\pi/80,\ \omega_3 = -78\pi/80,\ \omega_4 = -38\pi/80 \tag{3.65}$$

Denoting the negative frequencies is important for computing a time series to send into the simulation. The noise free simulated time response to this disturbance is shown in Fig 3.20. The higher frequency components introduce a low frequency tracking error. The magnitude scales are different from those in Figure 3.19. For this case, an input disturbance with size 1 introduces an output error of 1 track. Fortunately, the input disturbances are much smaller than this.

Simulation results computed for output, rather than input, disturbances are shown in Figures 3.22 and 3.21. For these output disturbances, frequencies aliased to the fundamental frequency were used. The worst case disturbance is quite small relative to the size of the best case disturbance, yet the size of the resulting repetitive control signals has the reverse relationship. In this case, the nominal feedback controller is cancelling a large part

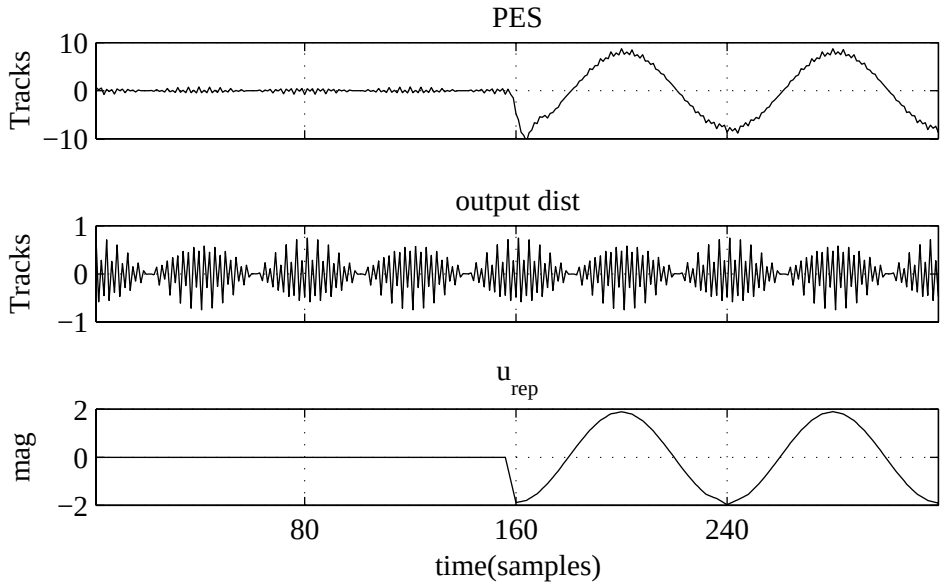

Figure 3.21: Simulated Example of Worst Case Periodic Output Disturbance

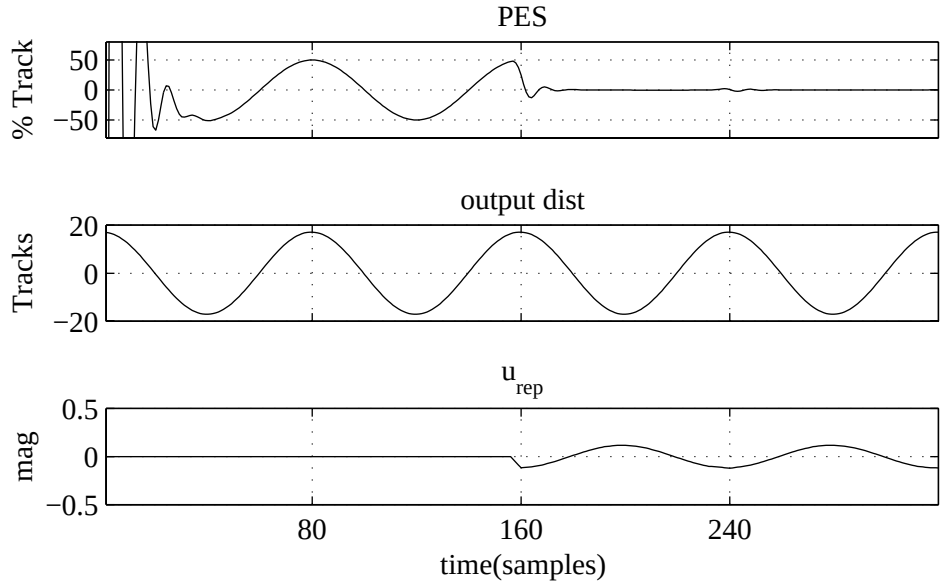

Figure 3.22: Simulated Example of Best Case Periodic Output Disturbance

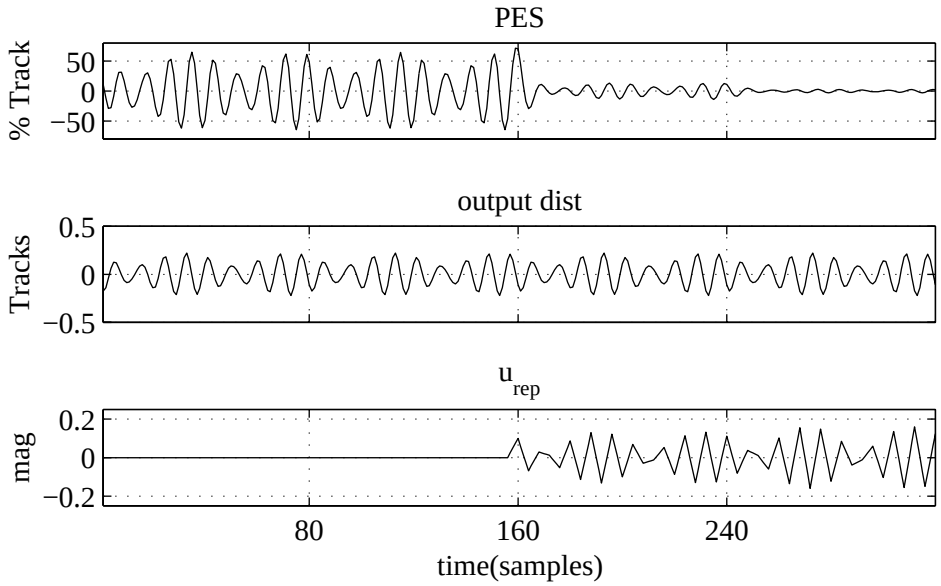

Figure 3.23: Simulated Example of Best Case Periodic Output Disturbance

of the repetitive control signal. The best case input is a sinusoidal signal at the fundamental periodic frequency.

Another example of the best and worst case output disturbances is given for the family of forcing frequencies based at $6\pi/80$ rad/sample. Simulations of the best and worst case output disturbance are shown in Figures 3.24 and 3.23. The best case disturbance is almost completely cancelled by the third cycle after repetitive control is turned on. The effect of the worst case disturbances is that they introduce significant tracking errors when compared with the nominal system.

The magnitudes of the components making up the worst case output disturbances are shown in Table 3.2. These are shown up to the 9th harmonic, as the 10th is at the slow rate Nyquist frequency. The low frequency components are in ω_1 and ω_4. The components at ω_2 and ω_3 are above a frequency of $\pi/2$ rad/sample and are larger in magnitude. The singular values of G_{ptv} associated with these worst case disturbances range from 15 to 18 (refer to the data in Table 3.4). This explains the amplification of these disturbances, though this amplification is associated with G_{ptv} rather than the closed loop system.

When G_{gain} instead is used for the inverse dynamics, these amplifications are

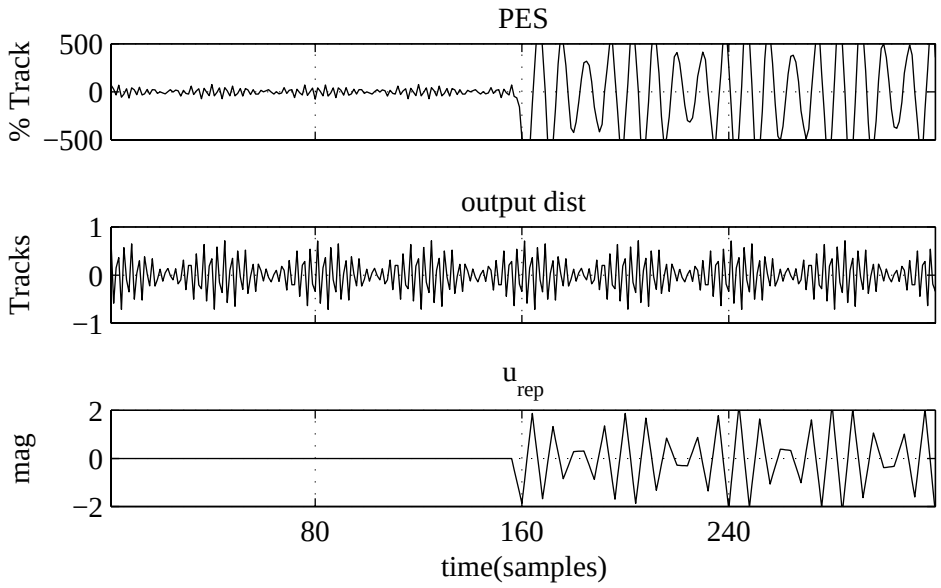

Figure 3.24: Simulated Example of Worst Case Periodic Output Disturbance

	Multiple of Fundamental Frequency								
	1	2	3	4	5	6	7	8	9
ω_1	0.0086	0.0082	0.0076	0.0068	0.0059	0.0050	0.0047	0.0053	0.0066
ω_2	0.2555	0.2990	0.3460	0.3960	0.4481	0.5015	0.5549	0.6076	0.6586
ω_3	0.9498	0.9426	0.9304	0.9131	0.8907	0.8632	0.8308	0.7937	0.7523
ω_4	0.1803	0.1487	0.1209	0.0968	0.0759	0.0581	0.0429	0.0293	0.0147

Table 3.2: Magnitude of frequency components of worst case output disturbances when G_{zpe} is used

	Multiple of Fundamental Frequency								
	1	2	3	4	5	6	7	8	9
ω_1	0.0157	0.0162	0.0170	0.0177	0.0184	0.0195	0.0230	0.0358	0.0759
ω_2	0.4675	0.4928	0.5183	0.5440	0.5698	0.5956	0.6211	0.6457	0.6688
ω_3	0.7787	0.7759	0.7713	0.7650	0.7571	0.7475	0.7360	0.7225	0.7067
ω_4	0.4180	0.3935	0.3690	0.3443	0.3191	0.2936	0.2683	0.2446	0.2180

Table 3.3: Magnitude of frequency components of worst case output disturbances when G_{gain} is used

	Multiple of Fundamental Frequency								
	1	2	3	4	5	6	7	8	9
G_{zpe}	16.02	16.26	16.66	17.24	17.96	18.55	18.12	15.53	11.79
G_{gain}	2.01	2.03	2.07	2.13	2.20	2.26	2.19	1.87	1.42
G_{zpe} w/ $q4$	4.03	3.99	3.93	3.86	3.77	3.62	3.28	2.63	1.90
G_{zpe}w/ $f(z^{-1})$	2.18	2.14	2.07	1.97	1.85	1.68	1.42	1.05	0.71

Table 3.4: Worst case singular values of G_{ptv} at harmonics

on the order of 2, as shown in Table 3.4. The worst case disturbances corresponding to these smaller gains include more of the ω_4 frequency component (Table 3.3). The addition of lowpass filtering in the form of $q4$ to G_{zpe} drops the size of this singular value to the range between 2 and 4, as shown in Table 3.4, with similar shifts of worst case disturbance components to ω_4. Further reduction of these worst case singular values is accomplished with the use of the binomial filter $f(z^{-1})$ defined in Eq 3.64 (Table 3.4). To compare this effect in terms of the worst case disturbances simulated for the design based on G_{zpe}, a worst case disturbance is simulated for a design based on $G_{zpe}f(z^{-1})$. The results shown in Figure 3.25 may be directly compared to that in Figure 3.24. Note the much more benign degradation of the nominal behavior of the system. It is amplified roughly by a factor of 2.

Realistic Simulations

Noise and disturbance signals based upon the experimental system are added to the simulation in this section. Gaussian distributed noise is inserted into the simulation at the input and output. As the output noise is meant to represent errors in measuring the PES, it is given a standard deviation of 1 percent of a track width. The input noise is

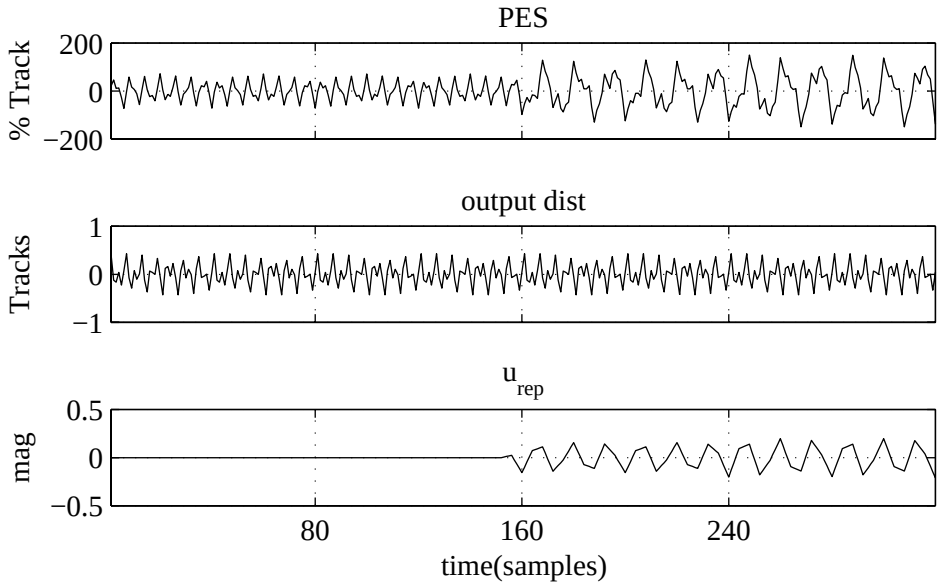

Figure 3.25: Worst case output disturbance for $G_{zpe}f(z^{-1})$

additive with the control. In the actual system, 14 bits are used to determine the control signal between -2 and 2 Volts. Thus, the standard deviation of this noise is set at the resolution of the control. This reflects the fact that the simulation is done in floating point, and the actual control will be done in finite precision. The simulated response of the nominal system to these noises in the absence of periodic disturbances is shown in Fig 3.26. The effect of these noises on the PES is shown over a single cycle. The PES lies roughly in the range of $\pm 4\%$ of a track. This meets the track following requirements for less than 10% of a track of positioning error.

A periodic output disturbance (track runout) is added to the system. It consists of a combination of sinusoidal disturbances at the fundamental, second, and sixth harmonic. The amplitudes are taken as 17, 2, and 0.25 tracks respectively. Comparisons of the performance of dual-rate repetitive control for $r = 1, 2, 4$ are shown. For the $r = 1$ design, G_{zpe} and $q4$ were used. For the $r = 2$ design, $q_r(z, z^{-1}) = q64$ was used and the inverse dynamics were taken as $G_{zpe}q4$. For the $r = 4$ design, $q_r(z, z^{-1}) = 1$ was used and the inverse dynamics were selected as $G_{zpe}f(z^{-1})$. The tracking errors which result with these different repetitive controllers are predominantly the same. For repetitive runouts in these

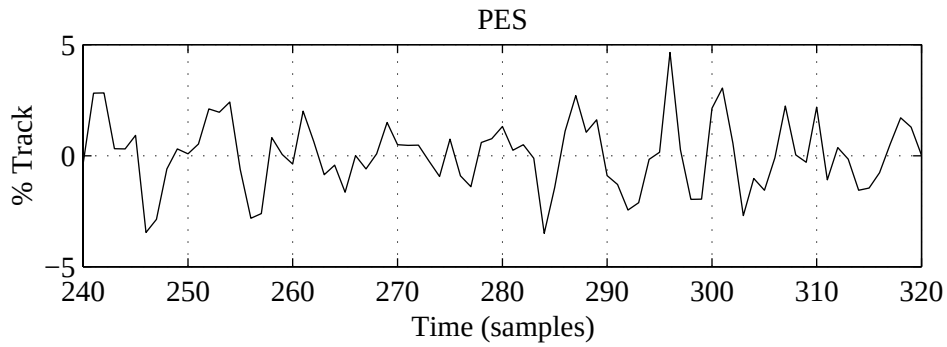

Figure 3.26: Noises and the nominal system

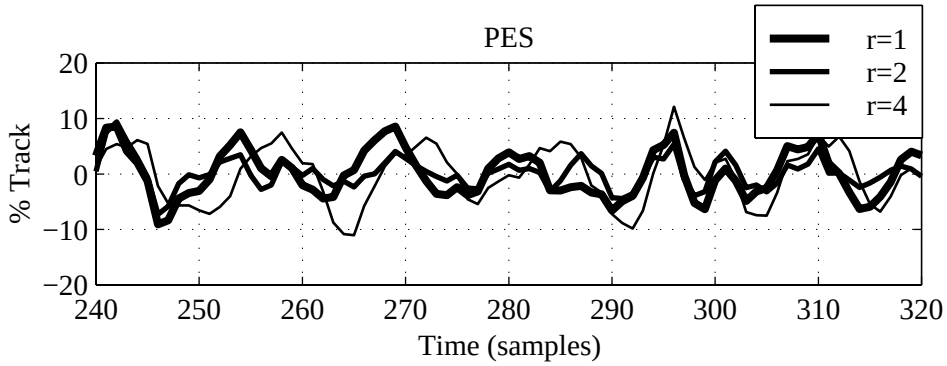

Figure 3.27: Simulated comparisons of $r = 1, 2, 4$ designs

lower frequency ranges, reduced order repetitive control makes sense.

Experimental Results

The experimental results presented are based upon time histories (over 12 revolutions) of internal digital signals of the microcontroller. The repeatable component of the error is computed as 80 separate averages of the 12 errors at each sector. This repeatable component of the error is used to describe the rejection of the periodic disturbance. The output of the repetitive controller over a cycle is also shown. For experiments, different values of $q(z, z^{-1})$ as described in Eq 3.60 were used with visible effects on performance. The inverse dynamics were scaled down, specifying cycle to cycle time constants of 0.5 and higher, mildly learning the periodic disturbance, and limiting the learning of noise.

In Figure 3.28, experimental results which show the introduction of aliased frequency components in the error are shown. These effects are easily seen in the magnitudes of the fundamental and harmonic components of the output shown in the top figure. Using a linear interpolation scheme is marginally more costly, but most probably worth its cost in terms of performance. The reduction ratio was set to 4, and a scaled down G_{gain} was used for the inverse dynamics. The filter $q(z, z^{-1})$ was set to $q32$. The two results are shown on the same plot, but because the data was collected separately, the phases relative to the data collection do not match. Note the holding and interpolated shape of the applied repetitive control signal.

In Fig 3.29, experimental results are shown which contrast designs with $r = 1$ and $r = 4$. The periodic component of the error is shown in the top figure, and a non-periodic component over one cycle is shown in the bottom figure. Notice that the non-periodic errors in each case are larger than the periodic errors – there are significant other disturbances. For this comparison, G_{gain} and $q4$ were used for the $r = 1$ design, and G_{zpe} was used with $q256$ for the $r = 4$ design. In both cases, gains of the inverse dynamics were reduced significantly to accomodate the other disturbances.

The experimental results in Fig 3.30 show the effect of $q(z, z^{-1})$ on the performance of the system. For this comparison, a scaled gain inverse, G_{gain}, was used. The frequency components of the periodic portion of the PES, show that moving $q(z, z^{-1})$ closer to unity corresponds to more attenuation of the fundamental component of runout. The peak at the 10th harmonic in this design corresponds to the Nyquist frequency associated with a

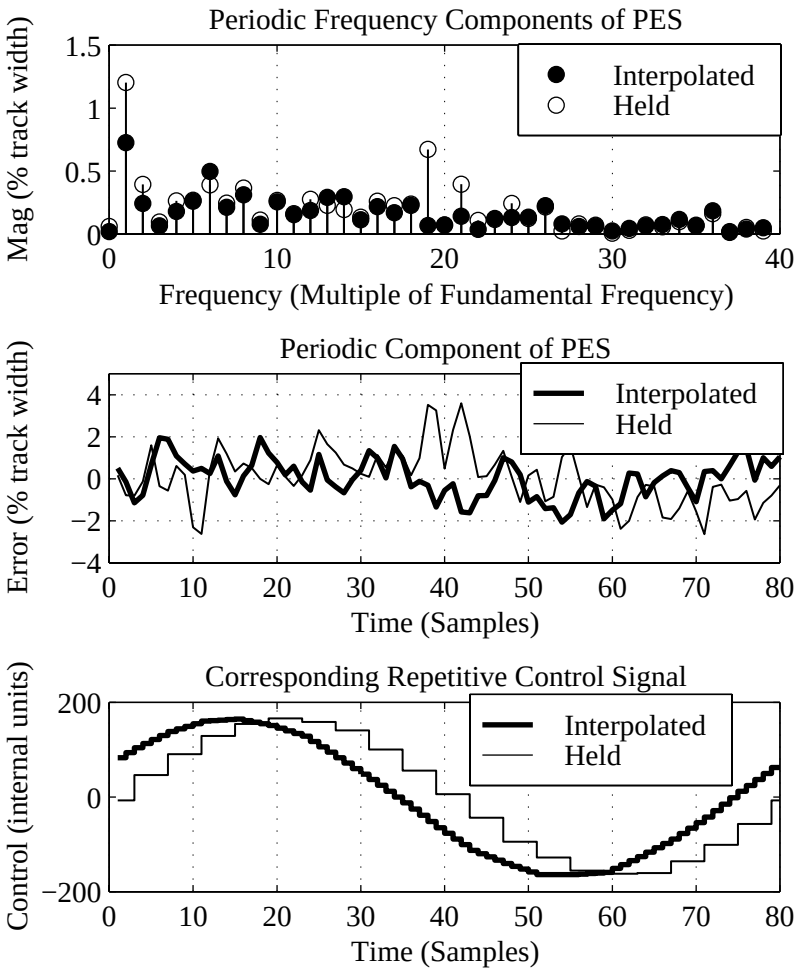

Figure 3.28: Experimental Comparison of Linear Interpolation and Holding of the Repetitive Control Signal for $r = 4$

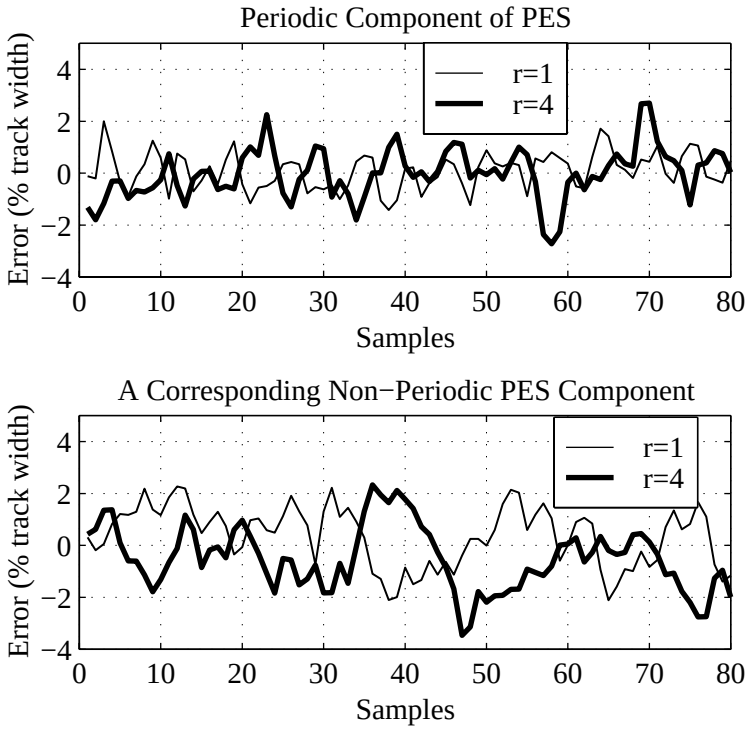

Figure 3.29: Experimental Comparison of $r = 4$ vs. $r = 1$

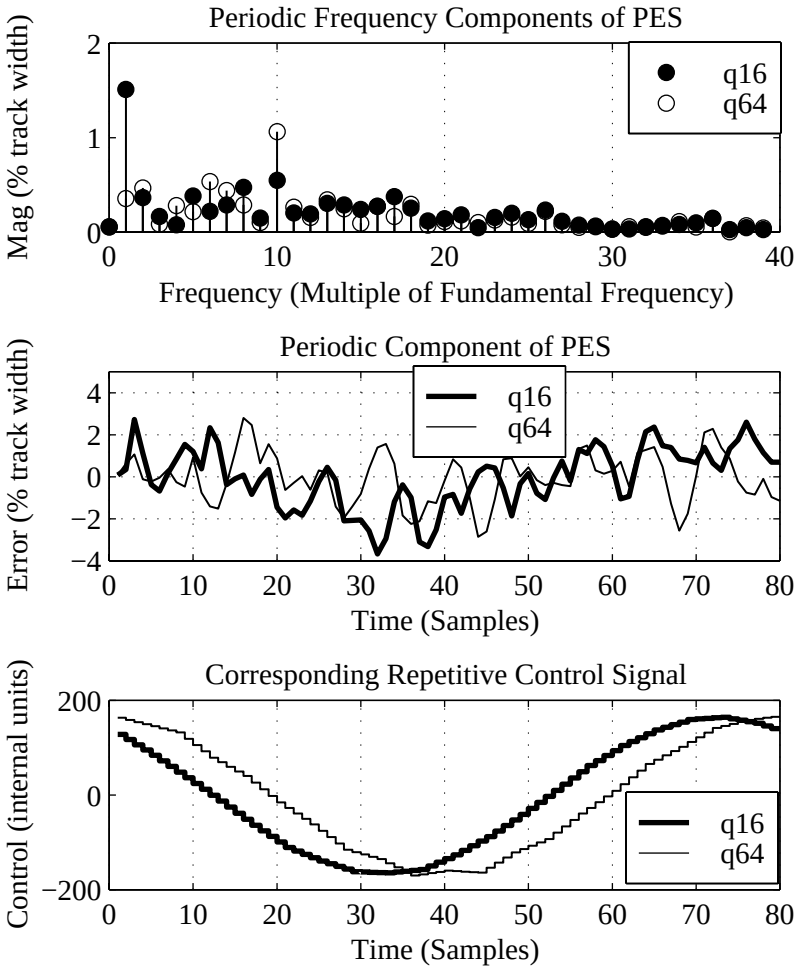

Figure 3.30: Experimental Results for $r = 4$ with $q(z, z^{-1})$ either $q16 = \frac{1}{16}z + \frac{14}{16} + \frac{1}{16}z^{-1}$ or $q64 = \frac{1}{64}z + \frac{62}{64} + \frac{1}{64}z^{-1}$

sampling rate 4 times slower than the measurement rate. The repetitive controller has no control authority at this frequency.

3.3 Concluding Remarks

The analysis and design techniques for dual-rate repetitive controllers described in Section 3.1 were applied to a disk drive servosystem. For repetitive control applied to this experimental setup, a 75% reduction in the memory usage of the repetitive controller was made while maintaining performance relative to the 1989 repetitive controller design. Reduced memory was appropriate for this application because of the concentration of periodic disturbances at lower frequency components of the periodic disturbances.

The effects of interpolation and decimation on the system were examined. The interpolation scheme is the predominant descriptor of which periodic disturbances can be rejected. Based on a given interpolation scheme, the combination of decimation and inverse dynamics determines worst case amplifications of these signals. When low-pass filtering action was added to G_{inv} in the form of $f(z^{-1})$ or $q4$, significant improvements in the performance of the repetitive controller were possible. The stability of such a design is guaranteed via the same proof as in Section 3.1.3, replacing occurrences of $\alpha(z, z^{-1})$ with $\alpha(z, z^{-1})f(z^{-1})$ or $\alpha(z, z^{-1})q4$. The computational load of this extra filtering action can be absorbed into the decimation scheme using the reverse of the decomposition in Eq 3.15. For the proposed filters, $q4$ or $f(z^{-1})$, which use powers of two, the decimation scheme will be computationally efficient. In this design example, they proved to be appropriate choices.

Chapter 4

Cascaded Repetitive Controllers

A new structure for discrete time repetitive controllers is proposed in this Chapter, with a design method based upon the $\mathcal{H}_\infty$ performance measure from Section 2.3. This new structure is motivated by efforts to minimize the complexity of repetitive control implementations. The addition of repetitive control to a system stabilized by observer state feedback is specifically described, but the ideas and methods should easily extend to other control systems. In a departure from existing design methods, the states of a stabilizing controller are used in addition to the plant output to drive the repetitive controller. The computation done by the stabilizing controller is done in series with that of the repetitive controller rather than parallel. The design method is applied to a model of a computer disk drive servosystem. The first section describes the controller and design method, and the second describes the results of applying this method to the disk drive servosystem model. Comparisons are made with the 1989 design.

4.1 Development

As noted above, the addition of repetitive control to a lumped system including an internal feedback controller is under consideration. This repetitive controller is designed as a multi-input-single-output controller. The regulated ouput of the lumped plant is augmented by the states of the internal feedback controller. Periodic errors at the output are the primary concern, but they cause periodic components in every internal signal of the control system. The internal states of the controller are typically available – it does not make sense to base designs only on the plant output. The internal feedback controller is nothing more

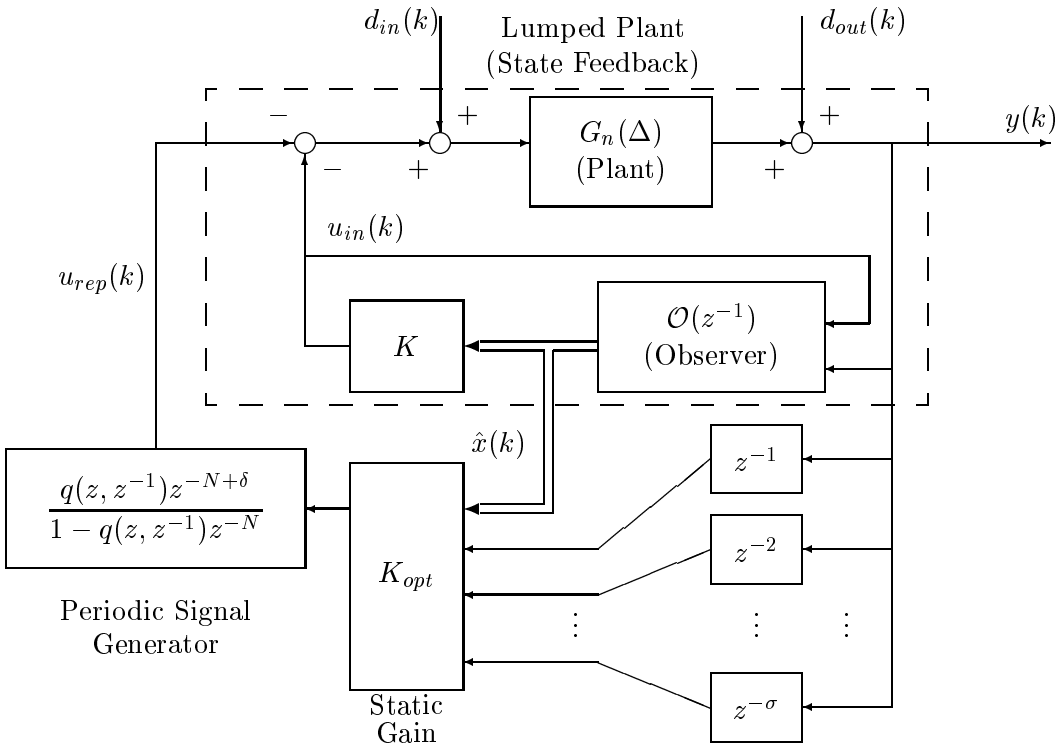

Figure 4.1: Cascaded Repetitive Control Structure

than a filter of the output signal. Since this filtering action could be reproduced by the repetitive controller in the outer loop, in some sense no extra information about the system is being used relative to the 1989 design. The additional benefit of using the filtered output is along the lines of the following analogy: if one has immediate access to both a number and its higher powers, the evaluation of a polynomial is possible with just the number, but far easier directly using all of its powers. A description of the cascaded discrete time repetitive controller structure is followed by a description of the design method.

4.1.1 Structure

A block diagram of the proposed repetitive controller structure (henceforth referred to as the Cascaded structure) is shown in Fig 4.1. There is significant similarity to the 1989 structure shown in Fig 2.3. The periodic signal generator is common to both designs. The system to which repetitive control is being applied (the lumped plant, including the assumed state feedback control action) is indicated. The observer states are directly accessed by the repetitive controller. This allows the computational effort expended in the observer to be

used for repetitive control.

The following assumptions are made:

- All systems and signals are in the discrete time domain.
- The period of the repetitive disturbances is N samples. The signals $d_{in}(k)$ and $d_{out}(k)$ may both have periodic disturbance components. These are lumped at $d_{in}(k)$, matched with the repetitive controller input $u_{rep}(k)$.
- The uncertainty in the plant is denoted by Δ, without specifying an uncertainty model. This is a bookkeeping measure directed at future work on robustness. This annotation of uncertainty is carried into closed loop transfer functions dependent on the plant.
- The observer state feedback control law is a given design. The closed loop behavior without repetitive control is appropriate and desirable in the absence of periodic disturbances.

The cascaded structure depicted in Figure 4.1 is parameterized by σ, K_{opt}, δ, and the filter $q(z, z^{-1})$. The choices of these parameters clearly depend on the lumped plant and the disturbance characteristics. Of these, δ and σ are nonnegative integers. In the PSG, δ is used to compensate for the delayed effect of disturbances on the output. The input to the periodic signal generator at time k is attributed to the repetitive disturbance at time $k - \delta$.

In addition to using the observer states, a delay chain with length parameterized by σ is applied to the output signal, allowing outputs up to σ steps in the past to be used by the repetitive controller. Therefore, the parameter σ determines the computational complexity of the design. Each additional stored output will add the computational cost of a multiply and an addition to the total computational cost associated with the controller.

The parameter K_{opt} is a row of static gains. Its length is the number of observer states plus σ. It contains weightings for each of these inputs, taking their linear combination and sending it to the PSG.

The filter $q(z, z^{-1})$ is a zero-phase moving average filter as in the 1989 structure. The effect of $q(z, z^{-1})$ on the PSG is decreased sensitivity to higher frequency components of the repetitive signals. These are typically more corrupted by non-periodic disturbances.

The stability and performance of the repetitive controller is also less susceptible to uncertainty in the plant at higher frequencies when a lowpass $q(z, z^{-1})$ is used (refer to Sections 2.1 and 2.3).

The repetitive control signal, $u_{rep}(k)$, though it is a control input, is not considered a control input by the observer. The observer state feedback control signal, $u_{in}(k)$, is taken as the only input to the plant for the purposes of the observer. This can be understood as follows: when $u_{rep}(k)$ successfully cancels the effect of periodic disturbances, the internal loop is operates in the conditions for which it was designed (with no repetitive disturbances).

Closing the feedback loop of $u_{in}(k)$ around the observer incorporates the state feedback control law into a new observer system, denoted by $\tilde{\mathcal{O}}(z^{-1})$, which has only $y(k)$ as an input, instead of both $y(k)$ and $u_{in}(k)$. Set K_{opt} in Fig 4.1 equal to zero (no repetitive control loop). The closed loop transfer function matrices then describe only the lumped plant. The transfer functions $\Gamma_y(\Delta)$ ($u_{rep}(k)$ to $y(k)$), $\Gamma_{\hat{x}}(\Delta)$ ($u_{rep}(k)$ to $\hat{x}(k)$) , and $\Gamma_{ext}(\Delta)$ ($u_{rep}(k)$ to the input signals to K_{opt}) are given below:

$$\Gamma_y(\Delta) = \frac{G_n(\Delta)}{1 + K\tilde{\mathcal{O}}(z^{-1})G_n(\Delta)} \tag{4.1}$$

$$\Gamma_{\hat{x}}(\Delta) = \frac{\tilde{\mathcal{O}}(z^{-1})G_n(\Delta)}{1 + K\tilde{\mathcal{O}}(z^{-1})G_n(\Delta)} \tag{4.2}$$

$$\Gamma_{ext}(\Delta) = \begin{bmatrix} \Gamma_{\hat{x}}(\Delta) \\ z^{-1}\Gamma_y(\Delta) \\ \vdots \\ z^{-\sigma}\Gamma_y(\Delta) \end{bmatrix} \tag{4.3}$$

A derivation of the closed loop transfer function from $u_{rep}(k)$ to $y(k)$, Φ_y, for some nonzero K_{opt} is made in terms of these transfer functions as follows:

$$\Phi_y = \frac{G_n(\Delta)}{1 + \left(K\tilde{\mathcal{O}} + \frac{qz^{-N+\delta}}{1-qz^{-N}}K_{opt} \begin{bmatrix} \tilde{\mathcal{O}} \\ z^{-1} \\ \vdots \\ z^{-\sigma} \end{bmatrix} \right) G_n(\Delta)} \tag{4.4}$$

$$= \frac{\Gamma_y(\Delta)}{1 + \frac{q(z,z^{-1})z^{-N+\delta}}{1-q(z,z^{-1})z^{-N}}K_{opt}\Gamma_{ext}(\Delta)} \tag{4.5}$$

and finally,

$$\Phi_y = \Gamma_y \frac{1 - q(z, z^{-1})z^{-N}}{1 + q(z, z^{-1})z^{-N+\delta}(z^{-\delta} - K_{opt}\Gamma_{ext}(\Delta))} \tag{4.6}$$

The term $K_{opt}\Gamma_{ext}(\Delta)$ manifests the linear combination of closed loop signals as a linear combination of closed loop transfer functions.

The elements of the transfer matrix $\Gamma_{ext}(\Delta)$ share a common characteristic equation modulo the effect of pure delays (that of the nominal closed loop). Therefore, this same characteristic equation is also that of $K_{opt}\Gamma_{ext}(\Delta)$ assuming there are no pole-zero cancellations. Similarly, the zeros of $G_n(\Delta)$ are zeros of each of the transfer functions which make up $\Gamma_{ext}(\Delta)$, so they will be zeros of $K_{opt}\Gamma_{ext}(\Delta)$ unless cancelled by an observer pole. The choice of K_{opt} determines the placement of the remaining zeros of $K_{opt}\Gamma_{ext}(\Delta)$. Appropriate selection of these zeros can cancel poles of the closed loop characteristic equation. Such pole-zero cancellations are used by the ZPE inverse when possible (Appendix A.1).

4.1.2 Design Method / Performance

The small-gain theorem can be used to arrive at a sufficient condition for the stability of the closed loop. This is done with a similar block diagram manipulation as for the dual-rate and 1989 designs. The closed loop system will be asymptotically stable when

$$\|(z^{-\delta} - K_{opt}\Gamma_{ext}(\Delta))q(z, z^{-1})\|_\infty < 1 \tag{4.7}$$

The proposed design method developed initially from using this condition to examine the stability of the cascaded structure. Making this quantity much less than 1 makes the performance of the repetitive control system defined roughly by $1 - q(z, z^{-1})z^{-N}$. These relationships inspired the definition of the repetitive control performance index described in Section 2.3 though now they are presented in reverse order.

The closed loop transfer functions associated with the cascaded structure and the convenient form of Φ_y given in Eq (4.6) are used to write the performance index described in Section 2.3 applied to a cascaded design. Assuming $q_w(z, z^{-1}) = q(z, z^{-1})$, the performance is written in terms of K_{opt}, δ, and σ as follows:

$$\mathrm{J_{rep}}(K_{opt}) = \max_{|z|=1} \left| \frac{qz^{-N+\delta}\left((1-\xi)z^{-\delta} - K_{opt}\Gamma_{ext}(\Delta)\right)}{1 - qz^{-N+\delta}(z^{-\delta} - K_{opt}\Gamma_{ext}(\Delta))} \right| \tag{4.8}$$

The functional dependence of the performance is given to K_{opt}, assuming fixed values for σ and δ. The design method for K_{opt} is to minimize this performance measure.

The process of designing cascaded repetitive controllers of various complexity (σ) based on the performance index parameters ξ and q_w proceeds as follows:

1. select $q(z, z^{-1}) = q_w(z, z^{-1})$
2. for $\sigma = 0, 1, 2, 3, ...$ (increasing complexity)
   (a) for each $\delta = 1, 2, 3, 4, ..., N$ find the best choice of K_{opt} according to Eq 4.8
   (b) use the best combination of δ and K_{opt} to define the design for this σ.

That other choices for $q(z, z^{-1})$ in the controller might be optimal is a possible topic for future research. When applied to the 1989 design, the boundaries between whether the design determines the performance index, or vice versa are difficult to draw. In this case, the performance index determines the design. It is hoped to match the closed loop behavior of an "ideal" repetitive control system described by the parameters q_w and ξ.

The portion of this objective requiring further explanation is the selection of the best K_{opt} for fixed values of σ and δ. A global search for the optimal K_{opt} is one option. The motivation for this design was predominantly that of saving computation cost. When the number of parameters is small, a global gridded search could restrict attention to values of K_{opt} which can be implemented with some fixed number of bit shifts and adds. This is an attractive approach. It was not taken here. The performance index $\mathrm{J_{rep}}(K_{opt})$ is not convex in K_{opt}. The potential to extend this design technique to include other criteria for which convex optimization tools may be useful motivates posing an objective which is convex in K_{opt}. The incorporation of tolerance to uncertainty is one example of such an extension. An approximation to the performance index therefore defined which is convex in K_{opt}. To make this approximation, first define

$$P_{K_{opt}} \doteq qz^{-N+\delta}\left((1-\xi)z^{-\delta} - K_{opt}\Gamma_{ext}(\Delta)\right), \tag{4.9}$$

which is affine in K_{opt}, and substitue into $\mathrm{J_{rep}}(K_{opt})$ as follows:

$$\mathrm{J_{rep}}(K_{opt}) = \max_{|z|=1}\left|\frac{P_{K_{opt}}}{1-\xi qz^{-N}-P_{K_{opt}}}\right|. \tag{4.10}$$

Notice that for $\mathrm{J}_{\mathrm{rep}}(K_{opt})$ to be small, the magnitude of the frequency response of $P_{K_{opt}}$ must be small. Define an approximate performance measure $\hat{\mathrm{J}}_{\mathrm{rep}}(K_{opt})$ as:

$$\hat{\mathrm{J}}_{\mathrm{rep}}(K_{opt}) \doteq \| \frac{P_{K_{opt}}}{1 - \xi q z^{-N}} \|_\infty \tag{4.11}$$

A bound on the error of this approximation can be formulated in terms of the value it achieves. Assume

$$\hat{\mathrm{J}}_{\mathrm{rep}}(K_{opt}) = \gamma \tag{4.12}$$

With this assumption,

$$\frac{\gamma}{1+\gamma} < \mathrm{J}_{\mathrm{rep}}(K_{opt}) < \frac{\gamma}{1-\gamma} \tag{4.13}$$

For stability, $\gamma < 1 - |\xi|$ is sufficient (compare Eqs 4.7 and 4.9). This implies that when the error of this approximation is important, γ will be less than 1. For larger values of $\xi \in [-1, 1]$, the approximation is guaranteed to improve. This new performance index, $\hat{\mathrm{J}}_{\mathrm{rep}}(K_{opt})$, *is* a convex function of K_{opt}. In the design example which follows, K_{opt} is designed by minimizing $\hat{\mathrm{J}}_{\mathrm{rep}}(K_{opt})$ instead of $\mathrm{J}_{\mathrm{rep}}(K_{opt})$. The performance may be measured in terms of $\mathrm{J}_{\mathrm{rep}}(K_{opt})$ using the optimal design for $\hat{\mathrm{J}}_{\mathrm{rep}}(K_{opt})$.

This concludes the development of this control algorithm. The development relies heavily on the use of the performance objective function described in Section 2.3.

4.2 Application to Magnetic Disk Drive

The cascaded design is applied to a model of a computer disk drive track following control system. This is an application where there is interest in saving computational complexity as described in previous chapters. The model data is given in Appendix B.3. Emphasis is placed on the design methodology. Simulation studies augment the analytical data in lieu of experiments.

The disk drive system consists of a third order model and a third order observer state feedback controller. Thus, for $\sigma = 0$, K_{opt} will be an 1×3 vector. The periodic disturbances to the system were assumed to have a period of 80 samples.

The design method depends on the performance index of Section 2.3, and hence on $q_w(z, z^{-1})$ and ξ. The filter $q_w(z, z^{-1})$ was selected as the zero-phase moving average filter $q_w(z, z^{-1}) = 0.25z + 0.5 + 0.25z^{-1}$. This choice is easy to implement via bit shifting.

Designs for $\xi = 0,\ 0.25,\ \&\ 0.5$ are compared to illustrate that the desired effect of ξ on the closed loop system described in Section 2.3 is achieved by the resulting designs of the cascaded repetitive controller.

4.2.1 Designing for different complexities (σ)

For given values of $q_w(z, z^{-1})$ and ξ, a design procedure was proposed in the previous section. The K_{opt} which minimizes the approximated performance index, $\hat{\mathrm{J}}_{\mathrm{rep}}(K_{opt})$, is used as the best design for a given δ and σ. When σ is increased, the number of parameters in K_{opt} changes. Every cascaded repetitive controller with $\sigma = \sigma_1$ is also possible when $\sigma > \sigma_1$, so increasing σ should decrease the optimal values of both $\mathrm{J}_{\mathrm{rep}}(K_{opt})$ and $\hat{\mathrm{J}}_{\mathrm{rep}}(K_{opt})$. The only barrier to continually increasing σ for performance enhancement is the additional cost associated with using larger values of σ. The performance gained for larger σ needs to be traded off with additional implementation costs.

The numerical procedure used to evaluate $\hat{\mathrm{J}}_{\mathrm{rep}}(K_{opt})$ used the MATLAB Optimization Toolbox function, `minimax`. The arguement of $\hat{\mathrm{J}}_{\mathrm{rep}}(K_{opt})$ is an affine function of K_{opt}. It was expanded into the following form using the elements of K_{opt}, $K_{opt}(i)$ for $1 \leq i \leq \sigma + 3$:

$$\frac{P_{K_{opt}}}{1 - \xi z^{-N}} = 1 + G_1(z^{-1})K_{opt}(1) + G_2(z^{-1})K_{opt}(2) + \cdots + G_{3+\sigma}K_{opt}(3+\sigma) \qquad (4.14)$$

The frequency responses of the scalar valued G_i were computed over a grid of frequency. Then the value of K_{opt} resulting in the smallest peak over frequency of this linear combination was found using a call to `minimax`.

The combination of δ and K_{opt} which minimizes $\hat{\mathrm{J}}_{\mathrm{rep}}(K_{opt})$ was found this way for each value of σ. Applied to the example system, a sixth order closed loop, the optimal values of K_{opt} were computed over a grid of σ and δ with $\xi = 0$. Table 4.1 shows the resulting minimum values of $\hat{\mathrm{J}}_{\mathrm{rep}}(K_{opt})$. The numbers in bold indicate the smallest cost and hence best choice of δ for each value of σ, the complexity. Notice that all of the values are less than 1, so all of these repetitive control systems will be asymptotically stable. The reduction in $\hat{\mathrm{J}}_{\mathrm{rep}}(K_{opt})$ from $\sigma = 1$ to $\sigma = 2$ is not as large (percentage-wise, or absolutely) as the reduction in $\hat{\mathrm{J}}_{\mathrm{rep}}(K_{opt})$ from $\sigma = 0$ to $\sigma = 1$. The best choice for δ varies with the value of σ. The minimizing K_{opt} for each bold (σ,δ) pair in Table 4.1 is shown in Table 4.2. Note the length of K_{opt} increasing with σ. The first three elements of K_{opt} weight the

Table 4.1: Optimal $\hat{\mathrm{J}}_{\mathrm{rep}}(K_{opt})$ for varying δ and σ

$\sigma \backslash \delta$	1	2	3	4	5
0	0.8380	0.4812	**0.4452**	0.6170	0.5557
1	0.5837	**0.1706**	0.4040	0.3282	0.5422
2	0.3997	0.1599	**0.1091**	0.3255	0.2741
3	0.3100	0.1290	**0.0484**	0.1062	0.2699

Table 4.2: Optimal values of K_{opt} as complexity varies

	K_{opt} (linear combination weights)					
$(\sigma,\ \delta)$	$\hat{x}_1$	$\hat{x}_2$	$\hat{x}_3$	$y(k)z^{-1}$	$y(k)z^{-2}$	$y(k)z^{-3}$
(0,3)	[0.283	1.644	3.412]			
(1,2)	[2.364	-3.351	-0.642	-2.501]		
(2,3)	[1.914	-8.280	1.569	0.639	-3.077]	
(3,3)	[0.901	-5.655	-4.888	0.960	-3.719	1.327]

internal controller states (state estimates in the observer for this system). The remaining σ elements define a FIR filter for the output.

The effect of σ may be seen in the time domain. Simulated time responses for the bold cascaded designs as σ varies, with $\xi = 0$, are shown in Fig 4.2. Notice the approach toward deadbeat cancellation of the periodic disturbance as σ increases. For these simulations, the initial conditions of the system and controller were set to zero. The periodic disturbance was selected as a sinusoidal signal with period 80 samples added to a triangular wave with period 10 samples. The higher frequency components of the repetitive disturbance due to the triangular wave can be seen to persist in the steady state, though with small amplitude. This was specified by the choice of q_w.

4.2.2 Effect of ξ on the resulting designs

To illustrate the effect of ξ on the closed loop performance, the proposed design method is carried out for $\xi = 0,\ 0.25,\ \&\ 0.5$ with the complexity fixed at $\sigma = 1$. Recall that ξ specifies the cycle to cycle time constant for rejecting the repetitive disturbance. The simulated responses of the controllers to the sinusoidal plus triangle wave periodic disturbance are shown in Fig 4.3. The parameters σ & δ were held fixed at 1 and 2 respectively, with K_{opt} designed to minimize $\hat{\mathrm{J}}_{\mathrm{rep}}(K_{opt})$ for each value of ξ shown. A side effect of choosing slower learning is that the system is less susceptible to learning large

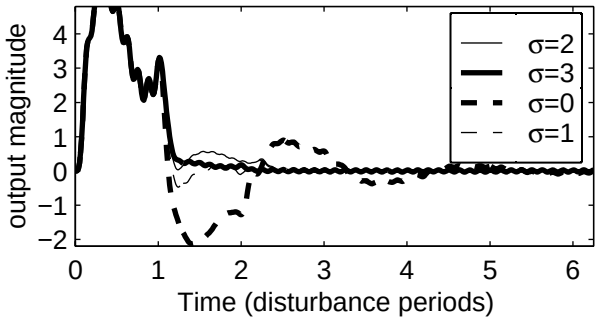

Figure 4.2: Effect of σ on the system shown in the time domain.

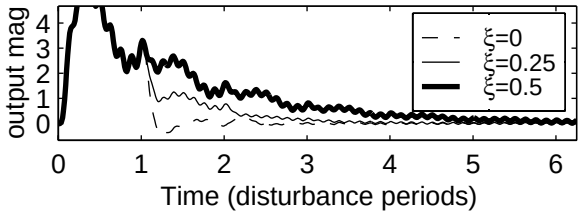

Figure 4.3: Simulation results for Cascaded designs with varying ξ and constant σ

Table 4.3: Performance Index Comparison

$J_{rep}(\cdot)$	1989	Cascaded
$\xi = 0$	0.2451	0.2057
$\xi = 0.25$	0.1551	0.1752
$\xi = 0.5$	0.1286	0.1384

one-time disturbances such a shocks.

4.2.3 Comparison to 1989 Design

The set of cascaded designs with $\sigma = 1$ is selected to compare with the 1989 design, under the assumption that more complexity is not merited by the performance it can achieve. The parameters δ and K_{opt} then depend upon the value of ξ used to define the approximated performance index, $\hat{J}_{rep}(K_{opt})$.

The 1989 controller design which will be compared to the Cascaded designs also depends on ξ. The component G_{inv} is initially set to be a fourth order approximation of the zero-phase-error inverse (see Appendix A.1) of Γ_y (the transfer function is given in Appendix B.3). For a given ξ, G_{inv} will be scaled by $1 - \xi$. This is the most appropriate modification to the 1989 structure to accomodate the design goal associated with ξ.

The difference in computation required to implement these two control schemes was a motivating concern. The G_{inv} block of the 1989 structure requires an additional five memories, 6 multiplies, and 5 additions. In contrast, the cascaded structure ($\sigma = 1$) needs 4 multiplies, 3 additions, and only 1 extra memory. The memory is not a major concern, as the majority of the memory costs are realized by the periodic signal generator which is common to both designs. However, an associated potential potential benefit of using less memory is that it means fewer states are added to the system (none if σ=0).

The original performance measure $J_{rep}(\Phi_y)$ rather than the approximated one can be used to compare the two controllers for different values of ξ. It does not depend upon the repetitive controller design method. Even though the cascaded controllers are designed using $\hat{J}_{rep}(K_{opt})$, they are compared to the 1989 designs using the unapproximated performance index. The values of $J_{rep}(\Phi_y)$ are shown in Table 4.3. The 1989 designs exhibits a lower cost in terms of the given performance index when ξ is not zero. With the chosen complexity, $\sigma = 1$, the structure of the cascaded design restricts performance in comparison to the 1989 design. In simulation, the forced responses of the two controllers to a particular repetitive

disturbance are nearly identical. Increases in the controller complexity (order) allow the cascaded design to surpass the 1989 design as measured by this performance index. These improvements may or may not be worth the cost. As a whole, the results of this example look promising for experimental application.

4.3 Concluding Remarks

This design method is based upon a performance index, so there are associated possibilities for its modification through the use of additional or different weightings. The inclusion of other design constraints to form a more complex convex optimization problem is possible when the approximated performance index is used for design. No guarantee that the given design method will result in an asymptotically stable closed loop system was given. A classification of the systems for which it does is an open question for research.

The cascaded design relies heavily on the design of the internal controller (observer state feedback as presented). The particular internal states which are available in an implementation setting depend upon the realization of the controller in software. If the realization is changed via a state transformation, the appropriate portion of K_{opt} can be transformed to reflect the new realization without changing the net effect of the repetitive controller design. Therefore, after designing the cascaded repetitive controller, a new realization of the internal feedback controller can make the equivalent K_{opt} sparse, reducing computation. The side effect is that it may make the implementation of the internal controller itself more complex. Exploring these integrative possibilities will move the design a step further toward minimal computational complexity.

Chapter 5

Conclusions

5.1 Summary of Results

The problem of cost effective repetitive control was addressed. Repetitive control is a control method aiming to eliminate the effect of periodic disturbances with known period on a control system. Periodic disturbances are common to many mechanical systems. For applications such as computer disk drives, implementation complexity plays an important role. This means that controllers achieving suboptimal performance at lesser complexity are of interest. Two discrete time repetitive controller designs which sacrifice performance for reduced implementation costs are described.

The memory burden of discrete time repetitive controllers is proportional to the known length of the periodic disturbance. To reduce this memory burden, a repetitive control system based on an internal model operating at a slower rate was developed. The resulting control system was a dual rate system. Simple designs of system components guaranteeing stability of the closed loop system were given. The system was analyzed through the use of lifting techniques to accomodate its dual rate nature within the context of linear time invariant systems. Modulated representations of these lifted systems were used to describe performance and to give conservative estimates of robustness.

This dual-rate design was applied to a computer disk drive servosystem. Analysis and simulation was carried out using a model of the experimental system. To reduce computational complexity, modifications to the nominal dual-rate design were made for this example. The analysis tools developed were used to show the stability of these modified designs, and compare properties of their performance. For example, the seventh order

zero-phase-error inverse of the closed loop system dynamics was approximated both with a second order inverse and with a constant gain (the inverse of the DC gain of the closed loop system). The performance of the system for these design choices was described in terms of several measures. Examples of the types of periodic disturbances the system is able to reject were given. Also given were examples of disturbances which capture the least desirable behavior of the system. Finally, experiments were conducted on the actual disk drive system which agree with the results of simulation and analysis.

Then, another new structure, the cascaded design, was developed to address implementation complexity from the point of view of computational complexity. For the use of this structure, repetitive control is assumed to be added to an existing control system. Rather than designing a SISO repetitive controller to map the measurement error to the control input, a controller which uses the internal states of existing controllers in addition to the measurement error was developed. An observer state feedback control scheme was taken for the internal feedback controller. The proposed design borrows the internal model structure from the 1989 repetitive controller design (Tomizuka et al., 1989).

Comparable performance to that of the 1989 repetitive controller was sought at a lesser computational cost. The problem was formulated in terms of a frequency domain $\mathcal{H}_\infty$ objective. This objective uses the existing feedback control system as a reference for the repetitive control design, defining the objective in terms of a deviation from its frequency response. The objective parameterizes this desired deviation in terms of a scalar value between -1 and 1, and a zero-phase lowpass filter. The scalar value describes a desired cycle to cycle rate of learning and the zero-phase lowpass filter describes the sensitivity to high frequency noises and model uncertainty.

The cascaded structure depends on several parameters, one of which describes computational complexity by specifying the order of a finite impulse response filter applied to the measurement signal. The coefficients of this filter and the weightings on observer states are free design parameters which can be selected optimally. When the proposed $\mathcal{H}_\infty$ objective is used for this purpose, the optimization problem is not convex. Rather than using a global optimization technique, the $\mathcal{H}_\infty$ objective was approximated with a convex objective to use for design. This was done looking toward future developments. Other constraints may be added to the design problem for which convex optimization methods will be useful. For now, convexity guaranteed that the minimum computed is a global minimum. Bounds on the error of the approximation to the original $\mathcal{H}_\infty$ objective are given.

A suggested design procedure for cascaded repetitive controllers of increasing complexity is given based upon the approximated performance objective.

For a model of a disk drive servosystem, a repetitive control problem is posed in terms of the performance objective, and various csacaded repetitive controller designs were carried out. For each level of complexity, a different cascaded design results. Before complexity exceeded that of the 1989 design, the cascaded repetitive controller performance compared favorably to the 1989 repetitive controller. At lesser computational cost, it exhibits nearly identical behavior in simulation and achieves similar performance in terms of the actual, rather than approximated, performance objective.

Steps toward leaner implementation of discrete time repetitive controllers were described, with applications to magnetic disk drives. Emphasis was placed on giving highly structured, parameterized designs. An engineer faced with questions of cost effectiveness can work within this framework to examine cost versus performance compromises.

5.2 Future Work

Related to the work presented in this dissertation, several directions for future research are described below.

- The philosophy behind the design of the cascaded controller has potential to be generalized. In many cases, a controller may be added as an "outer" loop control action to an existing system. The "outer" loop may be designed to capitalize upon computation in the inner loop, rather than duplicating computational effort.

- For disk drive servosystems, because of the typical mode switching between seeking and following, there is an interest in having fast integral action. Repetitive control has integral action in the steady-state, but through the interaction of its many modes a steady state error may persist for almost an entire cycle, even if deadbeat rejection of periodic disturbances is specified. Application of repetitive control in parallel with integral action leads to a hidden integrator in the total controller. Coupling fast integral action with the integral action of repetitive control can eliminate this hidden state. As always, there is an interest in minimal complexity.

- Consider the repetitive control problem as an observer state feedback scheme for a system augmented with a periodic signal generator. Assuming the augmented system

model has a computationally efficient realization (the PSG of repetitive control does have such a realization), imposing sparseness conditions on the state feedback and observer gains is one way to effect computational simplicity in the controller. Coupled with a performance objective, the design of such a controller may be addressed via optimization.

Bibliography

Astrom, K. J., Hagander, P. and Sternby, J. (1984). Zeros of sampled systems, *Automatica* **20**(8): 31–38.

Chiu, T.-C. et al. (1993). Compensation for repeatable and non-repeatable tracking errors in disk file systems, *Proceedings of the JSME International Conference on Advanced Mechatronics* pp. 710–717.

Ehrlich, R. (1999). Tpi growth is the key to delaying superparamagnetism's arrival, *Data Storage* **6**(10).

Evans, R. (1999). Extending bandwidth with dual-stage suspensions, *Data Storage* **6**(10).

Fliege, N. J. (1994). *Multirate Digital Signal Processing*, Chichester, Wiley, New York.

Francis, B. and Wonham, W. (1975). The internal model principle for linear multivariable regulators, *Applied Math and Optimization* **2**: 170–194.

Franklin, G. F., Powell, J. D. and Workman, M. (1997). *Digital Control of Dynamic Systems*, third edn, Addison Wesley. Chapter 14.

Goodwin, G. C. and Feuer, A. (1992). Linear periodic control: A frequency domain approach, *Systems and Control Letters* **19**: 379–390.

Hanson, R. and Tsao, T.-C. (1996). Discrete-time repetitive control of LTI systems sampled at a periodic rate, *Proceedings of the 13th World Congress of IFAC* **D**: 13–18.

Hara, S., Yamamoto, Y., Omata, T. and Nakano, M. (1988). Repetitive control system: A new type servo system for periodic exogenous signals, *IEEE Transactions on Automatic Control* **33**(7): 659–668.

Hernandez, D., Park, S.-S., Horowitz, R. and Packard, A. (1999). Dual-stage track following servo design for hard disk drives, *Proceedings of the American Controls Conference* pp. 4116–4121.

Hillerstrom, G. and Walgama, K. (1996). Repetitive control theory and applications – a survey, *Proceedings of the 13th World Congress of IFAC* **D**: 1–6.

Inoue, T., Nakano, M. and Iwai, S. (1981). High accuracy control of servomechanism for repeated contouring, *Proceedings of the 10th Annual Symposium on Incremental Motion Control Systems and Devices* pp. 285–292.

James, C. and Sadegh, N. (1999). Synthesis and stability of a multirate repetitive learning controller, *Proceedings of the American Control Conference* pp. 358–362.

Kempf, C., Messner, W., Tomizuka, M. and Horowitz, R. (1993). Comparison of four discrete-time repetitive control algorithms, *IEEE Control Systems Magazine* pp. 48–54.

Langari, A. and Francis, B. (1996). Robustness analysis of sampled-data repetitive control systems, *Proceedings of the 13th World Congress of IFAC* **D**: 19–24.

Poolla, P. K. K. and Tannenbaum, A. (1985). Robust control of linear time-invariant plants using periodic compensation, *IEEE Transactions on Automatic Control* **30**(11): 1088–1096.

She, J.-H. and Nakano, M. (1996). A design methodology for robust two-degree-of-freedom digital repetitive control, *Proceedings of the 13th World Congress of IFAC* **D**: 25–30.

Shroeck, S. J. and Messner, W. (1999). On controller design for linear time-invariant dual-input single-output systems, *Proceedings of the American Controls Conference* pp. 4122–4126.

Steinbuch, M. and Norg, M. L. (1998). Advanced motion control: An industrial perspective, *European Journal of Control* (4): 278–293.

Tenney, J. and Tomizuka, M. (1996). Effects of non-periodic disturbances on repetitive control systems, *Proceedings of the 13th World Congress of IFAC* **D**: 7–12.

Tomizuka, M. (1987). Zero phase error tracking algorithm for digital control, *ASME Journal of Dynamic Systems, Measurement, and Control* **109**: 65–68.

Tomizuka, M. (1997). Advanced control applications to servo systems for precision machines, *Proceedings of the International Confrence on Micromechatronics for Information and Precision Equipment* pp. 469–474.

Tomizuka, M., Chew, K. and Yang, W. (1990). Disturbance rejection through an external model, *ASME Journal of Dynamic System, Measurement, and Control* **112**: 559–564.

Tomizuka, M., Tsao, T.-C. and Chew, K.-K. (1989). Analysis and synthesis of discrete-time repetitive controllers, *ASME Journal of Dynamic System, Measurement, and Control* **111**: 353–358.

Tsao, T.-C. and Tomizuka, M. (1994). Robust adaptive and repetitive digital tracking control and application to a hydraulic servo for noncircular machining, *ASME Journal of Dynamic System, Measurement, and Control* **116**: 24–32.

White, M. and Tomizuka, M. (1996). Increased disturbance rejection in magnetic disk drives by acceleration feedforward control, *Proceedings of the 1996 IFAC World Congress* **O**: 489–494.

Yi, L. (2000). *Two Degree of Freedom Control for Hard Disk Drives*, PhD thesis, University of California at Berkeley.

Appendix A

Technical

A.1 Zero-Phase-Error Inverses

The zero-phase-error inverse dynamics described in what follows is based upon the zero-phase-error tracking controller developed by Tomizuka (1987). The underlying mathematical basis, and the reason that "zero-phase" is in the name, is the following:

$$\begin{aligned} &\forall\, z \ \in\ \mathbb{C} \text{ s.t. } |z| = 1 \\ &\text{and } p(z) = \alpha_0 + \alpha_1 z + \cdots + \alpha_n z^n \text{ s.t. } \alpha_i \ \in\ \mathbb{R} \text{ for } i = 0, 1, \ldots, n \\ &p(z)p(z^{-1}) = |p(z)|^2 \in \mathbb{R}^+ \end{aligned} \tag{A.1}$$

Evaluating the same real polynomial at a complex number on the unit disk and at its inverse yields results with complementary phase. This is used in the context of representing discrete time systems as ratios of polynomials in z^{-1}, the unit delay operator. Evaluations of z^{-1} along the unit circle correspond to the frequency response of the discrete time system.

Consider the following general form for a transfer function of a stable discrete time system:

$$\Gamma_y = \frac{z^{-d_p} B^+(z^{-1}) B^-(z^{-1})}{A(z^{-1})}, \tag{A.2}$$

where A, B^+, and B^- are polynomials with nonzero constant terms, and z^{-1} represents the one sample delay operator. Thus, this system has d_p pure delays. Furthermore, the numerator is factored such that B^+ has roots all outside or near the unit circle, and B^- has roots inside the unit circle. The denominator, A, has all roots inside the unit circle since the system was assumed to be stable.

If there are no zeros outside the unit disk ($B^+(z^{-1})$ constant), then define the zero-phase error inverse in terms of stable pole-zero cancellations as follows:

$$G_{zpe}(z^{-1}) = \frac{A(z^{-1})}{B^-(z^{-1})B^+(z^{-1})}. \tag{A.3}$$

With this definition, the transfer function of the series combination of Γ_y and G_{zpe} will be (after pole-zero cancellations):

$$\Gamma_y G_{zpe} = z^{-d_p}, \tag{A.4}$$

or that of pure delays.

If B^+ is not constant, define the zero-phase-error inverse in terms of the stable pole-zero cancellations as follows:

$$G_{zpe}(z^{-1}) = \frac{z^{-d}A(z^{-1})B^+(z)}{B^-(z^{-1})B^+(1)^2}, \tag{A.5}$$

where the "bad" pole-zero cancellations have been avoided, but their effect on the phase is addressed with $B^+(z)$. To enforce realizability, d delays are added to the ZPE inverse, where d is the order of B^+. Now, the transfer function of the series combination of Γ_y and G_{zpe} has the following form (again after pole-zero cancellations):

$$\Gamma_y G_{zpe} = z^{-(d+d_p)}\frac{B^+(z)B^+(z^{-1})}{(B^+(1))^2} \tag{A.6}$$

Referring back to the statement in Eq A.1, the frequency response of this series combination will have no phase due to the second factor – its phase will be that of $z^{-(d+d_p)}$. The second factor, though it may have zero-phase, will have a gain which changes with frequency.

A common source of zeros outside the unit circle for discrete time systems are so-called sampling zeros (Astrom et al., 1984). These commonly occur on the negative real axis. If for example, the above system has a single unstable zero at -2, then $B^+(z^{-1}) = 1+2z^{-1}$ modulo some constant gain. The zero-phase term involving $B^+(z)$ and $B^+(1)$ will be:

$$\frac{2z^{-1}+5+2z}{9} \tag{A.7}$$

which exhibits low-pass filter characteristics. In general, the zero-phase terms will have this symmetric, moving-average structure. When the zeros lie in the left half plane, the resulting zero-phase filter will have low-pass characteristics, becoming milder and milder the further away from the unit disk they are.

A.2 Multirate Systems

Mathematics relating to the dual rate systems found in the body of the paper is described here. The two sampling rates are referred to as the *slow* rate and *fast* rate. The fast rate is taken to be r times faster than the slow rate. The dual rate system in Fig 3.1 has both fast and slow rate signals. By considering scalar fast rate signals as r-dimensional slow rate signals (polyphase representation, or lifting), the interconnected system can be analyzed at the slow rate. That is, checking the stability of the multirate system is equivalent to checking the stability of a related single rate time invariant system at the slow sampling rate. Frequency domain performance interpretations must consider aliasing effects. Goodwin and Feuer (1992) discusses frequency response interpretations. Lifting is described nicely in (Poolla and Tannenbaum, 1985). This subject matter can also be found in signal processing textbooks, such as (Fliege, 1994), though in a significantly different form.

The proposed dual-rate repetitive control system is naturally represented using four types of single input single output systems: fast rate linear time invariant systems, slow rate linear time invariant systems, interpolation systems (creating a fast rate signal from a slow rate signal), and decimation systems (creating a slow rate signal from a fast rate signal). The form of Decimation and Interpolation as transfer function matrices at the slow rate is described in Section A.2.3 and A.2.4 with several examples. This is preceded by a discussion of lifting in Section A.2.1 and of frequency domain interpretations of lifted systems in Section A.2.2.

A.2.1 Lifting

Consider the single-input single-output (SISO) system G as a linear operator from input sequences of real numbers, $\{u_k\}$, to output sequences of real numbers, $\{y_k\} = G\{u_k\}$. Define the linear operator $\mathcal{L}^r(G)$, from sequences of r-dimensional vectors to sequences of r-dimensional vectors, such that $(\{\tilde{y}_k\} = \mathcal{L}^r(G)\{\tilde{u}_k\})$. Using loose notation, but indicating how the inputs and outputs are stacked (they still satisfy the relationship $\{y_k\} = G\{u_k\}$),

$\mathcal{L}^r(G)$ can be represented in the following way:

$$\begin{bmatrix} y(kr) \\ y(kr+1) \\ \vdots \\ y(kr+r-1) \end{bmatrix} = \mathcal{L}^r(G) \left(\begin{bmatrix} u(kr) \\ u(kr+1) \\ \vdots \\ u(kr+r-1) \end{bmatrix} \right)$$

The lifting operation, $\mathcal{L}^r(\cdot)$, is a mapping from single-input single-output(SISO) discrete systems to r-input r-output discrete systems. It is both linear, and an algebra homomorphism, $\mathcal{L}^r(U * V) = \mathcal{L}^r(U) * \mathcal{L}^r(V)$. We can apply $\mathcal{L}^r(\cdot)$ to general linear p-input m-output systems by applying it to each component. For example:

$$\begin{bmatrix} y_1(k) \\ y_2(k) \end{bmatrix} = \begin{bmatrix} G_{11} & G_{12} \\ G_{21} & G_{22} \end{bmatrix} \begin{bmatrix} u_1(k) \\ u_2(k) \end{bmatrix}$$

$$\Updownarrow$$

$$\begin{bmatrix} y_1(kr) \\ \vdots \\ y_1(k(r+1)-1) \\ y_2(kr) \\ \vdots \\ y_2(k(r+1)-1) \end{bmatrix} = \begin{bmatrix} \mathcal{L}^r(G_{11}) & \mathcal{L}^r(G_{12}) \\ \mathcal{L}^r(G_{21}) & \mathcal{L}^r(G_{22}) \end{bmatrix} \begin{bmatrix} u_1(kr) \\ \vdots \\ u_1(k(r+1)-1) \\ u_2(kr) \\ \vdots \\ u_2(k(r+1)-1) \end{bmatrix}$$

The result will be a rp-input rm-output system. Defined this way it is easy to verify that:

$$\mathcal{L}^r(G_1 * G_2) = \mathcal{L}^r(G_1) * \mathcal{L}^r(G_2)$$

where $G_1 * G_2$ denotes the series combination of two MIMO systems with compatible dimensions. Also,

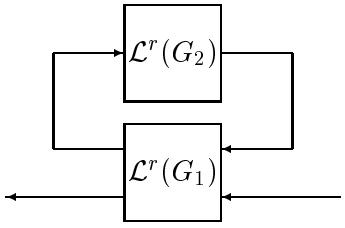

$$= \mathcal{L}^r \left(\right.$$

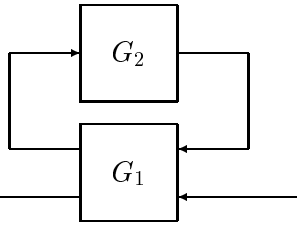

$$\left. \right),$$

When the induced 2-norm of G exists, $\|\mathcal{L}^r(G)\|_{2/2} = \|G\|_{2/2}$. This follows directly from the definition of the induced norm (for DLTI systems, the induced 2-norm will be the infinity

norm). $\mathcal{L}^r(\cdot)$ will be referred to as the lifting operator, and $\mathcal{L}^r(G)$ as the lifted version of G.

As an example, indicating the fast time index by k_f and the slow time index by k_s, consider a fast rate system, G_f with input $u(k_f)$ and output $y(k_f)$. The slow rate equivalent system, $G_s = \mathcal{L}^r(G_f)$, has r inputs and r outputs. The r inputs will be $u_i(k_s) = u(k_s r + i)$ for $i = 0 \ldots (r-1)$, and the outputs will similarly be $y_i(k_s) = y(k_s r + i)$ for $i = 0 \ldots (r-1)$. These are referred to as the polyphase components of the signal in the terminology of signal processing. As an example of lifting a SISO time-invariant discrete time system, consider $r = 3$ and $G_f = z^{-1}$. The following is the lifted representation of G_f:

$$G_s = \mathcal{L}^r(G_f) = \begin{bmatrix} 0 & 0 & z^{-1} \\ 1 & 0 & 0 \\ 0 & 1 & 0 \end{bmatrix}$$

The term z^{-1} represents the one-step delay (or shift) operator on sequences as usual in both instances. Using the above relations between inputs and outputs, it can be easily verified that G_f and G_s, represent the same mapping from input sequences to output sequences. A $r \times r$ transfer matrix can be found to represent any SISO transfer function. It is *not* true, however, that corresponding to any $r \times r$ transfer matrix, there exists a SISO transfer function such that the $r \times r$ transfer matrix is the lifted SISO transfer function. If the inputs and outputs of a generic $r \times r$ system are considered as the polyphase components of some faster rate signal, the $r \times r$system describes a periodically time varying (with period r) linear input-output mapping. Periodically time-varying characteristics can be described in the frequency domain according to the development in the next section.

A.2.2 Frequency Domain Interpretations

Consider an $r \times r$ transfer matrix, $H(z^{-1})$, representing a periodically time varying SISO discrete time system via lifting as described above. Thus, the r inputs and r outputs are the polyphase components of underlying fast rate signals. The frequency response of $H(z^{-1})$ defined up to the Nyquist frequency of the slow rate describes the gain from sinusoidal polyphase components of the input to sinusoidal polyphase components of the output.

An important result relates sinusoidal polyphase components of a signal to its sinusoidal components. Consider the following two descriptions of a signal $d(k)$ with sinusoidal

$(\omega < \pi/r)$ polyphase components:

$$d(k) = \begin{cases} A_1 e^{j\omega k} & \text{for} \quad k \bmod r = 0 \\ A_2 e^{j\omega(k-1)} & \text{for} \quad (k-1) \bmod r = 0 \\ \vdots & \\ A_r e^{j\omega(k-r+1)} & \text{for} \quad (k-r+1) \bmod r = 0 \end{cases} \tag{A.8}$$

and

$$d(k) = F_1 e^{j\omega_1 k} + F_2 e^{j\omega_2 k} + \cdots + F_r e^{j\omega_r k} \tag{A.9}$$

where ω_i are defined as follows:

$$\begin{aligned} &\omega_1 = \omega && \omega_r = \omega - 2\pi/r \\ &\omega_2 = \omega + 2\pi/r && \omega_{r-1} = \omega - 4\pi/r \\ &\vdots && \vdots \\ &\omega_{(r+1)/2} = \omega + (r-1)\pi/r && (r \quad \text{odd}) \\ &\text{OR} \\ &\omega_{r/2} = \omega + (r-2)\pi/r && \omega_{r/2+1} = \omega - \pi \qquad (r \quad \text{even}) \end{aligned} \tag{A.10}$$

These ω_i describe the aliased frequencies of $\omega < \pi/r$. Note that $-\pi < \omega_i < \pi$ for all i, thus all below the Nyquist frequency associated with the signal $d(k)$. With some algebra, it can be shown that the coefficients F_i and A_i satisfy the following relationship:

$$\begin{bmatrix} F_1 \\ F_2 \\ \vdots \\ F_r \end{bmatrix} = W_r^{-1} \operatorname{diag}(1,\, e^{-j\omega},\, \ldots,\, e^{-j(r-1)\omega}) \begin{bmatrix} A_1 \\ A_2 \\ \vdots \\ A_r \end{bmatrix} = S_r^{-1}(\omega) \begin{bmatrix} A_1 \\ A_2 \\ \vdots \\ A_r \end{bmatrix} \tag{A.11}$$

with W_r being the conjugate of the standard $r \times r$ discrete fourier transform matrix defined as follows:

$$\gamma_r = e^{j2\pi/r}, \quad [W_r]_{(i,j)} = \gamma_r^{(i-1)(j-1)} \tag{A.12}$$

The inverse relationship can also be formed, defining A_i in terms of F_i.

$$\begin{bmatrix} A_1 \\ A_2 \\ \vdots \\ A_r \end{bmatrix} = \operatorname{diag}(1,\, e^{j\omega},\, \ldots,\, e^{j(r-1)\omega}) W_r \begin{bmatrix} F_1 \\ F_2 \\ \vdots \\ F_r \end{bmatrix} = S_r(\omega) \begin{bmatrix} F_1 \\ F_2 \\ \vdots \\ F_r \end{bmatrix} \tag{A.13}$$

It is easily verified that $\frac{1}{\sqrt{r}}S_r$ is unitary from the using the following known property of W_r:

$$W_r^{-1} = \frac{1}{r}W_r^* \tag{A.14}$$

Using the above relationships, specific frequency components of polyphase input or output signals can be isolated.

For example, consider a SISO system forced with a sinusoid at frequency $\omega < \pi/r$. Let the system be realized as an $r \times r$ transfer matrix, $H(z^{-1})$, mapping polyphase components of input to polyphase components of the output as described above. The polyphase components of the input can be described using the relationship of Eq A.13, assuming $F_i = 0$ for $i > 1$. This amounts to restricting the polyphase input signals to be in the direction of the first column of $S_r(\omega)$, denoted by $C_1(\omega)$. Then the steady-state polyphase components of the output of the system can be found using the gain $H(e^{-jr\omega})$. The relationship in Eq A.11 then leads to the frequency components of the output. The first row of $S_r^{-1}(\omega)$, denoted by $R_1(\omega)$, thus extracts the component of the output at the forcing frequency ω. So, the gain and phase shift of the component of the output at the forcing frequency $\omega < \pi/r$ can be found by evaluating:

$$R_1(\omega)H(e^{-jr\omega})C_1(\omega) \tag{A.15}$$

The components at other aliased frequencies can likewise be found. The set of all of these transfer function like quantities forms the modulated representation of the system.

Modulated Form of SISO LTI system

For any SISO linear time invariant system G at the fast rate, define an $r \times r$-valued function of ω, $\hat{G}$, as follows:

$$\hat{G}(\omega) = S_r^{-1}(\omega)\left(\mathcal{L}^r(G)|_{z=e^{jr\omega}}\right)S_r(\omega) \tag{A.16}$$

The $r \times r$ value of $\hat{G}(\omega)$ will be diagonal for each value of ω, and will be referred to as the modulated form of G. The values along the diagonal will be the frequency response of G at the aliased frequencies ω_1 to ω_r.

A.2.3 Decimation

Decimation is written as a $1 \times r$ transfer matrix. For example, consider

$$\mathcal{D}_1 = \begin{bmatrix} 1 & 0 & 0 \end{bmatrix} \quad \mathcal{D}_2 = \begin{bmatrix} 0 & 1 & 0 \end{bmatrix} \quad \mathcal{D}_3 = \begin{bmatrix} 1/3 & 1/3 & 1/3 \end{bmatrix}$$

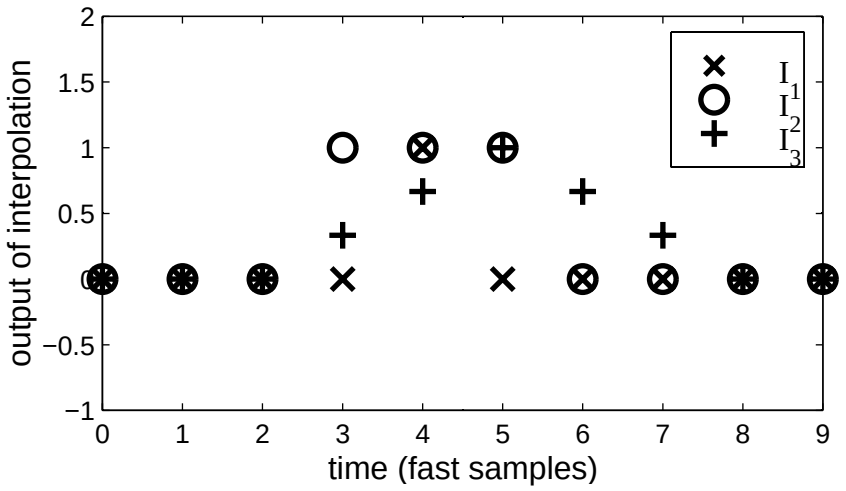

Figure A.1: Several interpolation schemes

The generation of a slow rate signal by taking every rth value of a fast rate signal is represented by the transfer matrices $\mathcal{D}_1$ or $\mathcal{D}_2$ which select from different polyphase components of the input signal. The decimation $\mathcal{D}_3$ generates a slow rate signal by averaging r fast rate values associated with a single slow sample.

A.2.4 Interpolation

Likewise, interpolation is a $r \times 1$ transfer matrix. Consider for example,

$$\mathcal{I}_1 = \begin{bmatrix} 0 \\ 1 \\ 0 \end{bmatrix} \quad \mathcal{I}_2 = \begin{bmatrix} 1 \\ 1 \\ 1 \end{bmatrix} \quad \mathcal{I}_3 = \begin{bmatrix} 2z^{-1}/3 + 1/3 \\ z^{-1}/3 + 2/3 \\ 1 \end{bmatrix}$$

Defining the input/ouput relationship of the interpolation as

$$\begin{bmatrix} u_f(3k) \\ u_f(3k+1) \\ u_f(3k+2) \end{bmatrix} = \mathcal{I}u(k) \tag{A.17}$$

and letting the slow input signal be $u(k) = 1$ for $k = 1$ and zero elsewhere, Figure A.1 shows $u_f(k)$ for $\mathcal{I}$ equal to the different interpolation schemes above.

Appendix B

Design Example Data

B.1 Experimental Equipment

The experimental system was a removable media magnetic disk drive under development. The disk rotation rate was 90Hz. With 80 sectors, and a sector servo scheme, the resulting PES measurement sample rate was 7200Hz. Actuator arm resonances were present near 3000Hz. The distance from the pivot point of the arm to the head was 5.4 cm. The radial track density was 13200TPI, corresponding to a track pitch of 1.9μm. This means that the positioning accuracy required for accurate track following was roughly one tenth of this value, or 0.2μm.

The dynamics from the command input to head position were modeled in terms of physical parameters to achieve good agreement with experimental data. The system model was as a double integrator with delay, and the controller is modeled as implemented. The frequency responses for the system are given in Section 3.2. Integral action of the internal feedback controller was disabled, as the repetitive controller applies integral action of its own. A feedback controller with integral action alone was not sufficient to meet track following requirements.

The servo controller was implemented with an on-board 16 bit microcontroller with no built-in multiplication. The PES measurements had a resolution of 10 bits per track. The source of voice coil motor current was an amplifier whose input DAC had a resolution of 14 bits. Computational, ADC, and DAC delays combined for a delay of approximately 0.25 of the measurement sample interval. An analog notch filter was used between the DAC and the amplifier to prevent excitation of the actuator arm resonance. To collect data,

the developmental interface was used to monitor the system. The time histories of digital signals internal to the microcontroller were collected. Through the developmental interface, commands to seek a new track, or to follow a single data track could be issued to the servo controller. The amplitude of periodic track runouts was in the vicinity of 17tracks, requiring reduction of their effects by more than 60dB in order to have a chance to meet tracking requirements in the presence of other disturbances.

B.2 Disk Drive Servosystem Model used in Chapter 3

In this section, a state space representation of the plant and controller used for the analytical and simulation studies in Chapter 3 are given. These numerical models are based on the physical parameters of the experimental system described in Appendix B.1. The plant (input: control signal; output: head position) is the zero-order hold equivalent of a continuous double integrator plant with an input delay of 0.258 samples. The controller is implemented digitally in discrete time.

The nominal discrete time third order plant model incoporating delay is described by the following state space data:

$$A = \begin{bmatrix} 1 & 1 & 0.22164 \\ 0 & 1 & 0.25893 \\ 0 & 0 & 0 \end{bmatrix} \quad B = \begin{bmatrix} 0.22789 \\ 0.64013 \\ 1 \end{bmatrix} \tag{B.1}$$

$$C = \begin{bmatrix} 1 & 0 & 0 \end{bmatrix} \qquad D = 0$$

The third order feedback control scheme is described by the following state space realization:

$$A_c = \begin{bmatrix} 0.0046656 & -0.33365 & 0.021067 \\ -0.015124 & 0.02143 & -0.23812 \\ 0 & 0.34892 & -0.30241 \end{bmatrix} \quad B_c = \begin{bmatrix} 0.60615 \\ -0.24051 \\ -.91608 \end{bmatrix} \tag{B.2}$$

$$C_c = \begin{bmatrix} 0 & 0 & 0.9562 \end{bmatrix} \qquad D_c = 0.93011$$

A zero-phase error inverse of the closed loop system will have a high order. The following is the second order approximation to this zero-phase error inverse which is used in the text:

$$\frac{0.91333(1 - 1.32z^{-1} + 0.6708z^{-2})}{(1 + 0.2591z^{-1} + 0.08977z^{-2})} \tag{B.3}$$

B.3 Disk Drive Servosystem Model used in Chapter 4

In this appendix section, the model of a computer disk drive servosystem used in Chapter 4 is given. This system is similar to the experimental system described in Appendix B.1. The plant and nominal feedback controller state space descriptions are given, along with the form of a fourth order approximation to the zero-phase error inverse of the closed loop system.

Continuous plant characteristics are those of a double integrator. Application of discrete time digital control to this plant leads to the zero-order hold (ZOH) equivalent of this plant. A time delay of 0.25 samples is included in the system model. The sources of this delay are the A/D and D/A conversions times, along with the time necessary to compute the control action. As with the experimental system, the period of the repetitive disturbance is taken to be 80 samples. The appropriateness of this model can be verified through examination of the material in Appendix B.1.

The feedback controller is estimator state feedback, designed with a pole placement scheme. The predictor/corrector equations and the parameters of the design are given below. The design of this feedback controller was based on the typical concerns for computer disk drives (Tomizuka, 1997; Franklin, Powell and Workman, 1997; Steinbuch and Norg, 1998). A summary of these concerns was given in Section 2.2.

The state space matrices corresponding to the nominal discrete time plant along with the state feedback and observer design comprising the internal controller are included below. Frequency responses describing the nominal feedback system are shown in Fig B.1. The loop transfer function is that of the plant in series with the controller. The gain and phase margins are shown. The disturbance to error transfer function shown is from the plant intput to its output, with the controller in feedback.

The plant and observer nominal system are described by the following state, output, predictor, corrector, and control equations:

$$\begin{aligned} x(k+1) &= Ax(k) + Bu(k) \\ y(k) &= Cx(k) \\ \hat{x}(k+1|k) &= (A - BK)\hat{x}(k|k) \\ \hat{x}(k|k) &= \hat{x}(k|k-1) + L\left(y(k) - C\hat{x}(k|k-1)\right) \\ u(k) &= -K\hat{x}(k) + u_{rep}(k) \end{aligned} \tag{B.4}$$

The insertion point for the repetitive control signal is indicated by $u_{rep}(k)$ corresponding

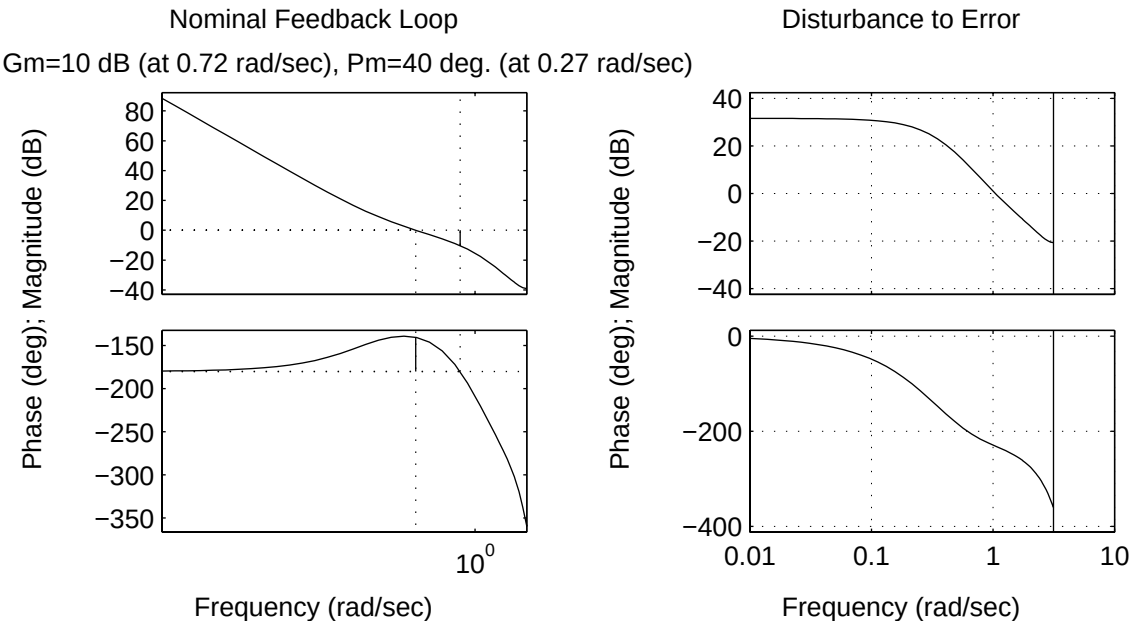

Figure B.1: Bode plots for observer state feedback system.

to the block diagram in Fig 4.1. The numerical values of the above matrices are:

$$A = \begin{bmatrix} 1 & 1 & 0.21875 \\ 0 & 1 & 0.25 \\ 0 & 0 & 0 \end{bmatrix} \qquad B = \begin{bmatrix} 0.28125 \\ 0.75 \\ 1 \end{bmatrix}$$

$$C = \begin{bmatrix} 1 & 0 & 0 \end{bmatrix} \qquad L = \begin{bmatrix} 0.6279 \\ 0.1697 \\ 0 \end{bmatrix} \tag{B.5}$$

$$K = \begin{bmatrix} 0.0728 & 0.4718 & 0.0874 \end{bmatrix}$$

The filter G_{inv} used for the 1989 repetitive controller design in Chapter 4 is the following fourth order ZPE inverse of a third order approximation to the closed loop system:

$$G_{inv} = \frac{0.754(1 - 0.776z^{-1})(1 + 0.474z^{-1})(1 - 1.51z^{-1} + 0.592z^{-2})}{(1 - 0.173z^{-1})} \tag{B.6}$$

The phase of a zero outside the unit circle of the closed loop at -2.4 is approximately cancelled with the term $(1 + 0.474z^{-1})$ in the numerator of these inverse dynamics.